Review of main QCD ideas: proton structure, parton evolution and saturation

Anna Staśto

PennState
Eberly College of Science

UPC2023, Student day, Playa del Carmen, December 10, 2023

Outline

- Exploration of proton structure: brief historical overview
- DGLAP evolution
- BFKL evolution at small x
- Dipole model
- Parton saturation

Atomic structure revealed

Geiger-Marsden experiment 1909

Scattering of alpha particles off the gold foil.
Observation of large angle scattering.

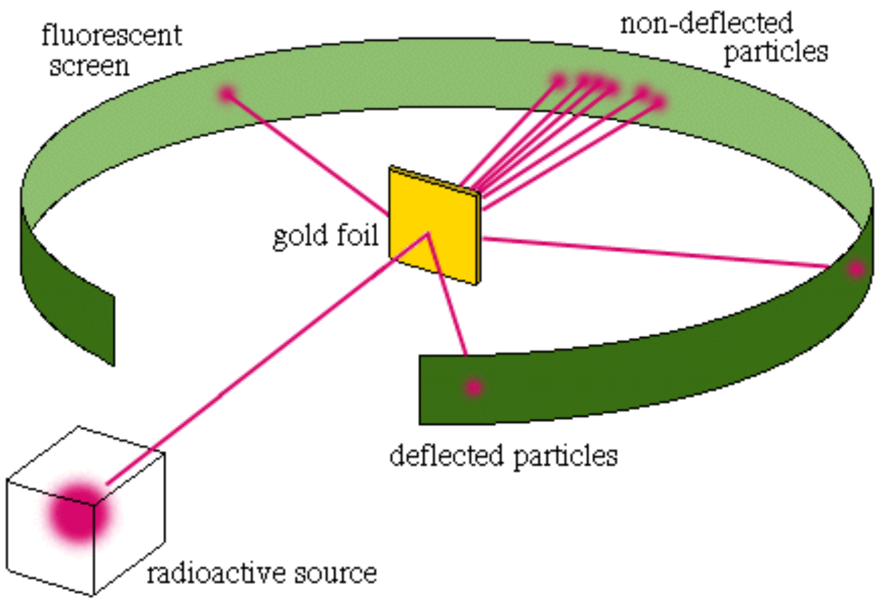

Rutherford model 1911

Atomic structure: positively charged small nucleus

LXXIX. *The Scattering of α and β Particles by Matter and the Structure of the Atom.* *By* Professor E. Rutherford, *F.R.S., University of Manchester* *.

traversed. The observations, however, of Geiger and Marsden † on the scattering of α rays indicate that some of the α particles must suffer a deflexion of more than a right angle at a single encounter. They found, for example, that

It seems reasonable to suppose that the deflexion through a large angle is due to a single atomic encounter, for the chance of a second encounter of a kind to produce a large deflexion must in most cases be exceedingly small. A simple calculation shows that the atom must be a seat of an intense electric field in order to produce such a large deflexion at a single encounter.

Atomic structure revealed

Geiger-Marsden experiment 1909

Scattering of alpha particles off the gold foil.
Observation of large angle scattering.

Rutherford model 1911

Atomic structure: positively charged small nucleus

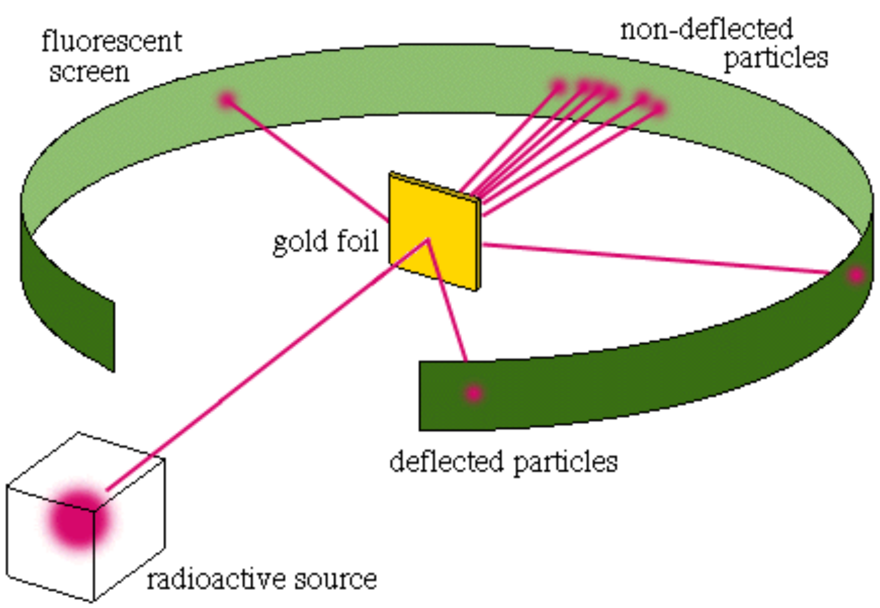

LXXIX. *The Scattering of α and β Particles by Matter and the Structure of the Atom. By* Professor E. RUTHERFORD, *F.R.S., University of Manchester* *.

traversed. The observations, however, of Geiger and Marsden † on the scattering of α rays indicate that some of the α particles must suffer a deflexion of more than a right angle at a single encounter. They found, for example, that

It seems reasonable to suppose that the deflexion through a large angle is due to a single atomic encounter, for the chance of a second encounter of a kind to produce a large deflexion must in most cases be exceedingly small. A simple calculation shows that the atom must be a seat of an intense electric field in order to produce such a large deflexion at a single encounter.

Later on addressing a Royal Society anniversary meeting as its President, Rutherford commented prophetically, “It would be of great scientific interest if it were possible in experiments to have a supply of electrons... of which the individual energy of motion is greater even than that of the α particle”.

Nucleon size

Hofstadter experiments in 1950-1957

<u>Electron</u> scattering off nuclei, determining the charge and shape of nuclei, and measuring the finite size of protons.

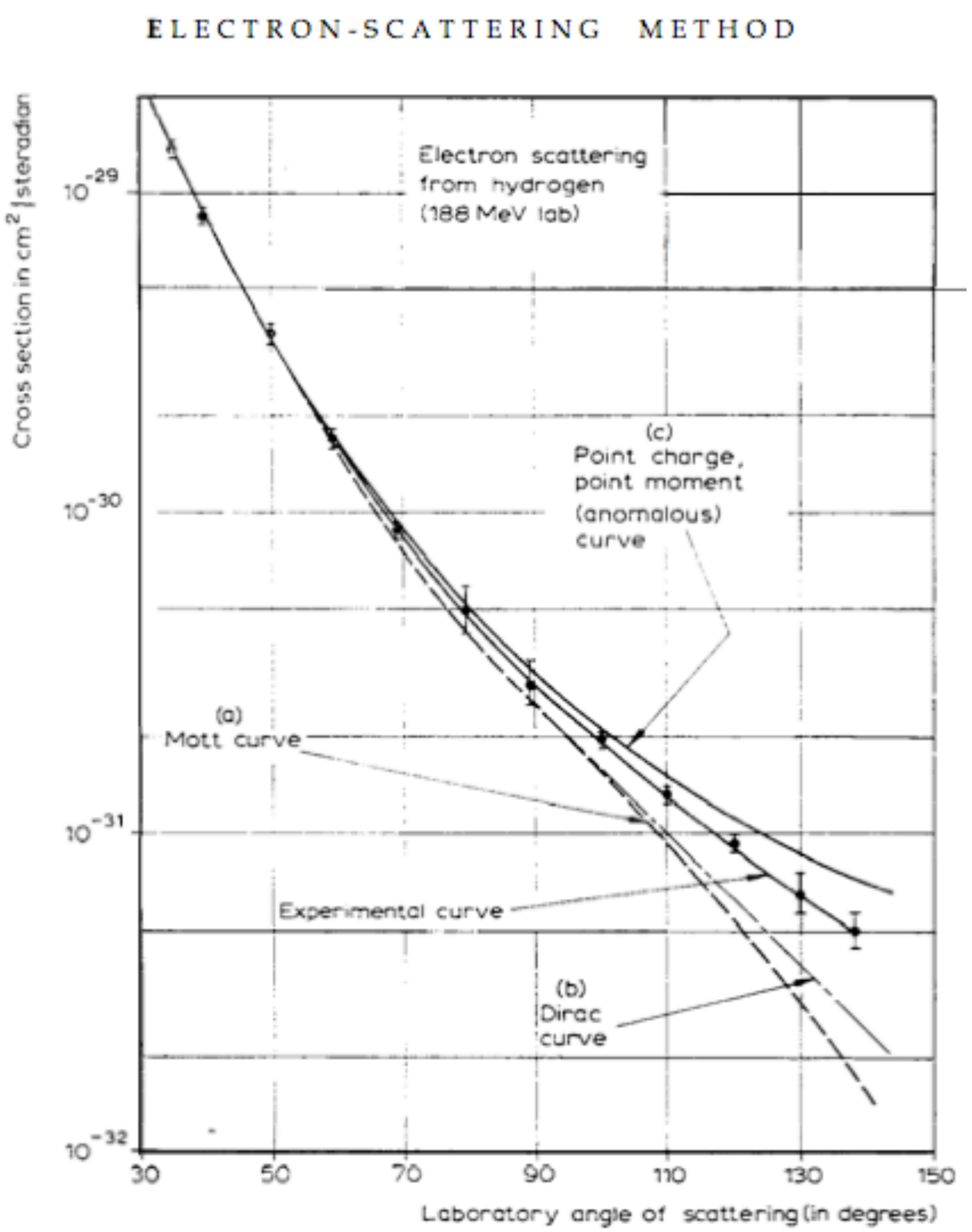

Energy of electrons 188 MeV

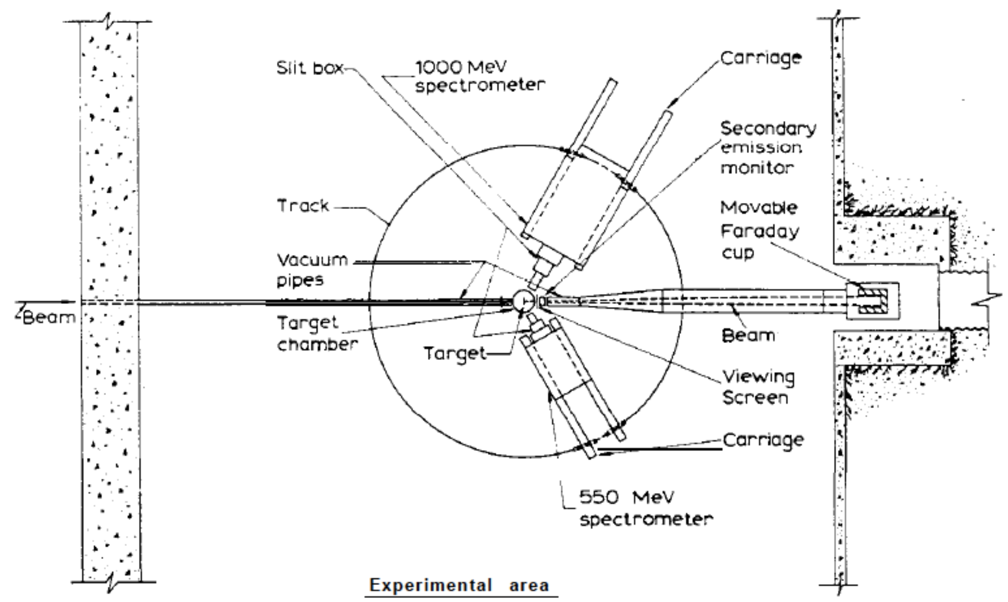

Fig. 2. This figure shows a schematic diagram of a modern electron-scattering experimental area. The track on which the spectrometers roll has an approximate radius of 13.5 feet.

Current experimental value (measured with electrons):

$$R_p = 0.87 \text{ fm}$$

$$1 \text{ fm} = 10^{-13} \text{ cm}$$

First observation of proton structure

VOLUME 23, NUMBER 16 PHYSICAL REVIEW LETTERS 20 OCTOBER 1969

OBSERVED BEHAVIOR OF HIGHLY INELASTIC ELECTRON-PROTON SCATTERING

M. Breidenbach, J. I. Friedman, and H. W. Kendall
Department of Physics and Laboratory for Nuclear Science,*
Massachusetts Institute of Technology, Cambridge, Massachusetts 02139

and

E. D. Bloom, D. H. Coward, H. DeStaebler, J. Drees, L. W. Mo, and R. E. Taylor
Stanford Linear Accelerator Center,† Stanford, California 94305
(Received 22 August 1969)

20 GeV electron beam scattering off protons

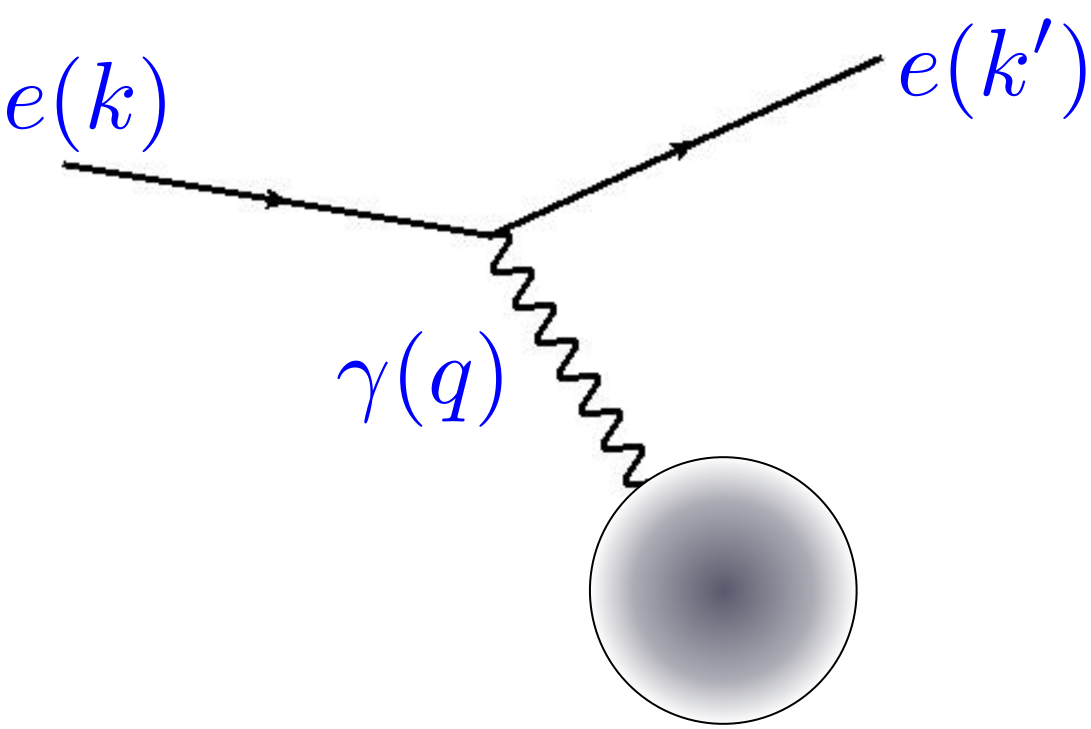

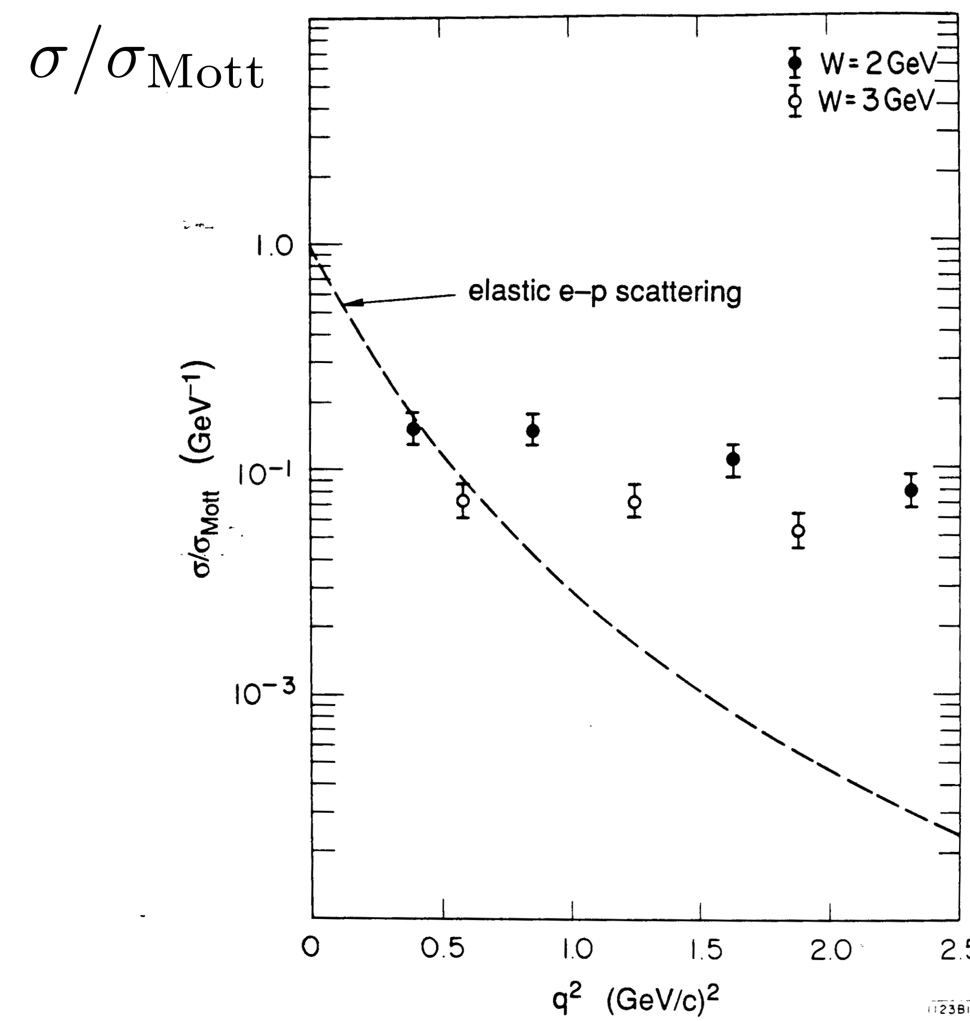

$Q^2 = -q^2$:resolving power of interaction

First observation of proton structure

VOLUME 23, NUMBER 16 PHYSICAL REVIEW LETTERS 20 OCTOBER 1969

OBSERVED BEHAVIOR OF HIGHLY INELASTIC ELECTRON-PROTON SCATTERING

M. Breidenbach, J. I. Friedman, and H. W. Kendall
Department of Physics and Laboratory for Nuclear Science,*
Massachusetts Institute of Technology, Cambridge, Massachusetts 02139

and

E. D. Bloom, D. H. Coward, H. DeStaebler, J. Drees, L. W. Mo, and R. E. Taylor
Stanford Linear Accelerator Center,† Stanford, California 94305
(Received 22 August 1969)

20 GeV electron beam scattering off protons

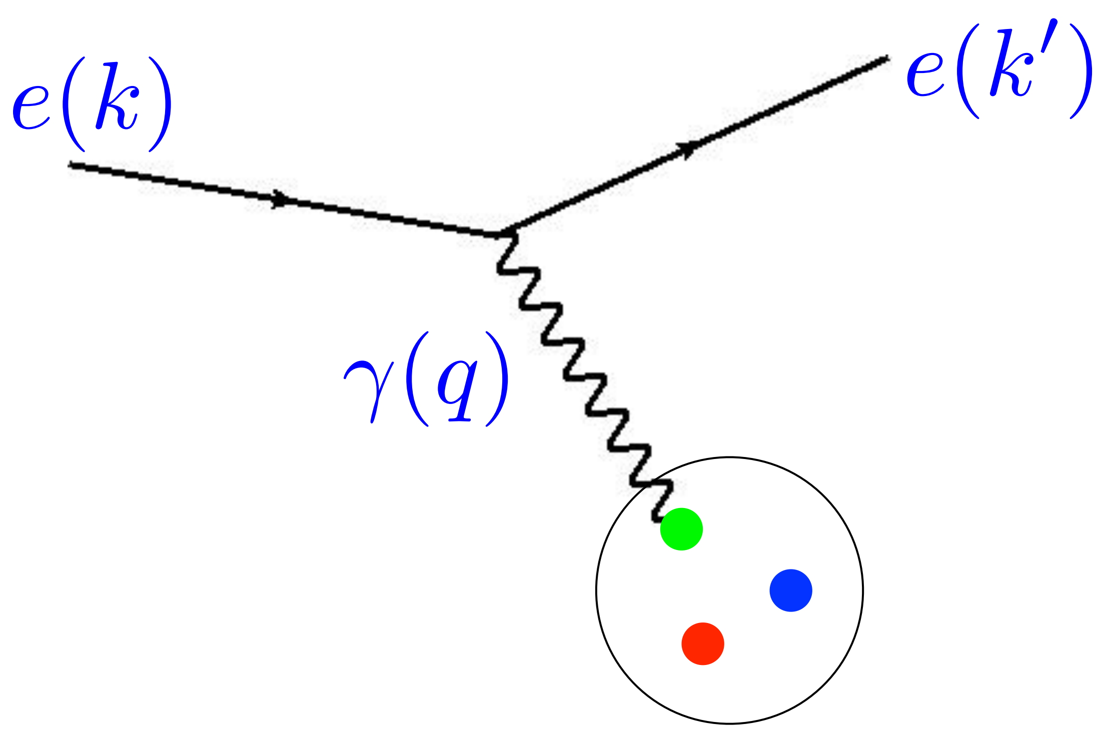

$\sigma/\sigma_{\text{Mott}}$

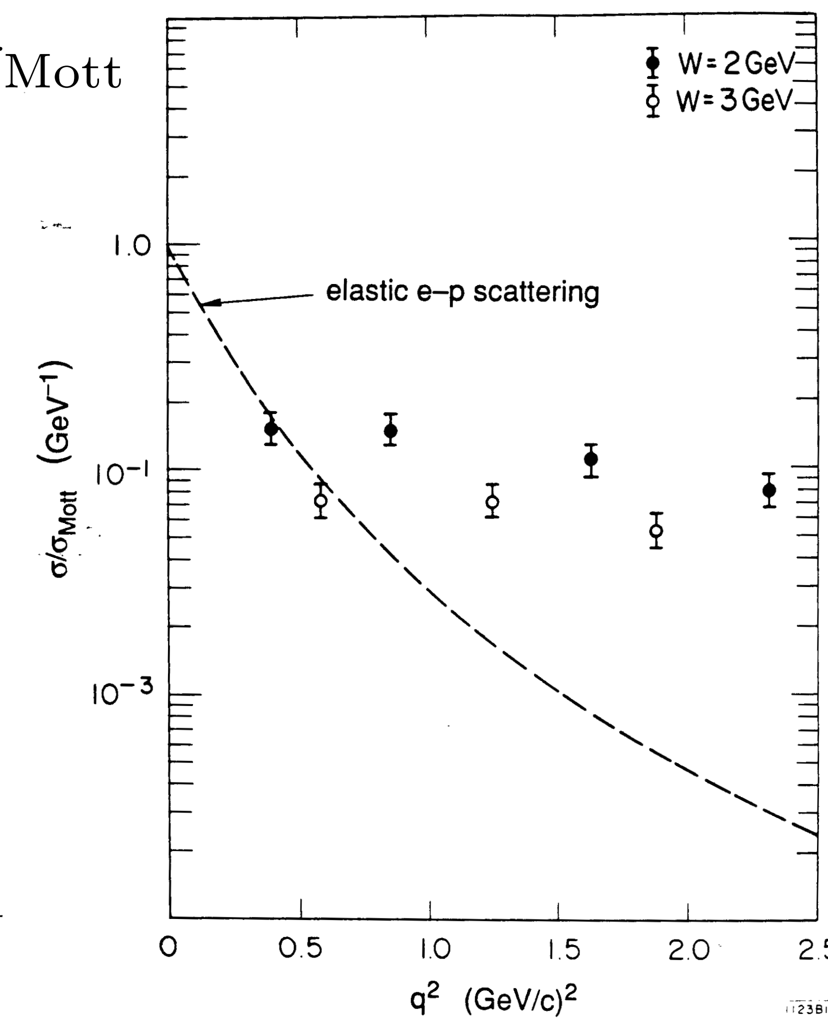

$Q^2 = -q^2$:resolving power of interaction

Feynman-Bjorken scaling: existence of partons

Inelastic scattering off proton → Elastic scattering off parton (quark)

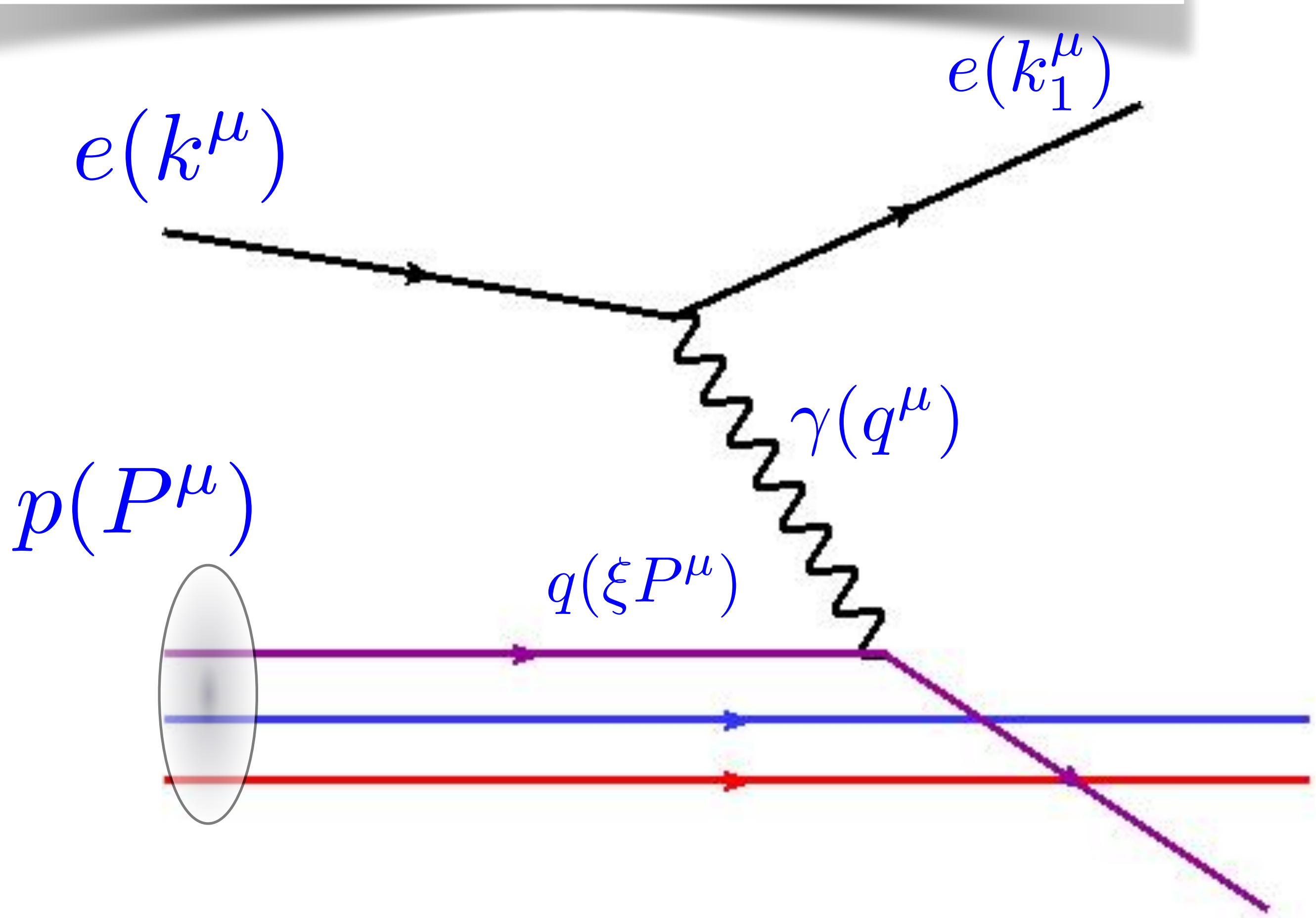

$$Q^2 = -q^2$$ Photon virtuality : resolving power

$$x = \frac{Q^2}{2P\cdot q} \simeq \frac{Q^2}{Q^2+W^2}$$ Bjorken x

$$W^2 = (p+q)^2$$ total energy of photon-proton system

$$s = (p+k)^2$$ total cms energy

x has the interpretation of the longitudinal momentum fraction of the proton carried by the struck quark (in the frame where proton is fast) $x \simeq \xi$

DIS: structure functions

Inclusive DIS cross section for $lp \to lX$ (l charged lepton, $Q^2 \ll M_Z^2$, $s \gg M_p^2$)

$$\frac{d^2\sigma}{dx dQ^2} = \frac{2\pi\alpha_{\rm em}^2}{Q^4 x}\left[\left(1+(1-y)^2\right)F_2(x,Q^2) - y^2 F_L(x,Q^2)\right]$$

structure functions

$$y = \frac{p\cdot q}{p\cdot k} = Q^2/(sx)$$ inelasticity

Structure functions encode all the information about the **proton(hadron) structure**

$$F_T(x,Q^2) = F_2(x,Q^2) - F_L(x,Q^2)$$ transversely polarized photons

$$F_L(x,Q^2)$$ longitudinally polarized photons

Often experiments give **reduced cross section**

$$Y_+ = 1 + (1-y)^2$$

$$\sigma_{r,NC} = \frac{d^2\sigma_{NC}}{dx dQ^2}\frac{Q^4 x}{2\pi\alpha_{\rm em} Y_+} = F_2 - \frac{y^2}{Y_+}F_L$$

Dominated by the F_2 structure function except for large y

Revealing proton structure

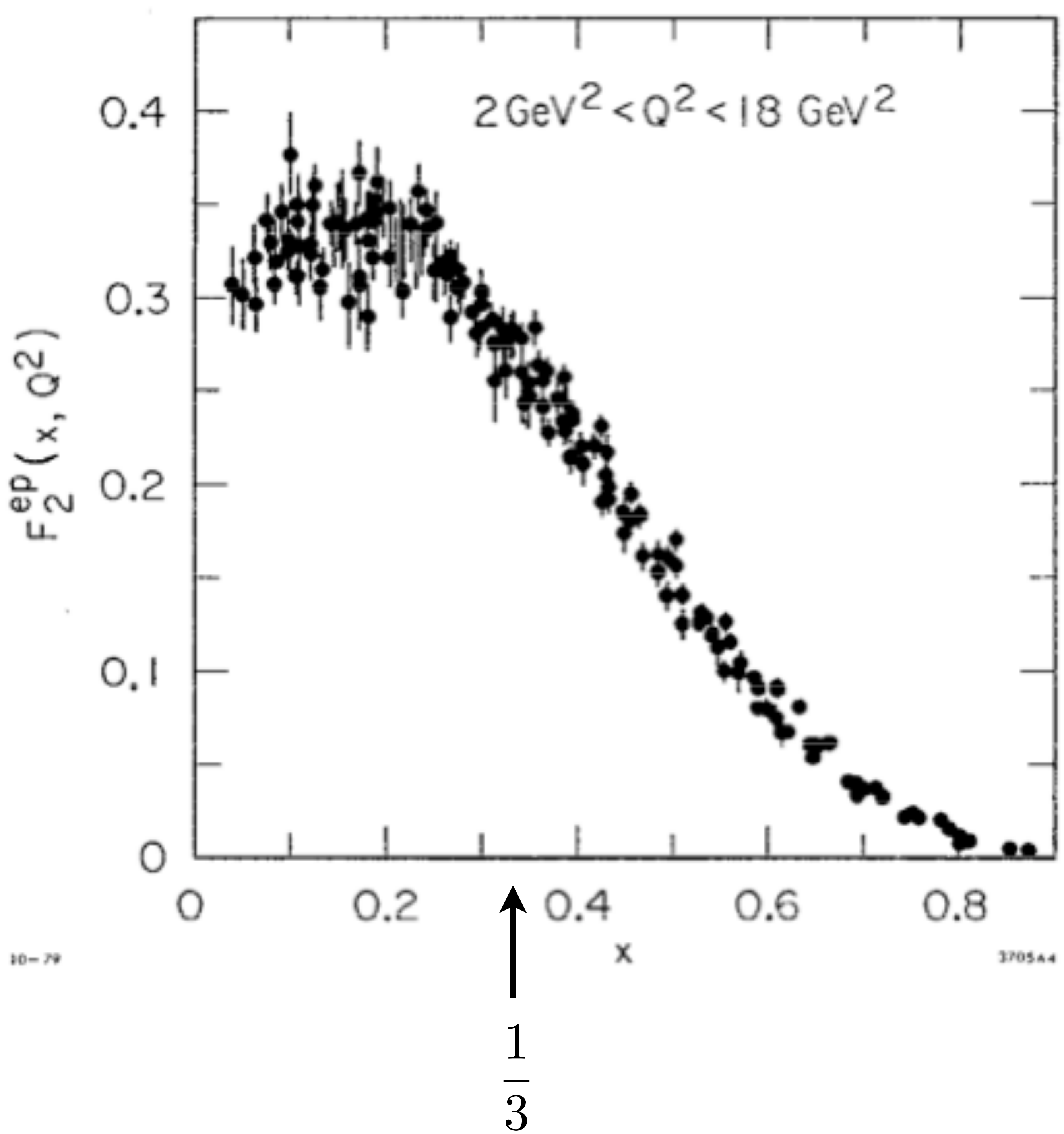

Measured cross section

Momentum distribution of partons inside the proton

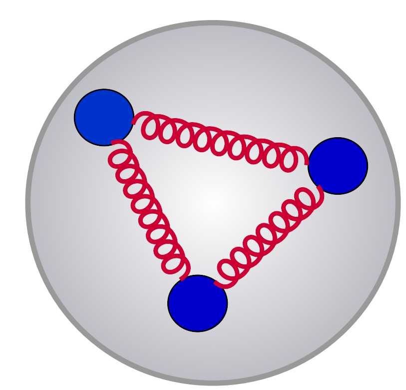

Exploring proton structure at high energy

DESY - Hamburg
HERA Collider
1992-2007

The only electron(positron)-proton collider ever built

Center of mass energy:

$$E_{\mathrm{cm}} = 320\ \mathrm{GeV}$$

equivalent to 50 TeV electron beam on a fixed proton target...about 2500 times more than at SLAC

Measurements of proton structure function

low energy

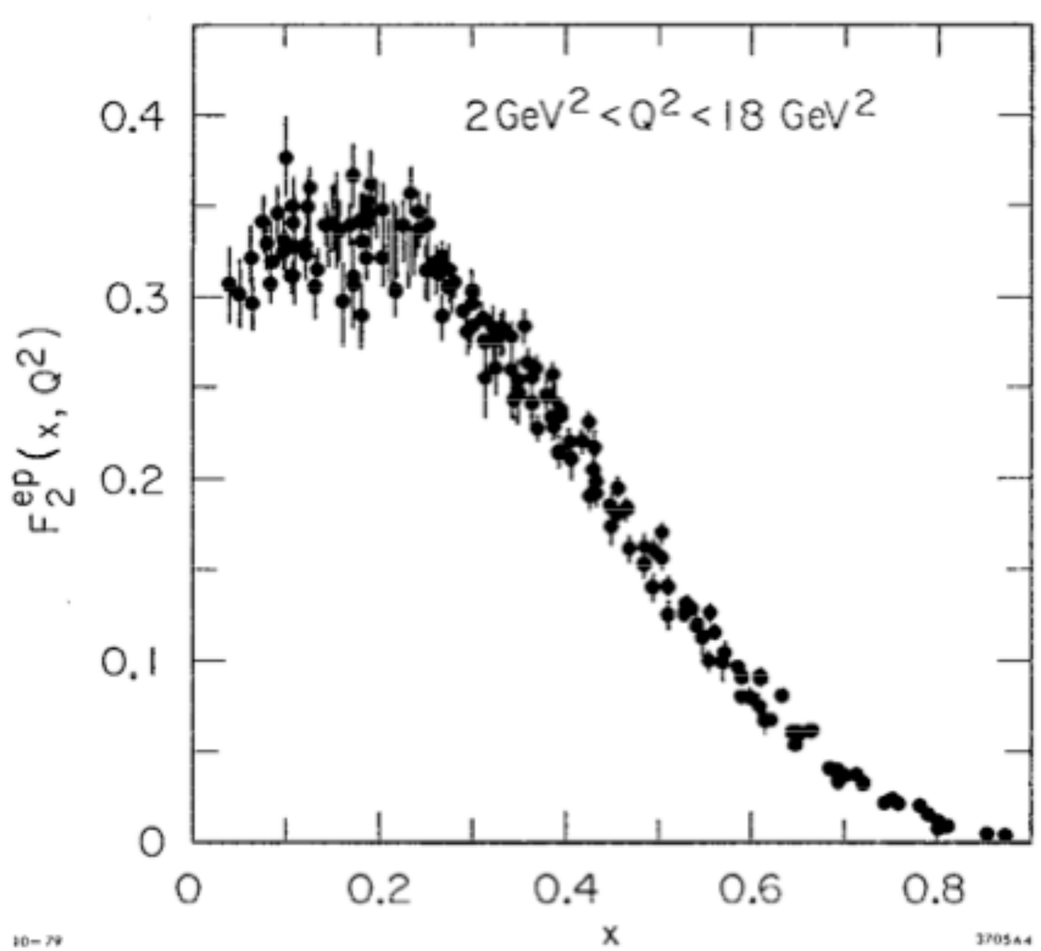

high energy

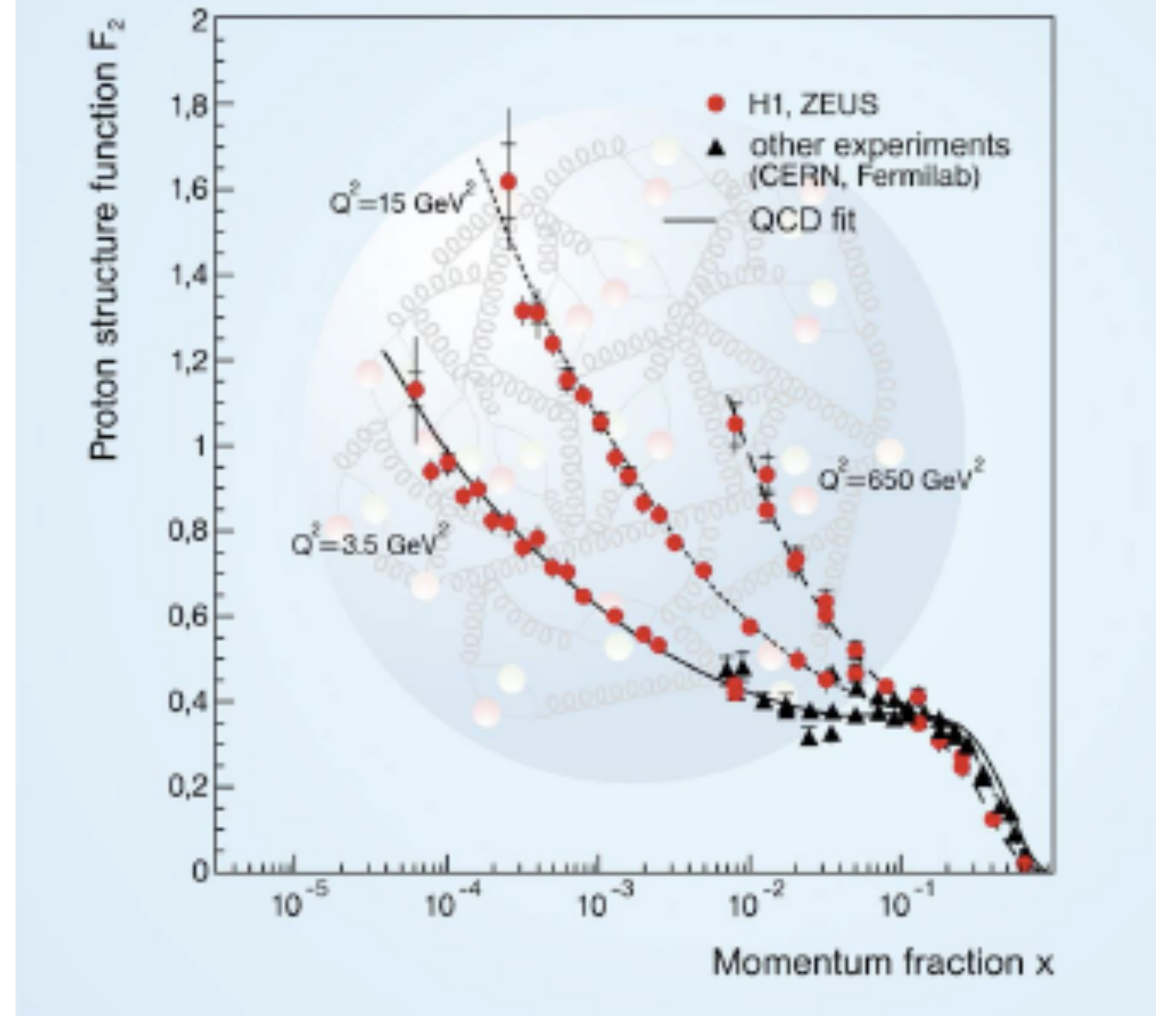

Measurements of proton structure function

low energy

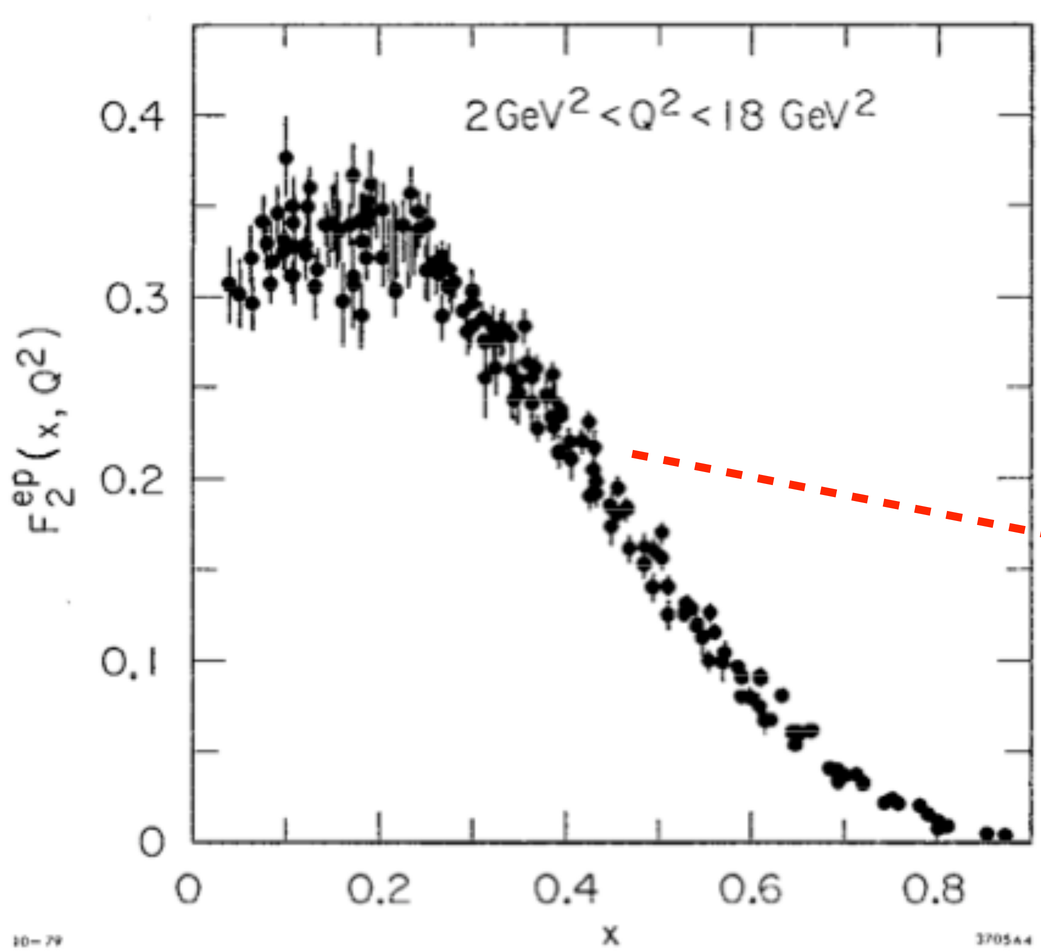

high energy

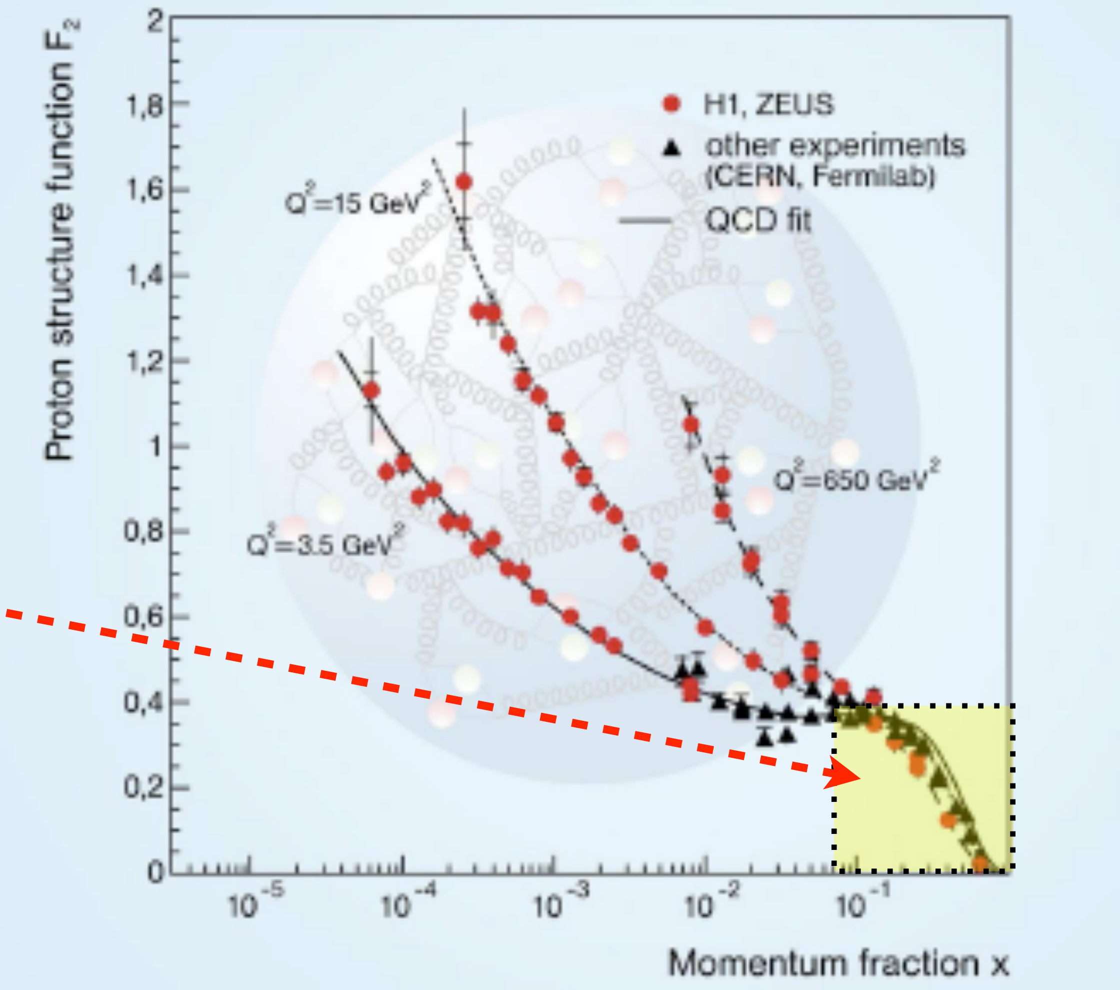

Measurements of proton structure function

low energy

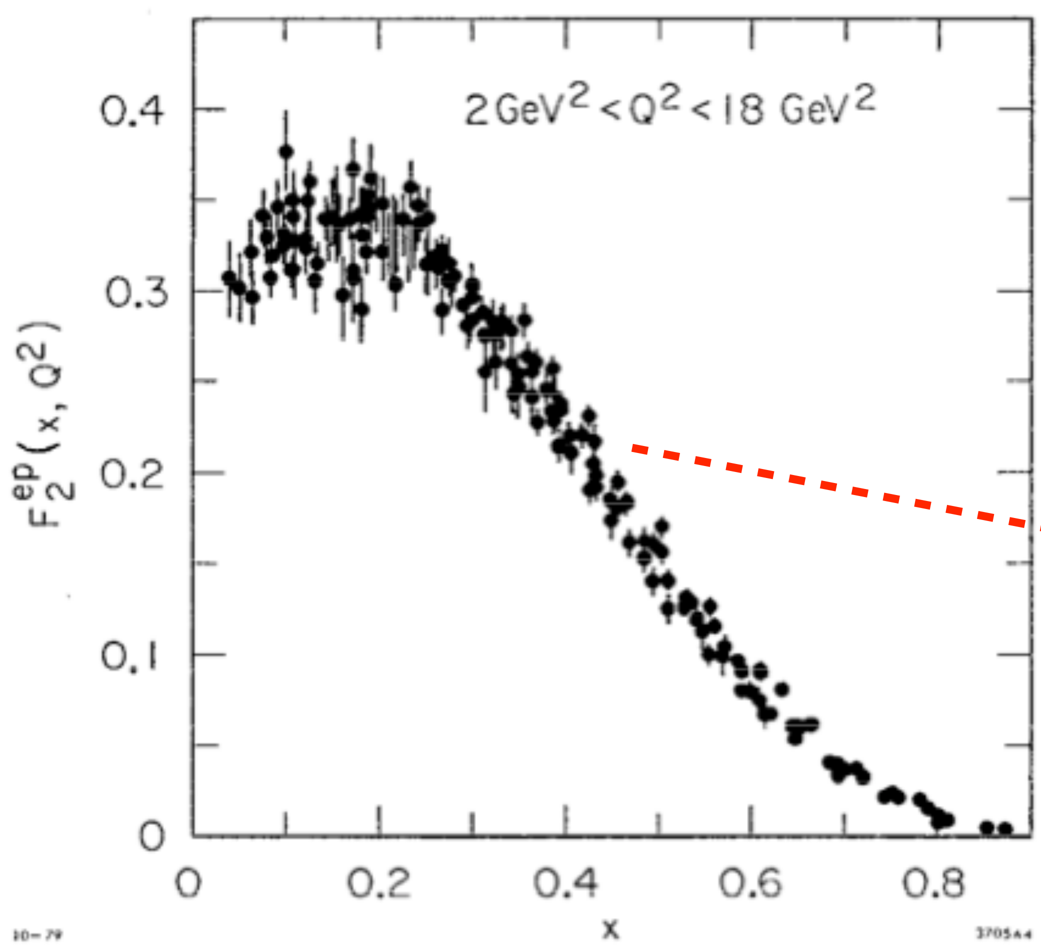

high energy

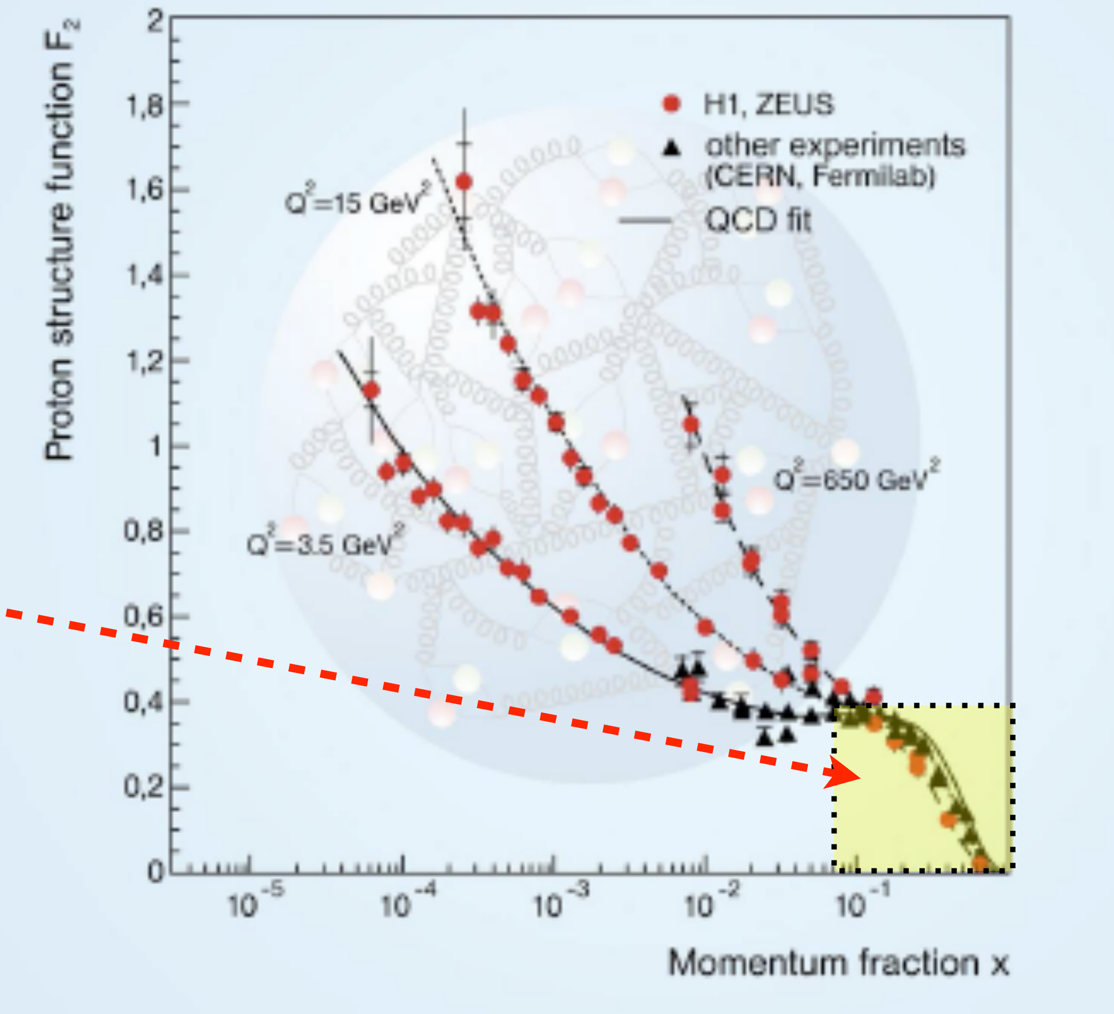

Cross section and that means parton density increases:

- with decreasing x
- with increasing scale Q

Measurements of proton structure function

low energy

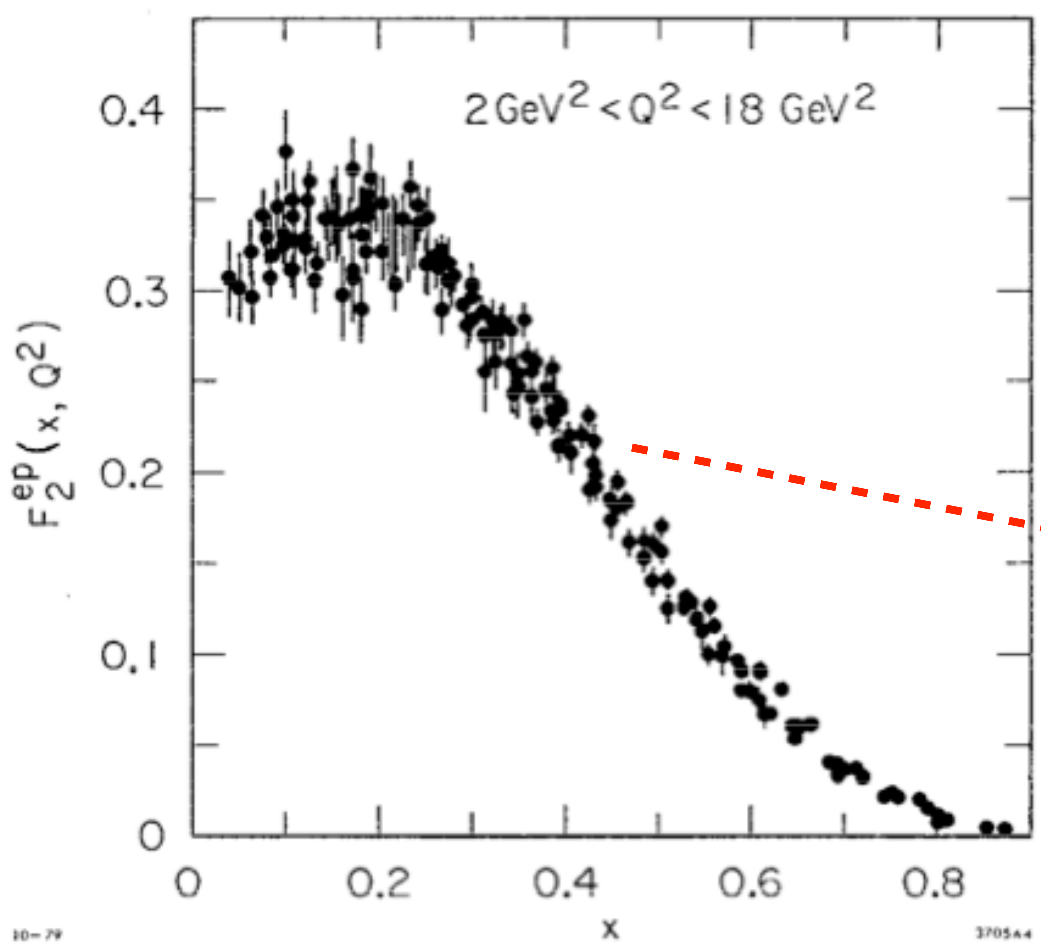

high energy

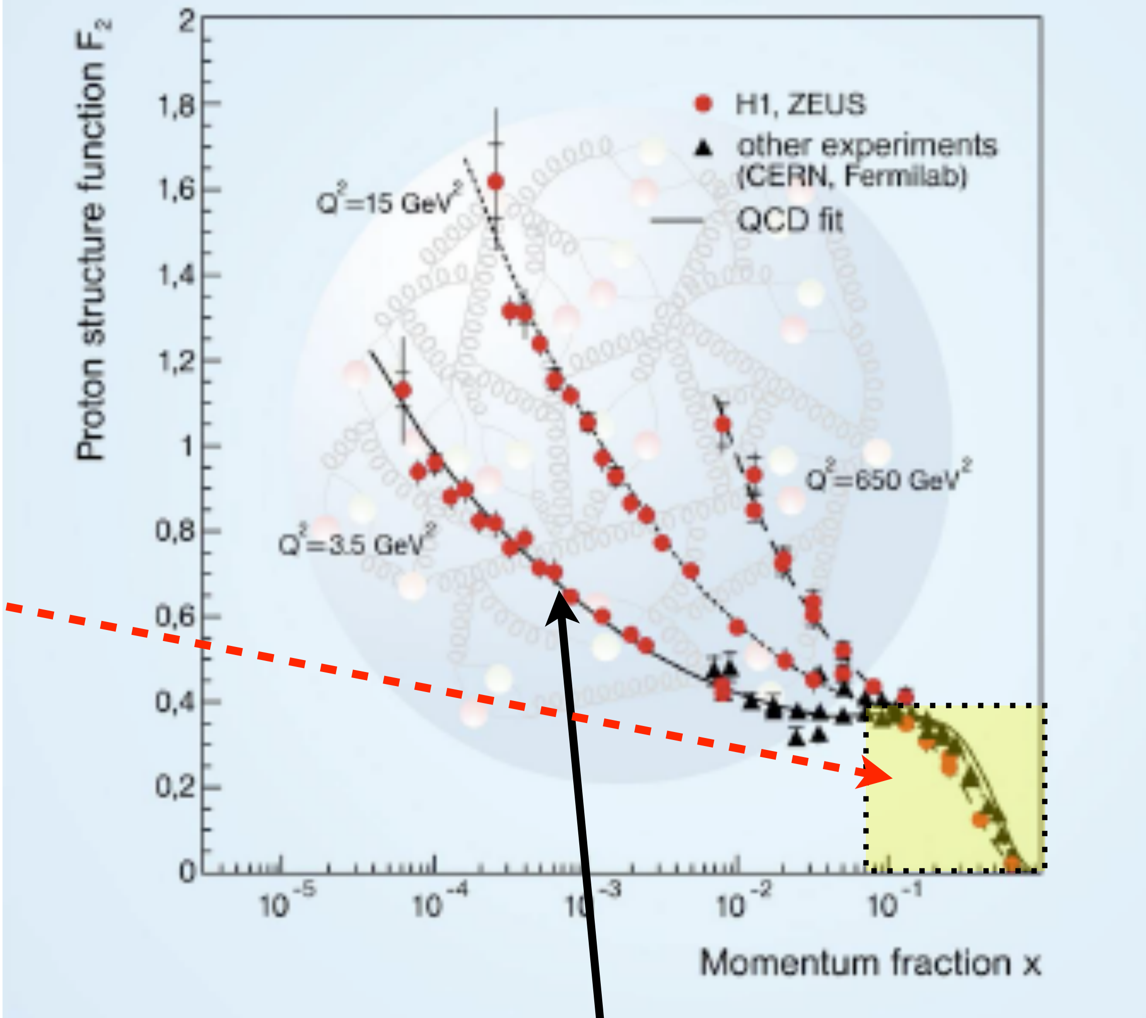

Cross section and that means parton density increases:

- with decreasing x
- with increasing scale Q

Where does this rise come from?

Answer: QCD radiation

Parton model

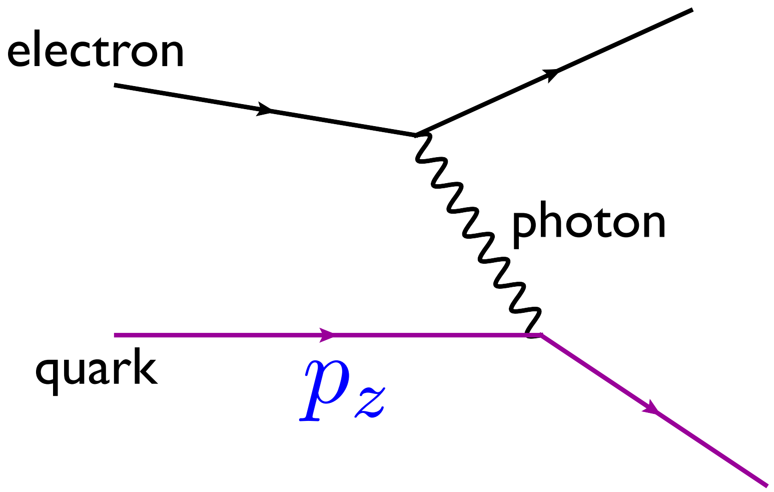

Parton model

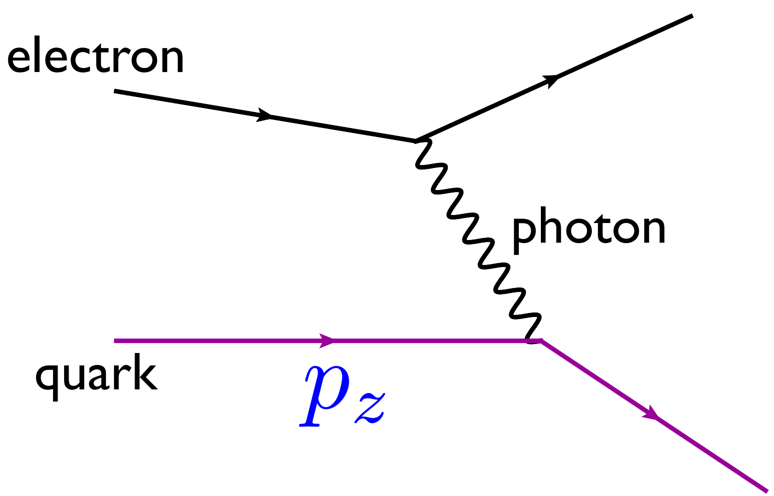

QCD radiation

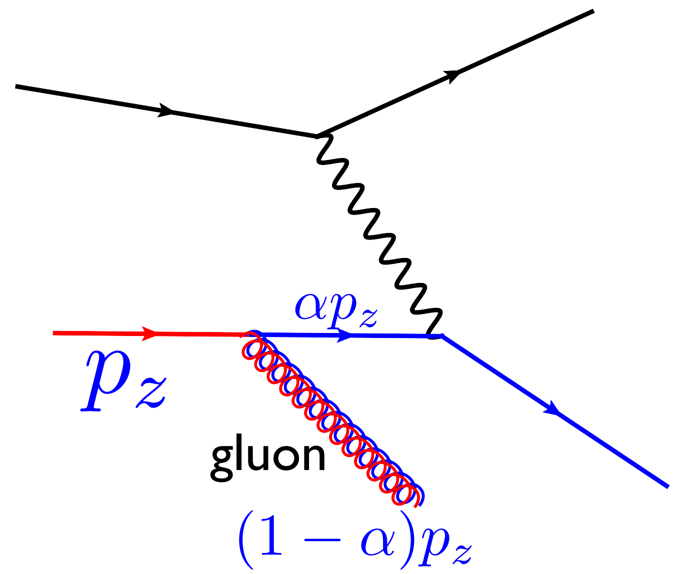

Parton model

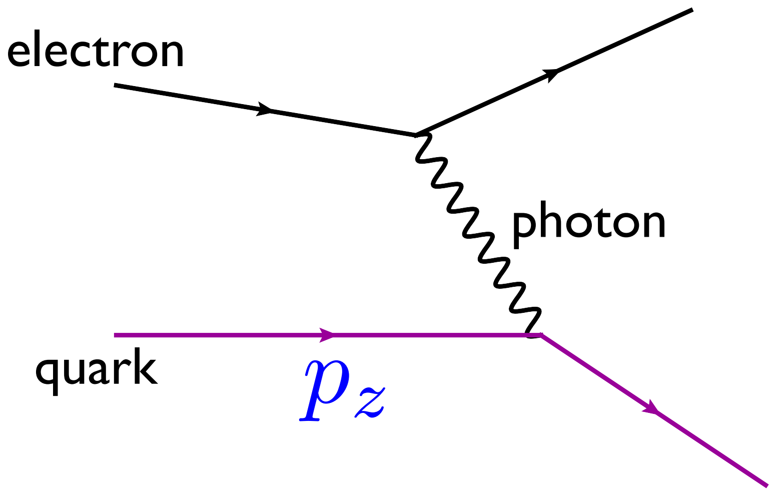

QCD radiation

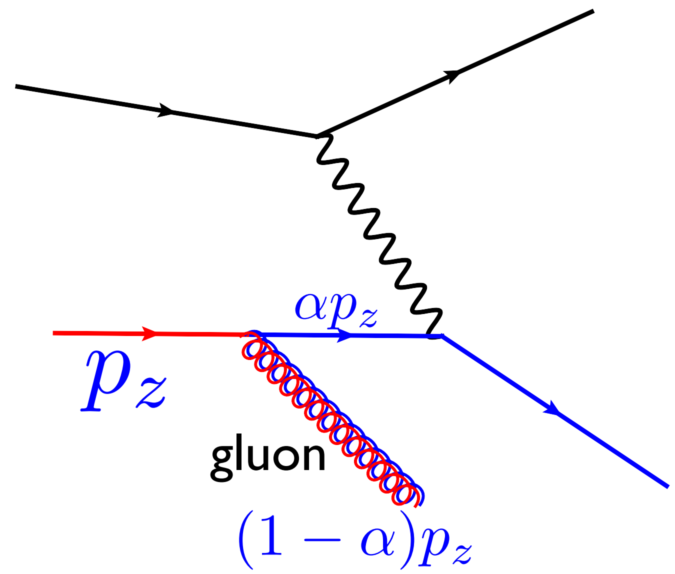

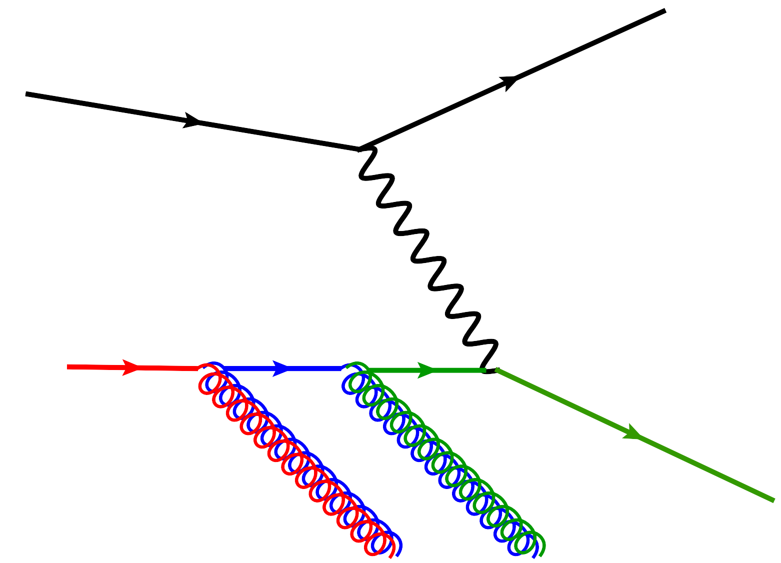

Parton model

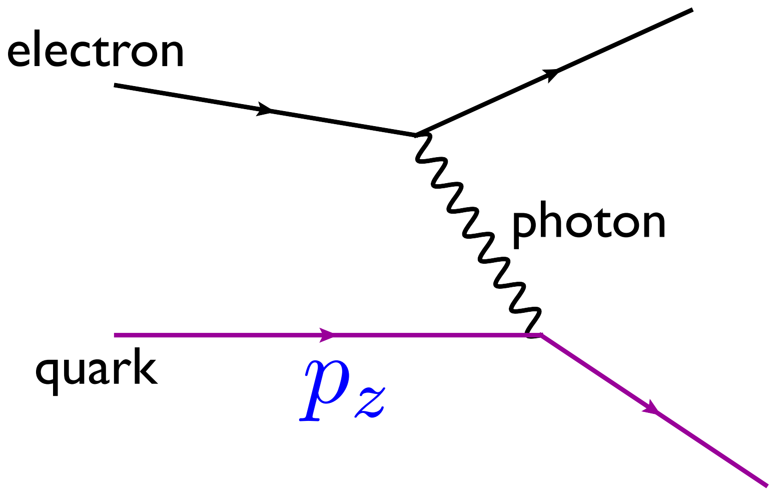

QCD radiation

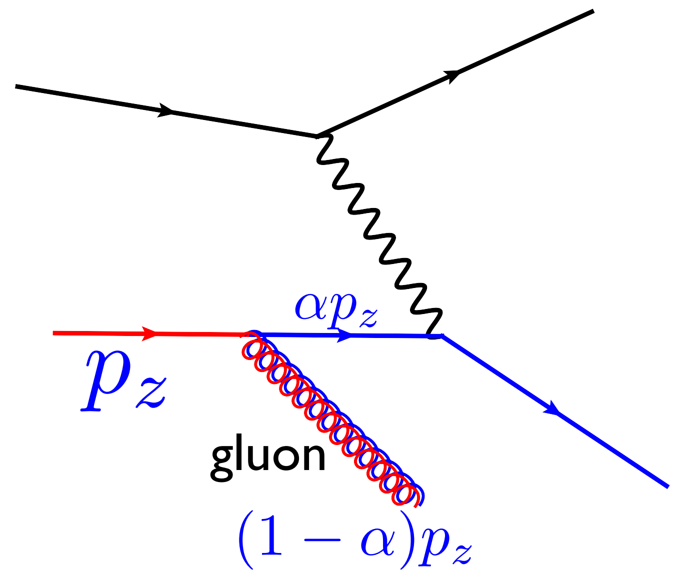

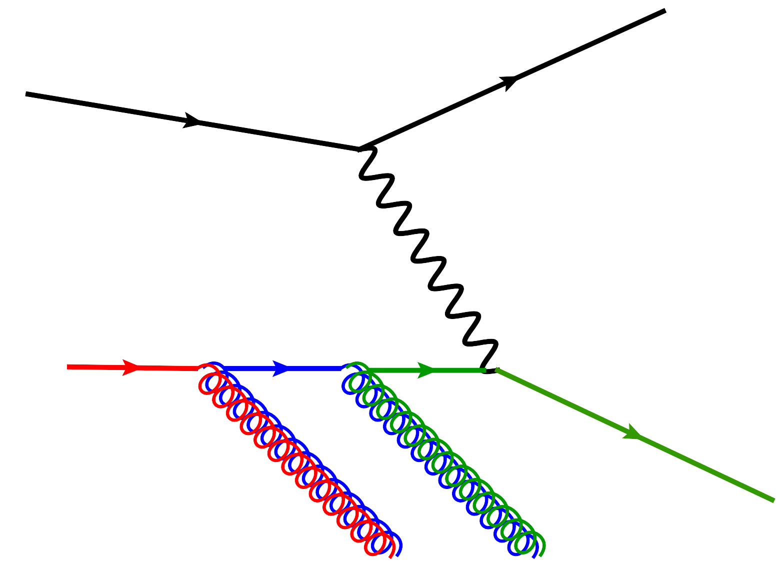

Pair production of sea quarks

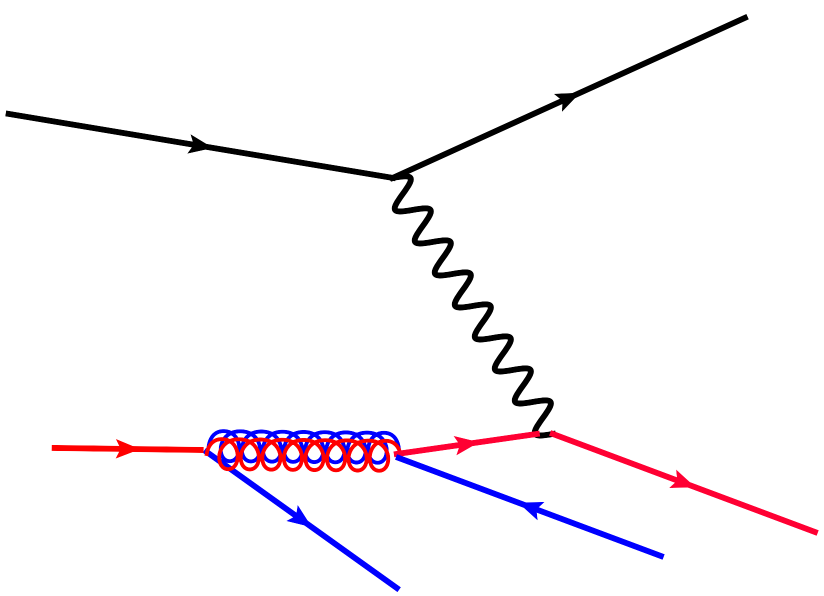

Parton model

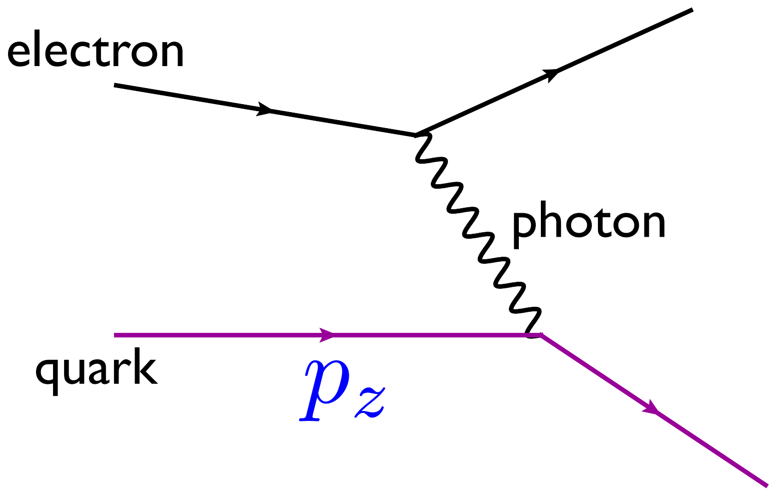

QCD radiation

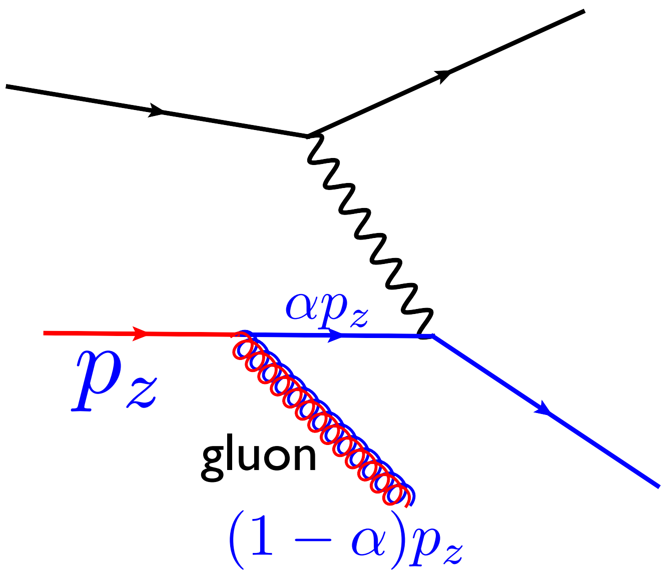

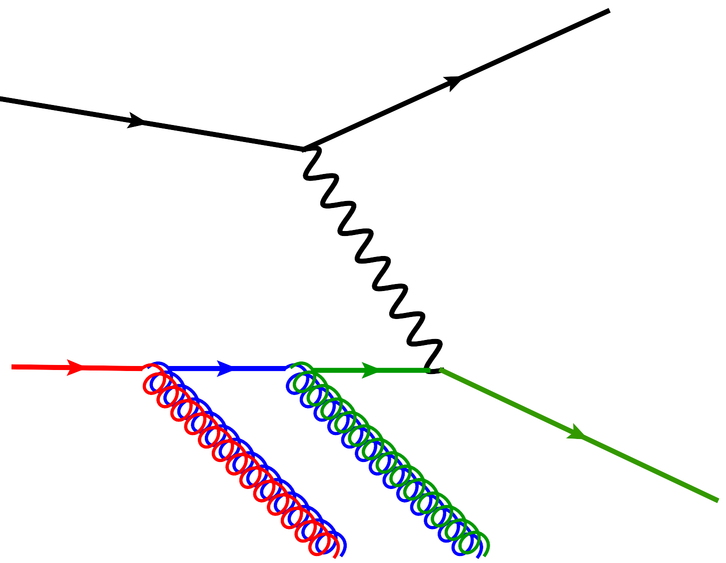

Pair production of sea quarks

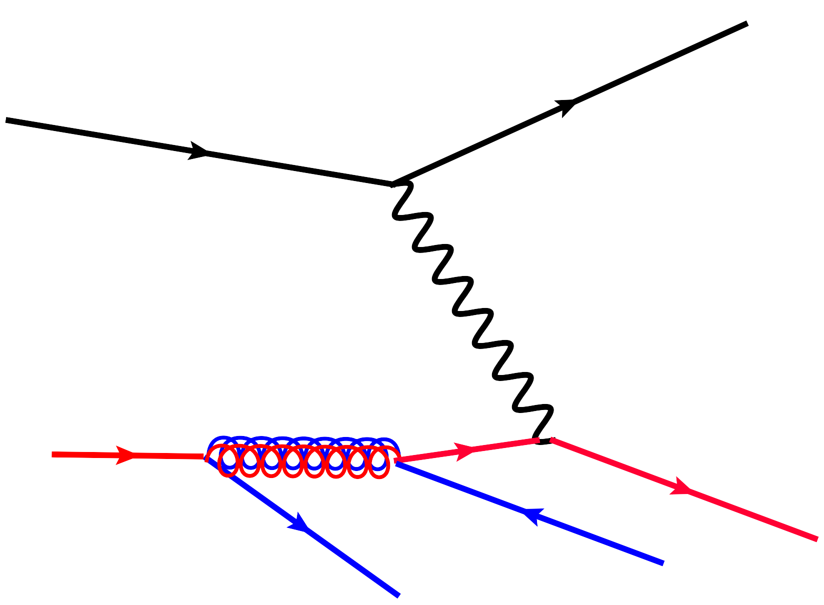

Gluon splitting

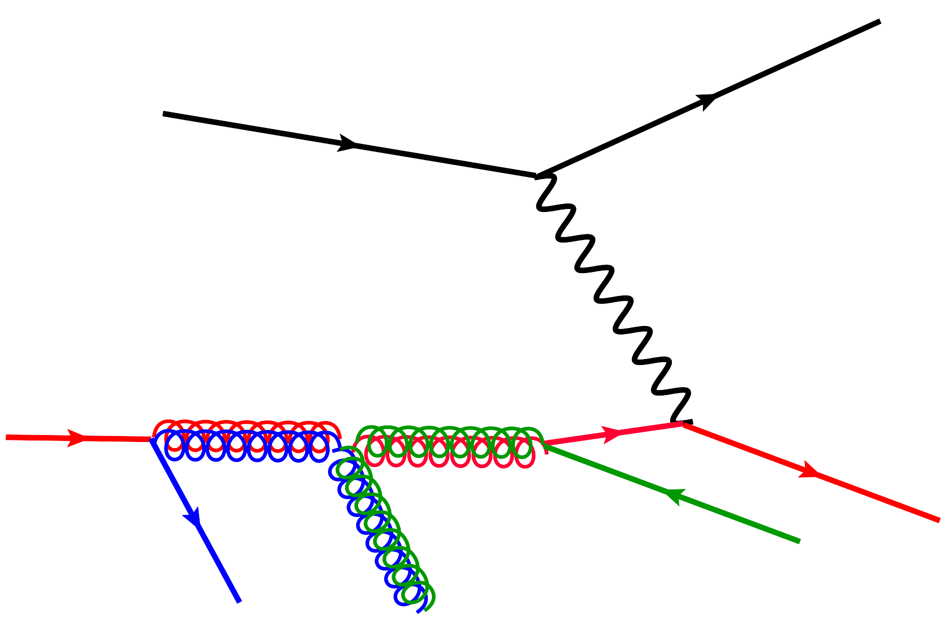

Parton model

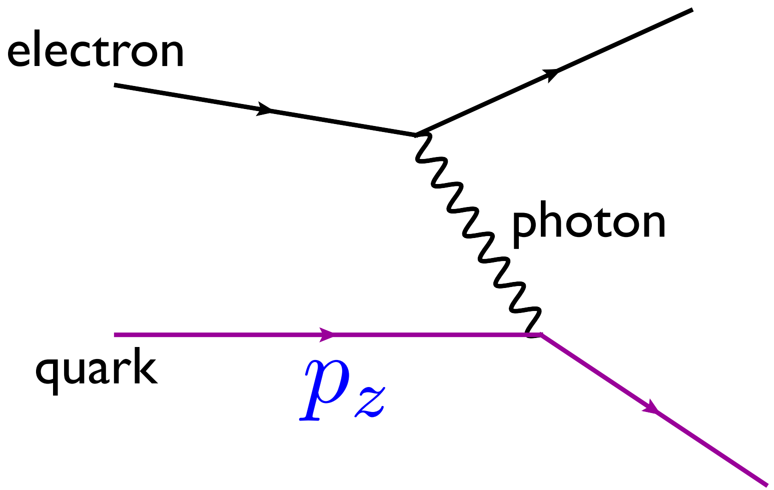

QCD radiation

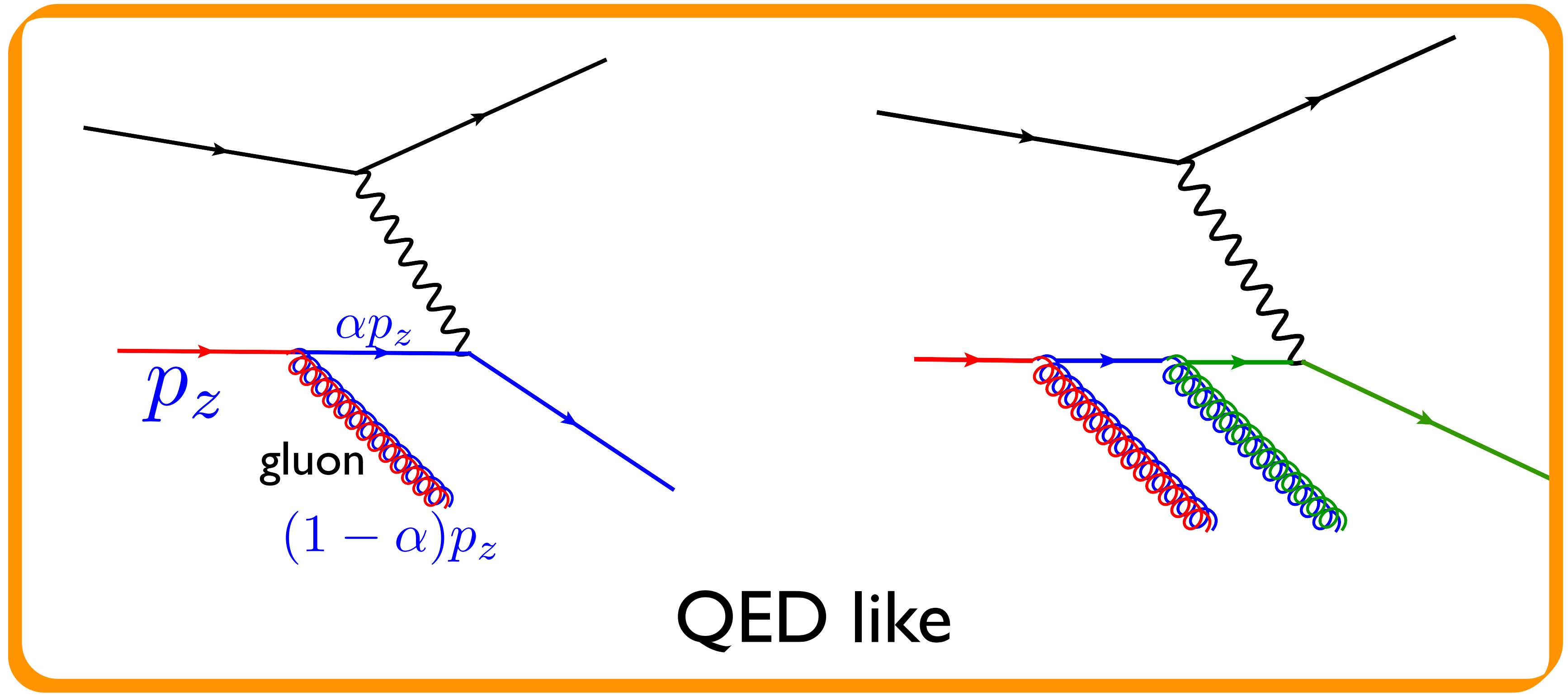

Pair production of sea quarks

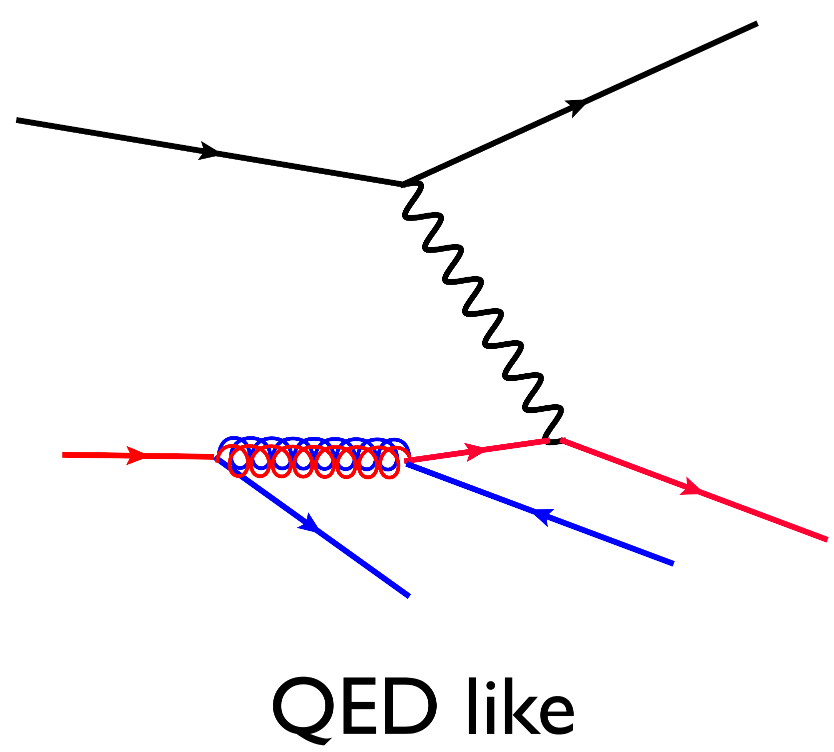

Gluon splitting

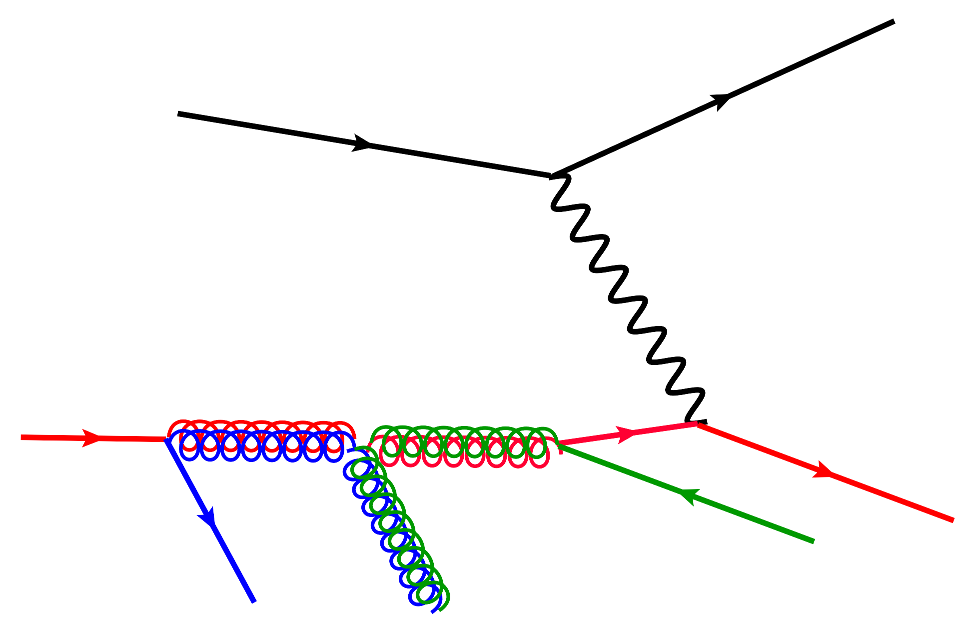

Parton model

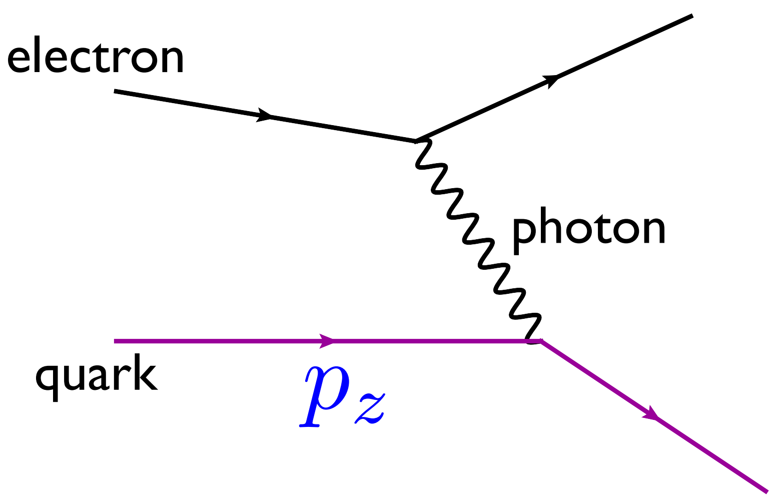

QCD radiation

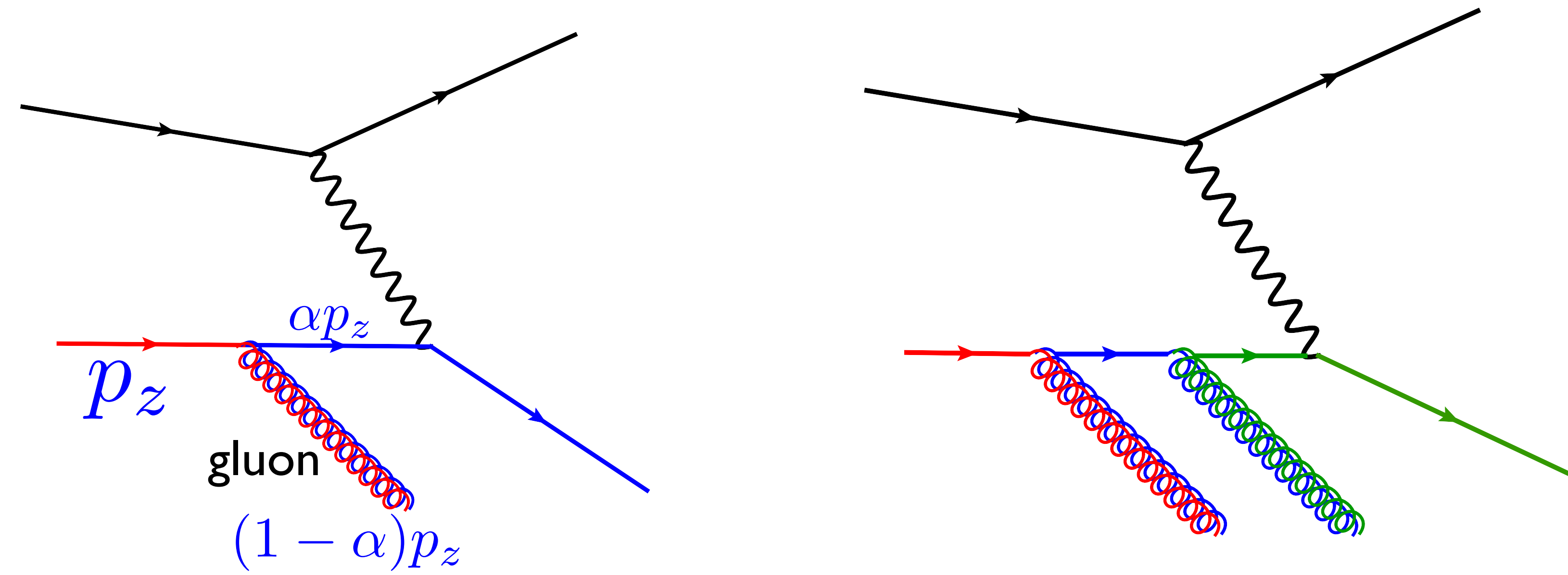

QED like

Pair production of sea quarks

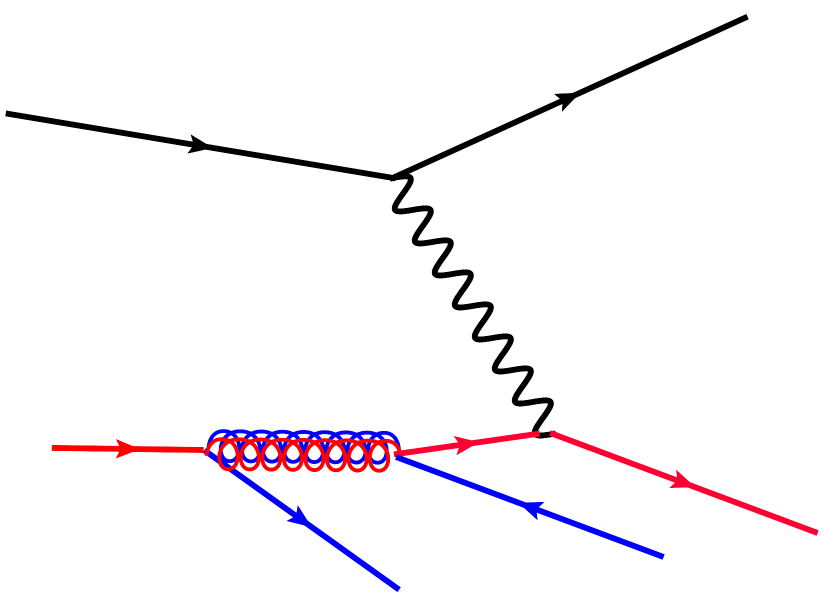

QED like

Gluon splitting

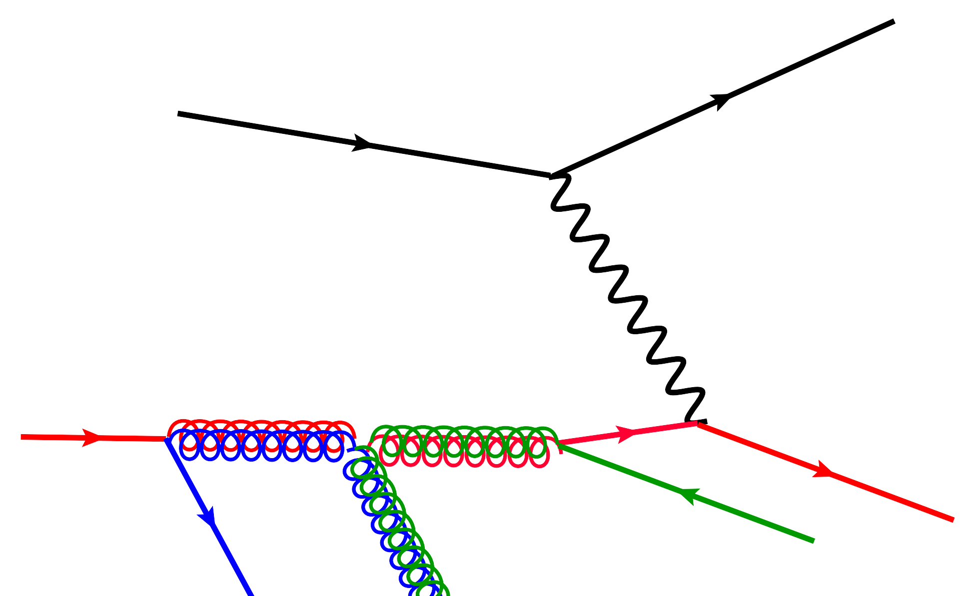

Unique to non-abelian theory

More gluons

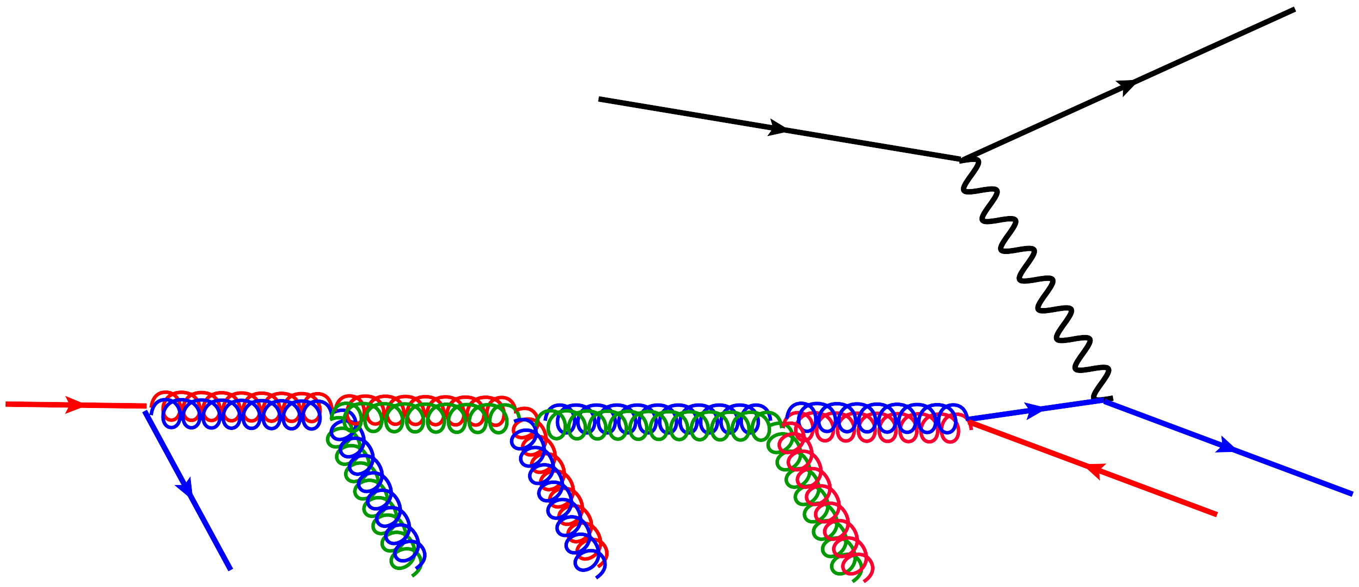

...and even more...

More gluons

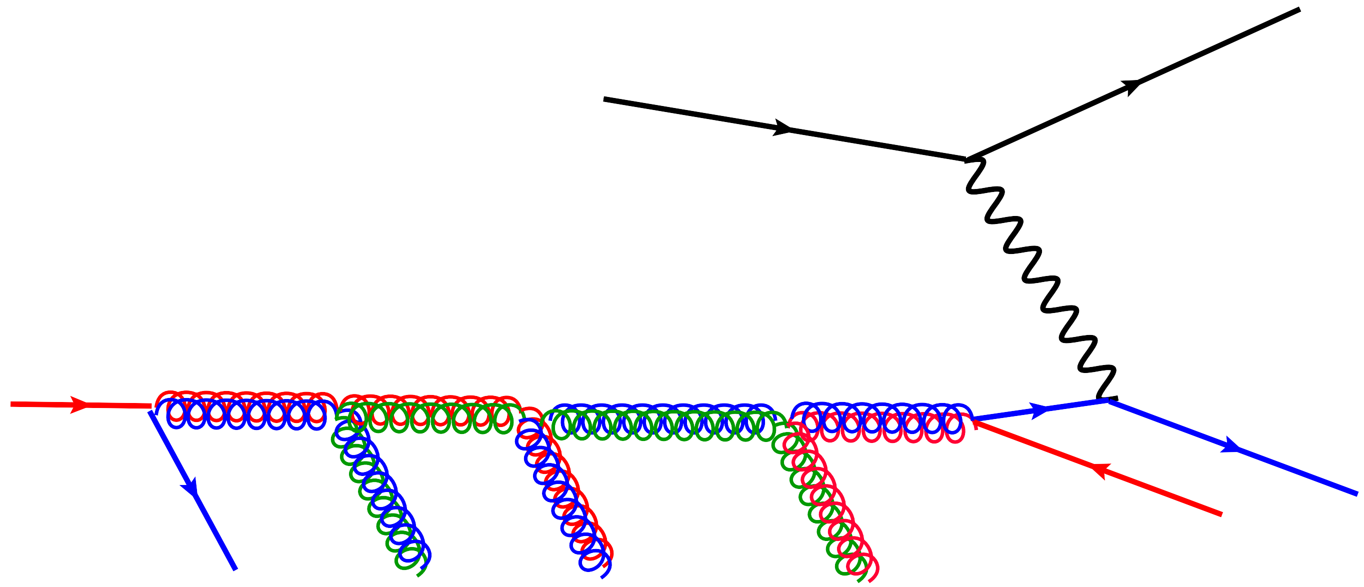

...and even more...

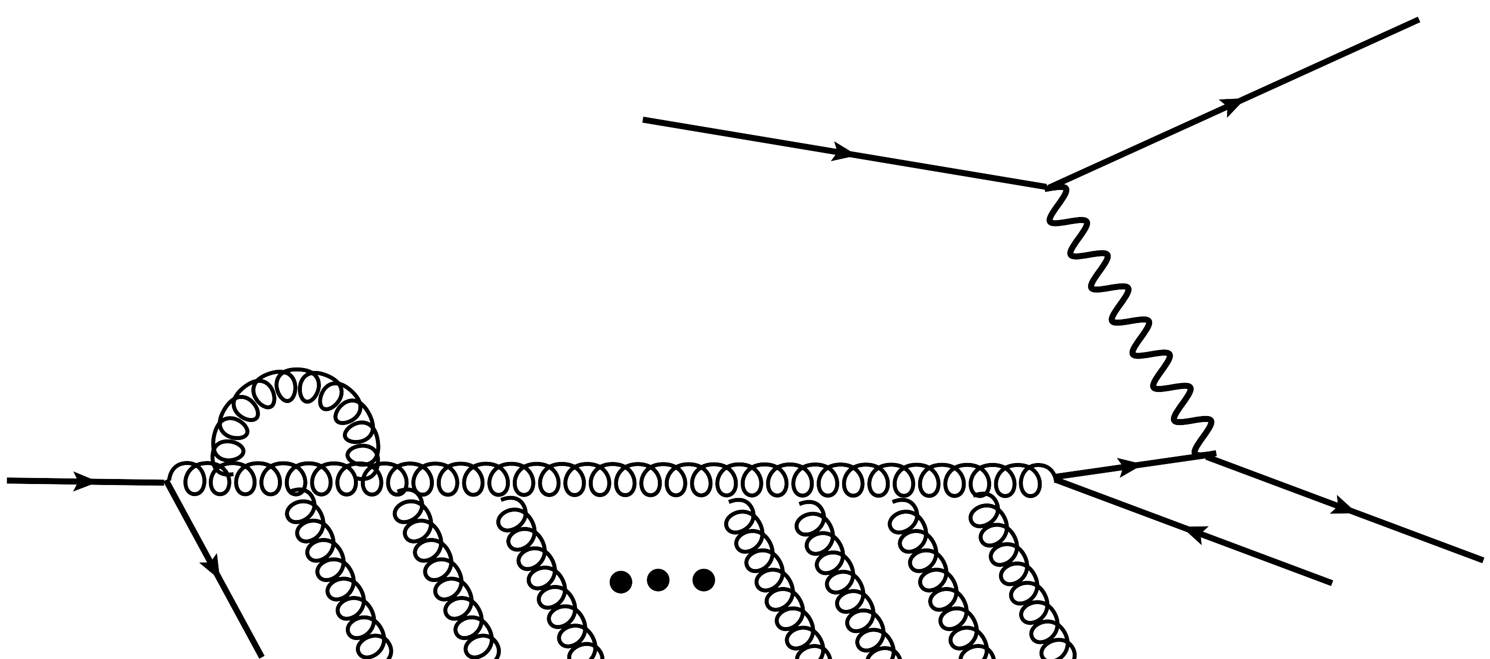

More gluons

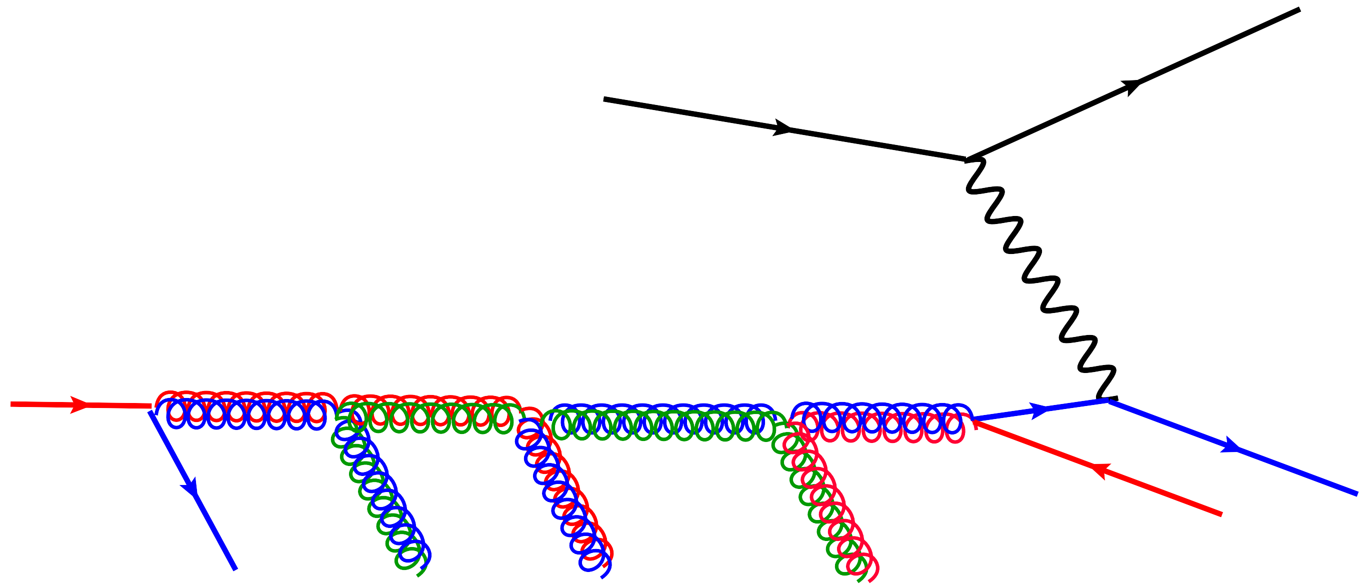

...and even more...

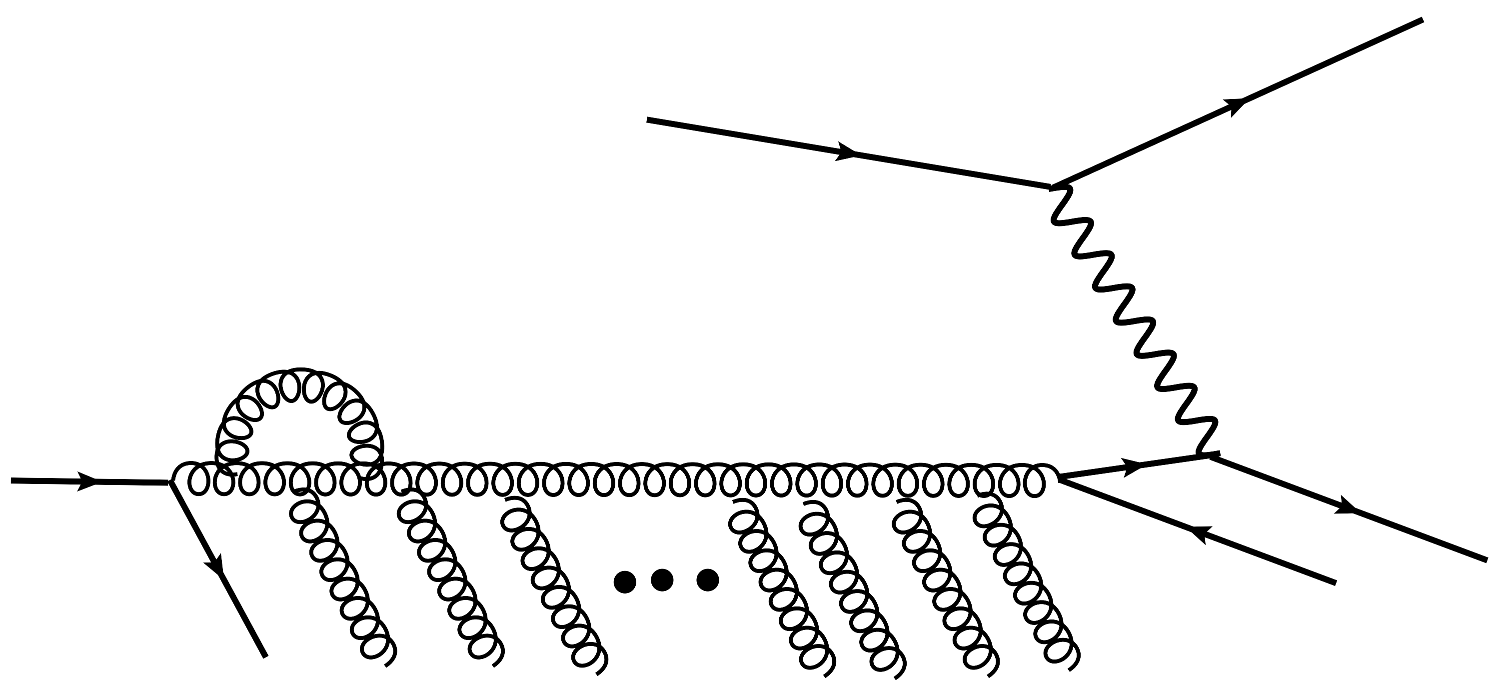

These emissions suppressed by powers of coupling constant but enhanced by large (kinematical) logarithms

Arbitrarily many gluon emissions

Cross section vs parton density

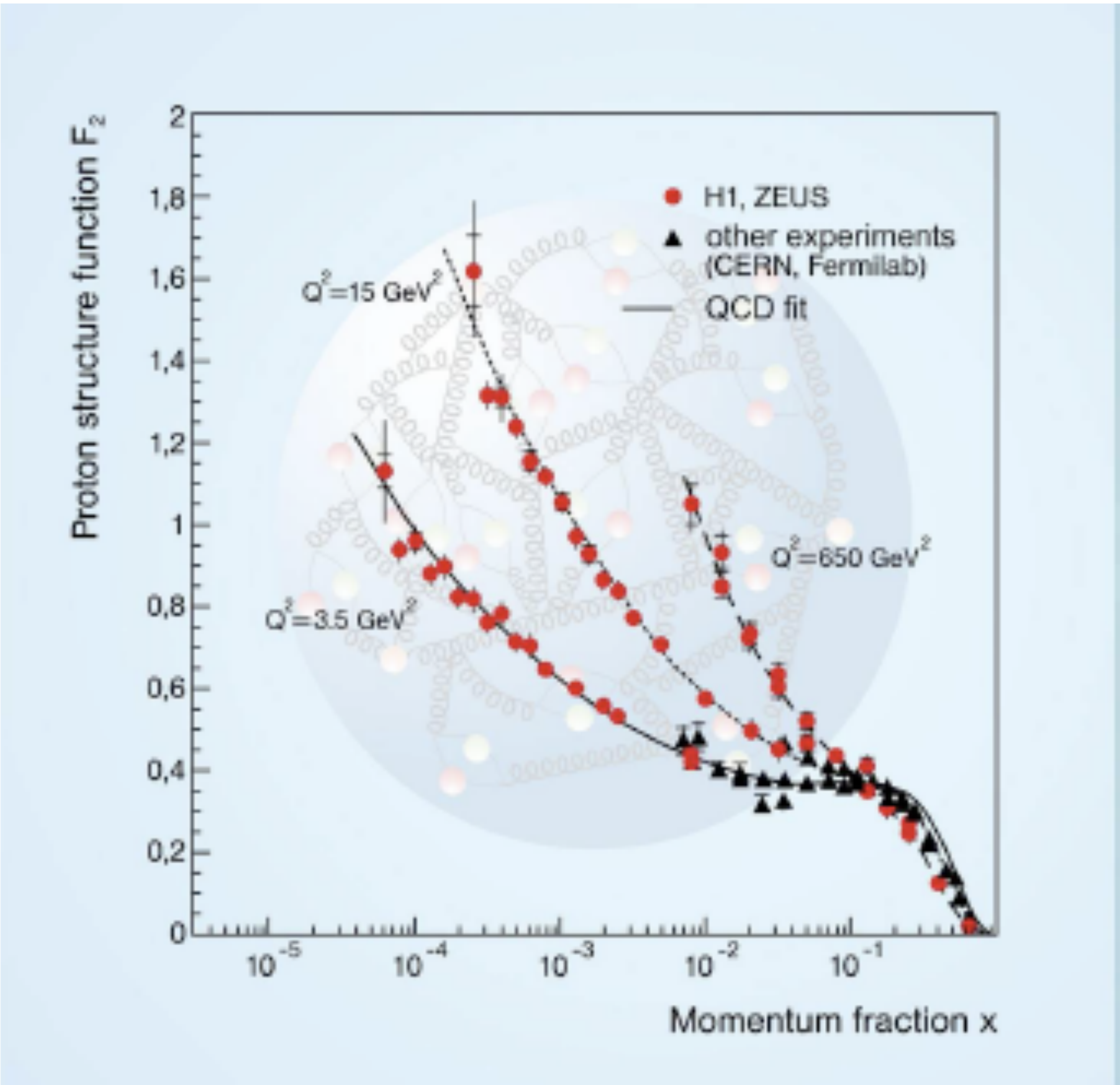

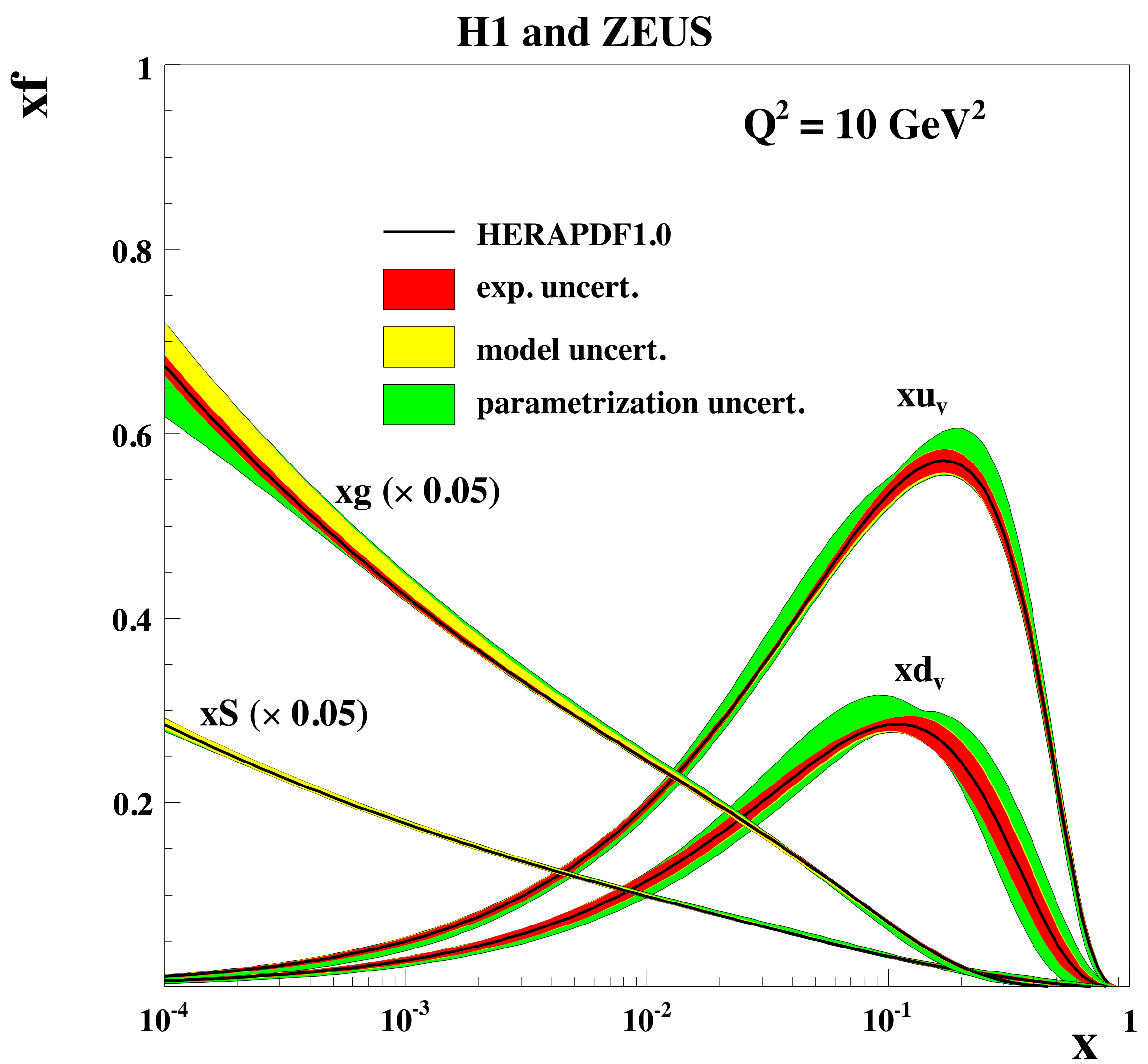

Data demonstrate the growth of the gluon and sea quark distributions with decreasing x

Parton densities

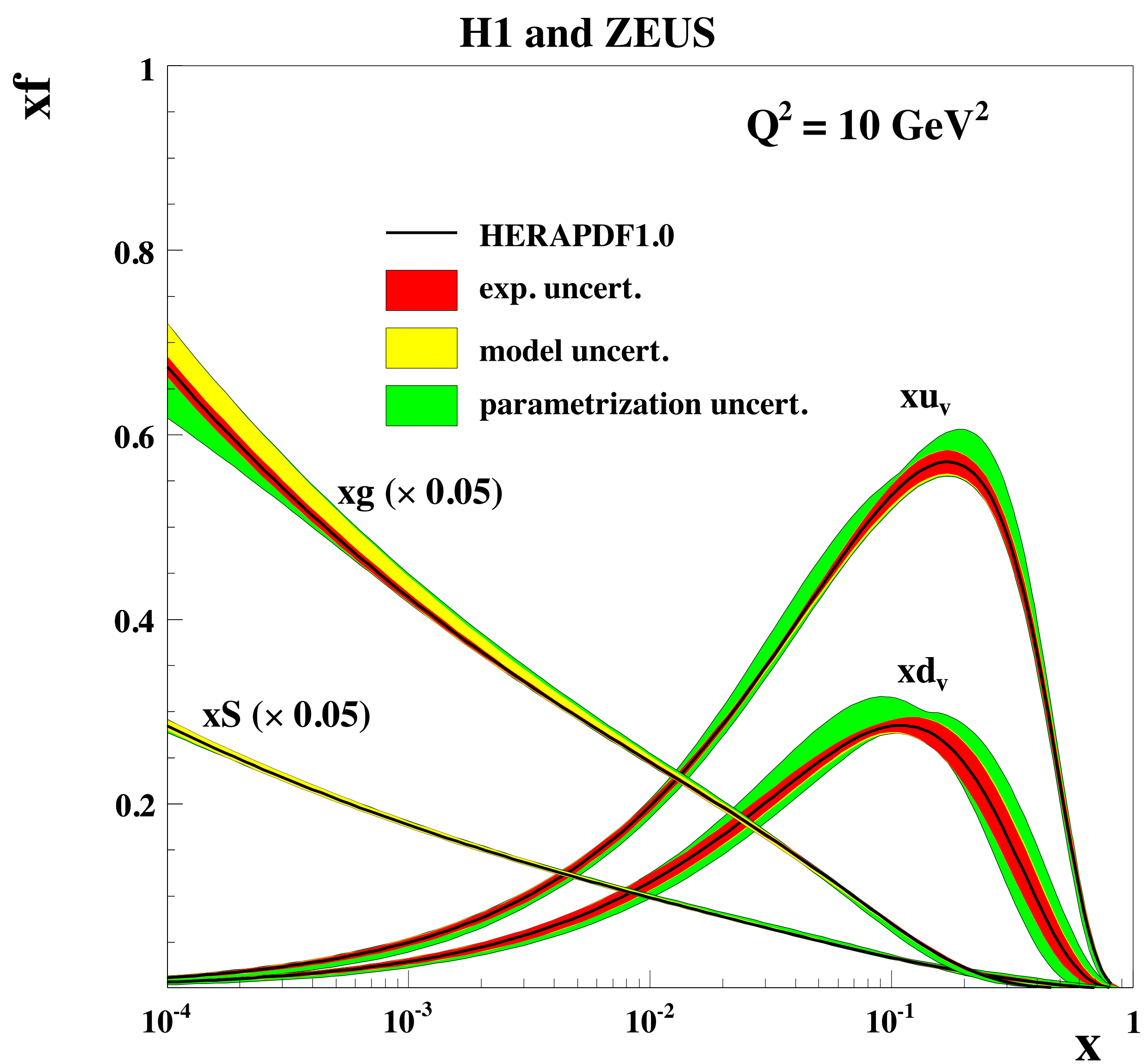

Gluon density increases rapidly with x and with Q

Gluons dominate over the quark density

Parton densities

valence quarks

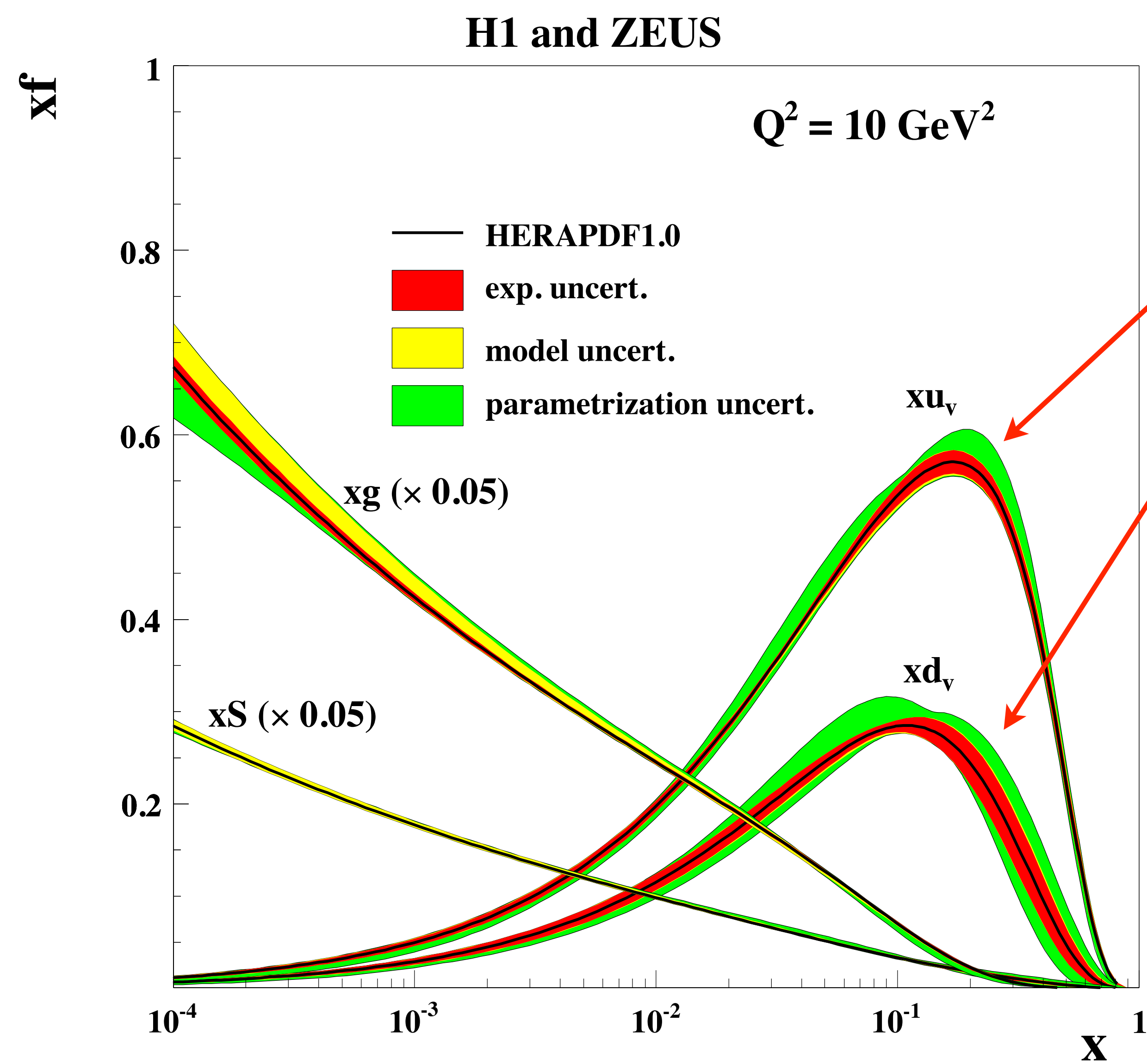

Gluon density increases rapidly with x and with Q

Gluons dominate over the quark density

Parton densities

gluons

valence quarks

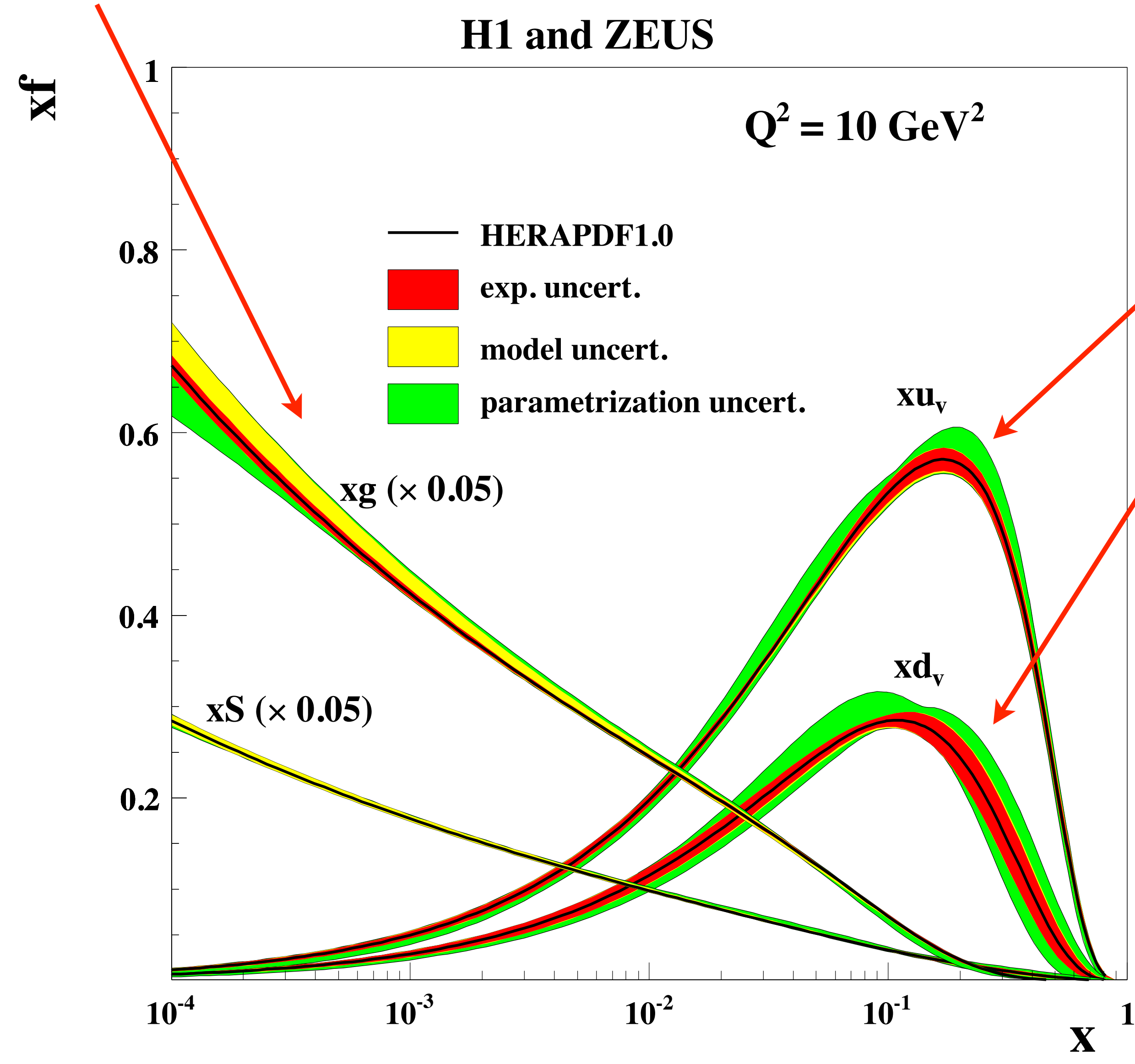

Gluon density increases rapidly with x and with Q

Gluons dominate over the quark density

Parton densities

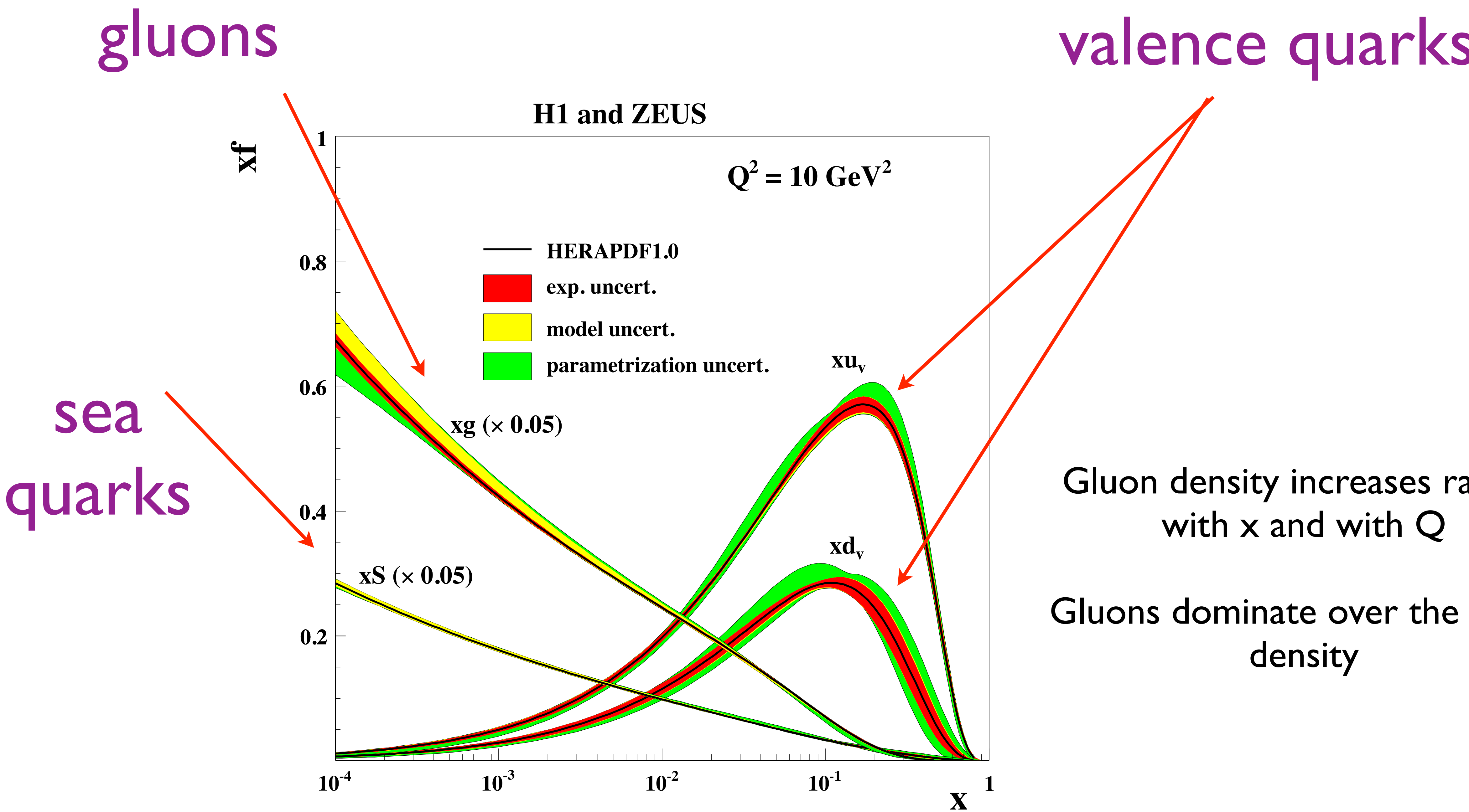

Gluon density increases rapidly with x and with Q

Gluons dominate over the quark density

Parton densities

gluons

valence quarks

sea quarks

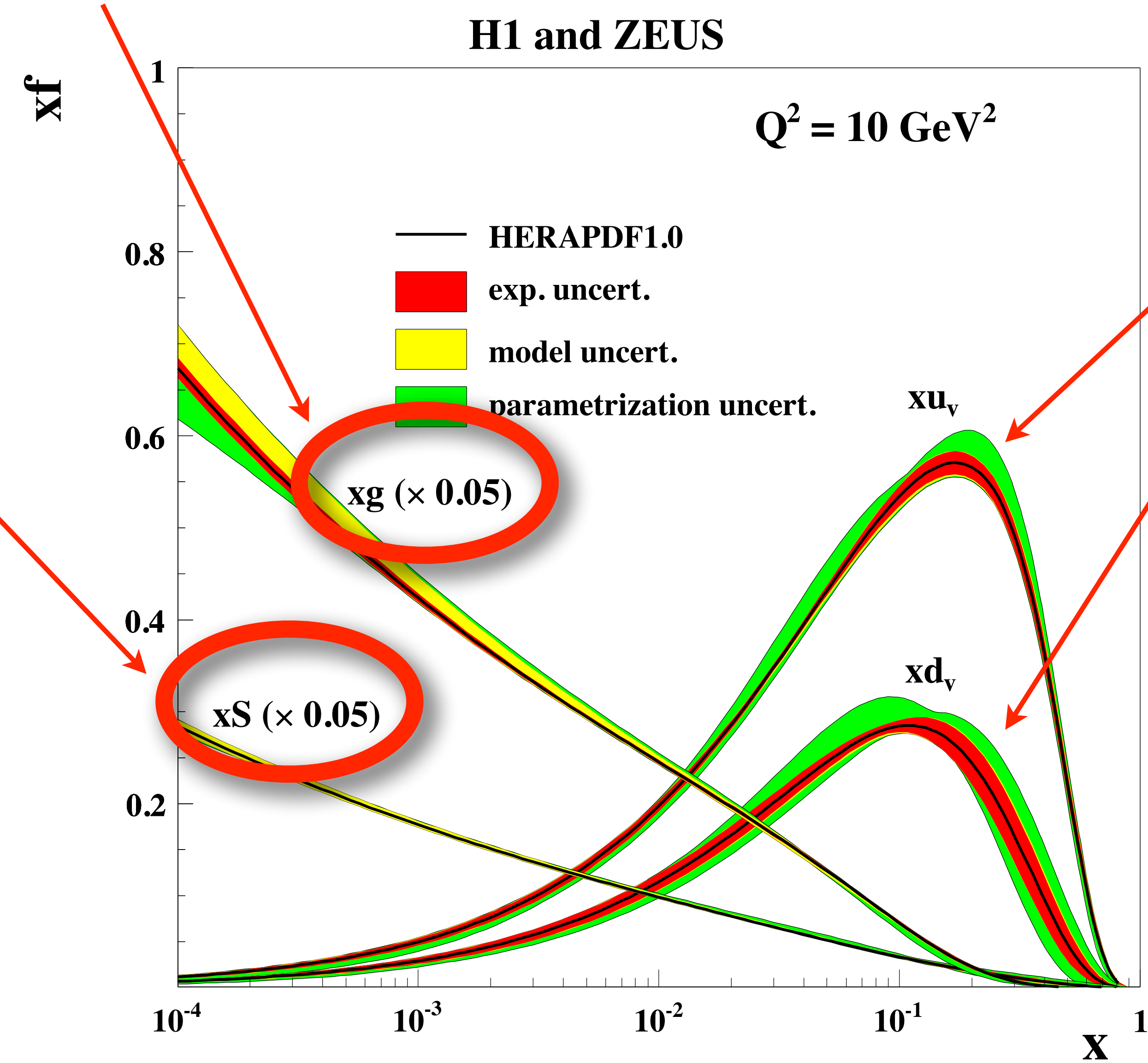

Gluon density increases rapidly with x and with Q

Gluons dominate over the quark density

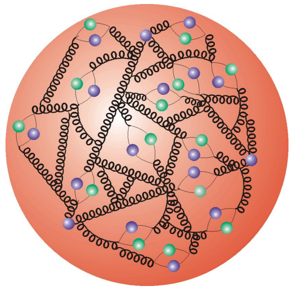

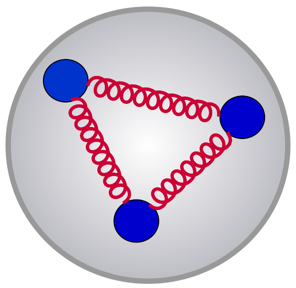

Parton densities

gluons

valence quarks

sea quarks

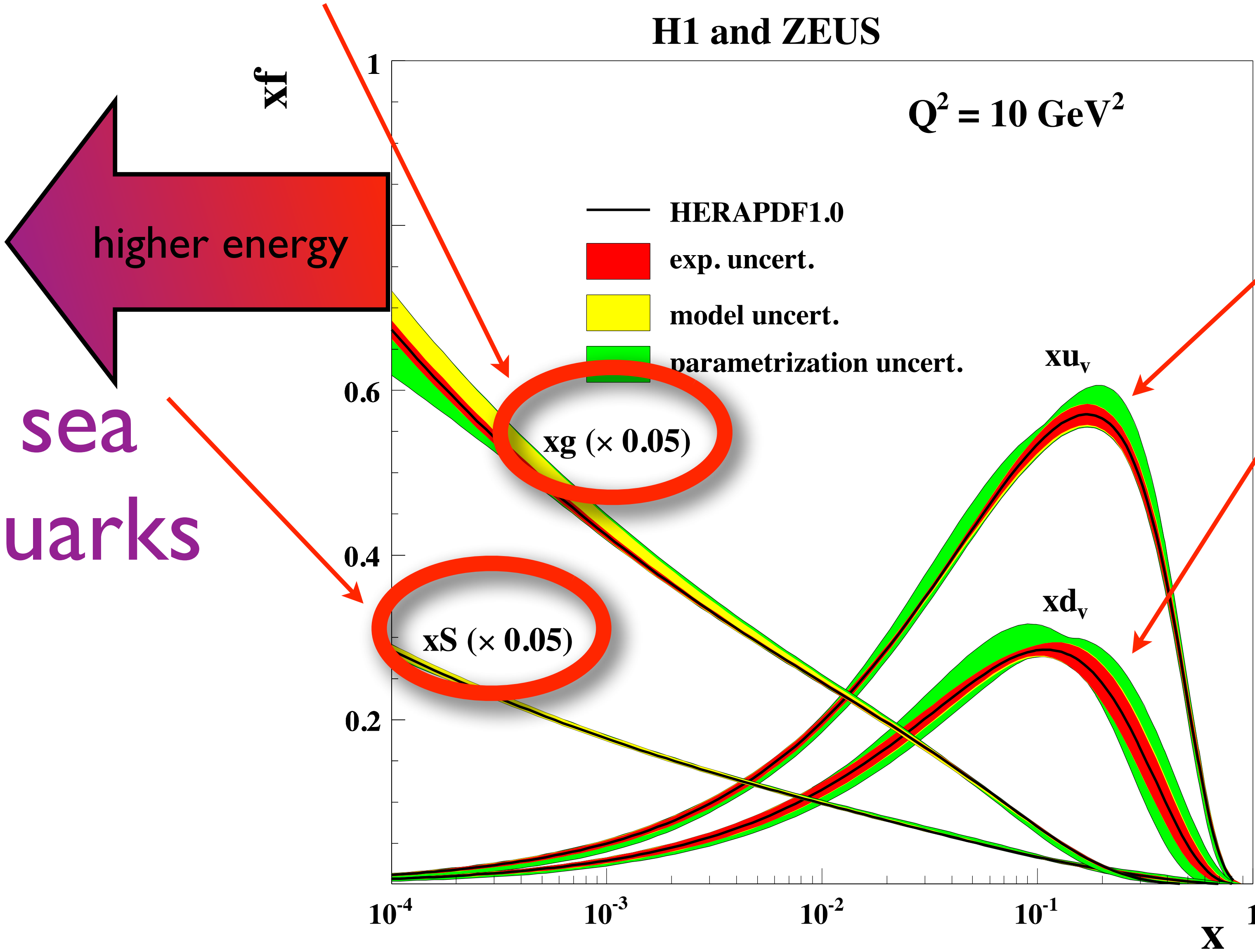

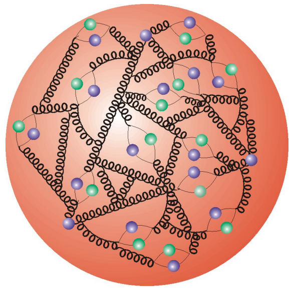

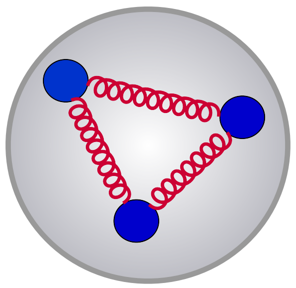

Gluon density increases rapidly with x and with Q

Gluons dominate over the quark density

Rise of cross sections

Rise of cross sections

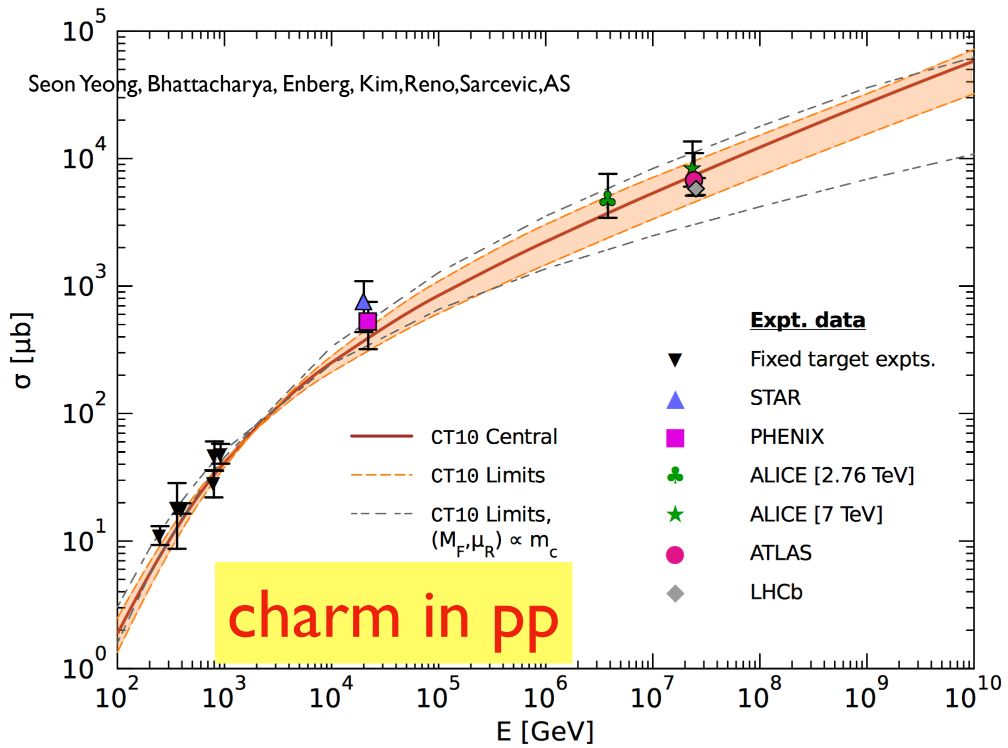

Rise of cross sections

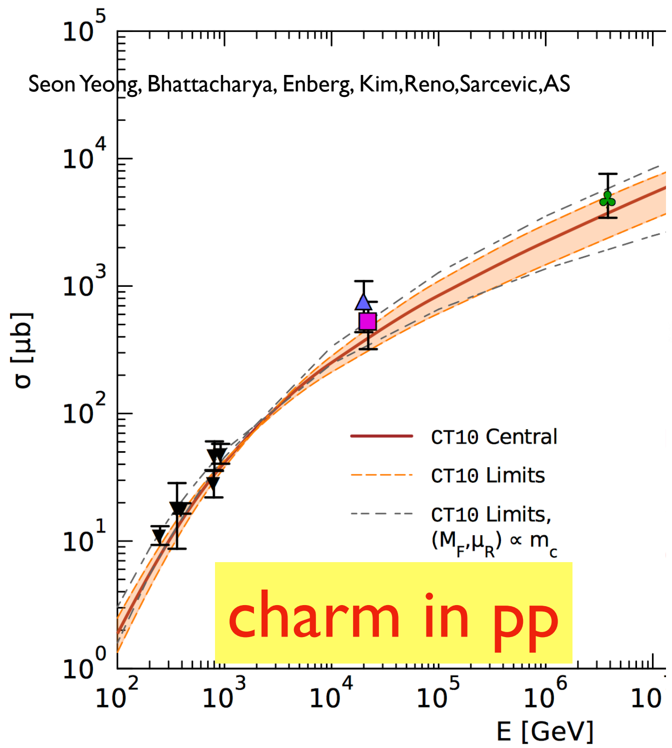

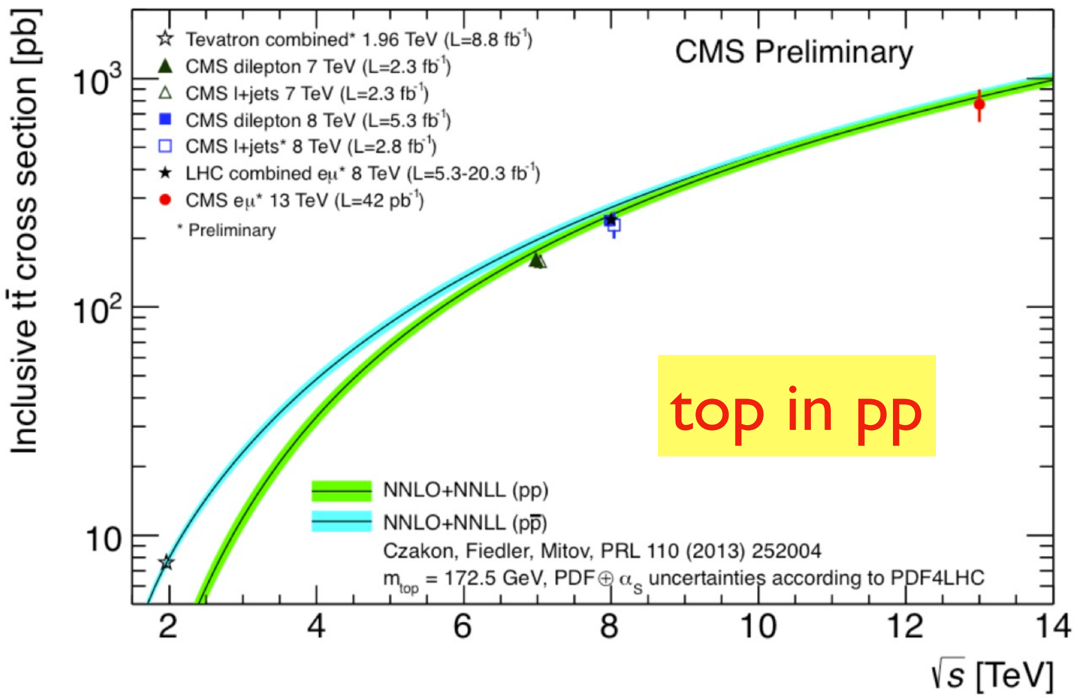

Rise of cross sections

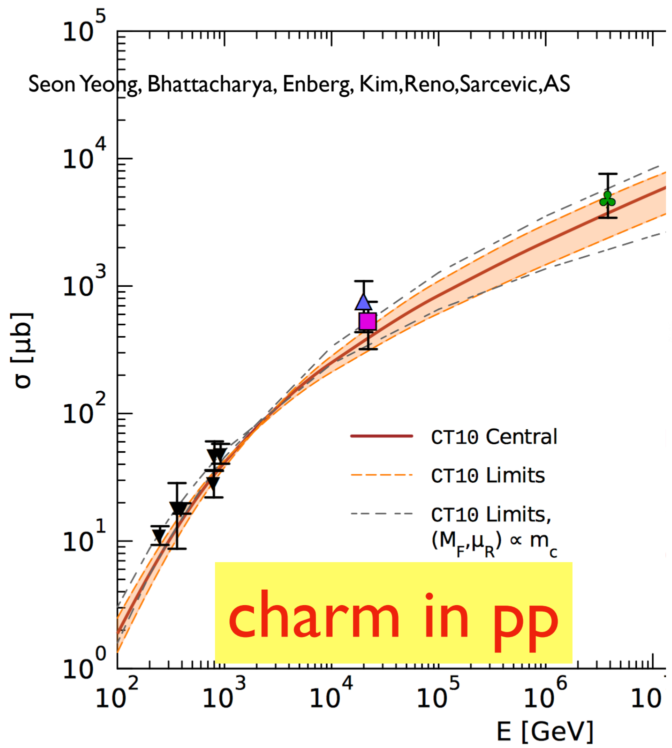

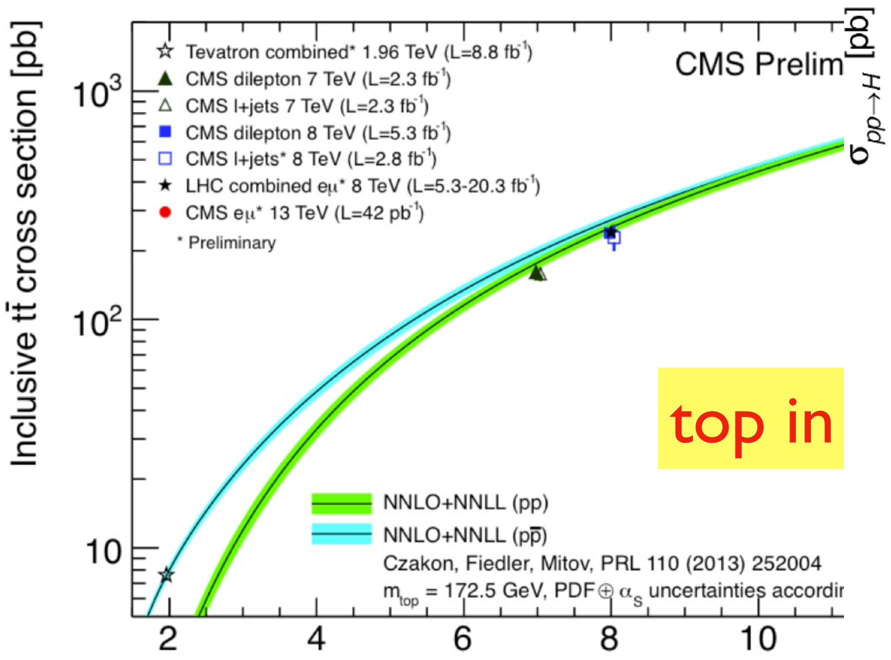

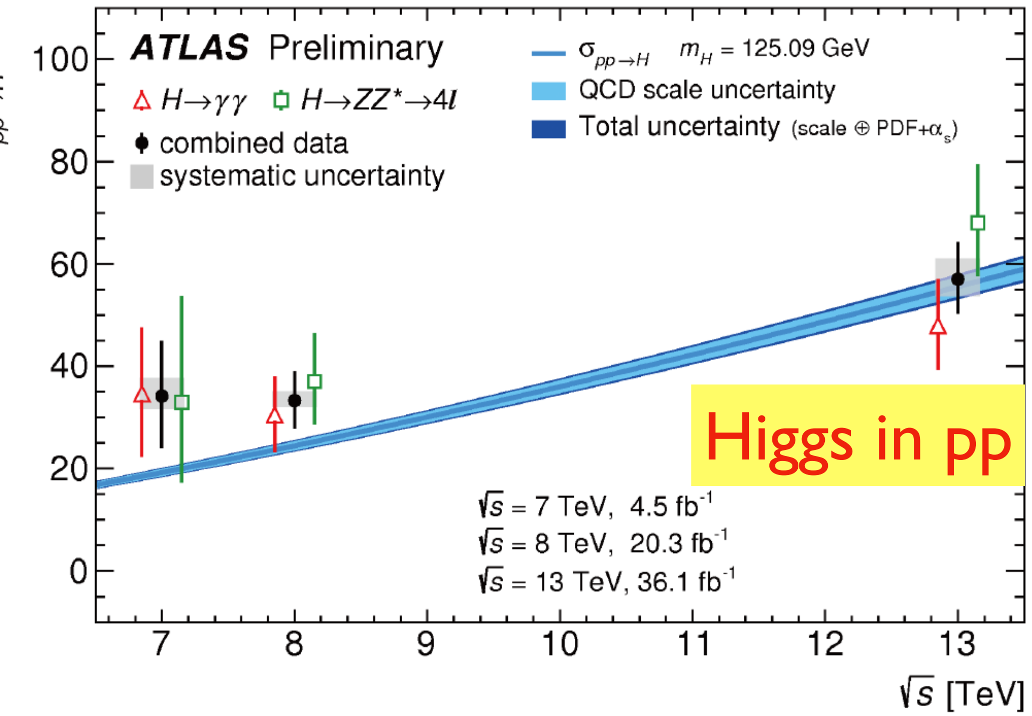

Rise of cross sections

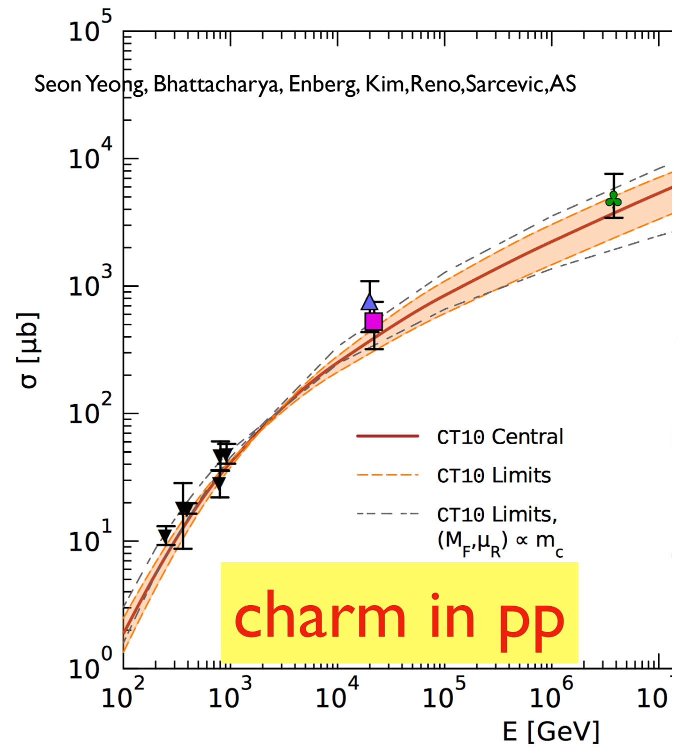

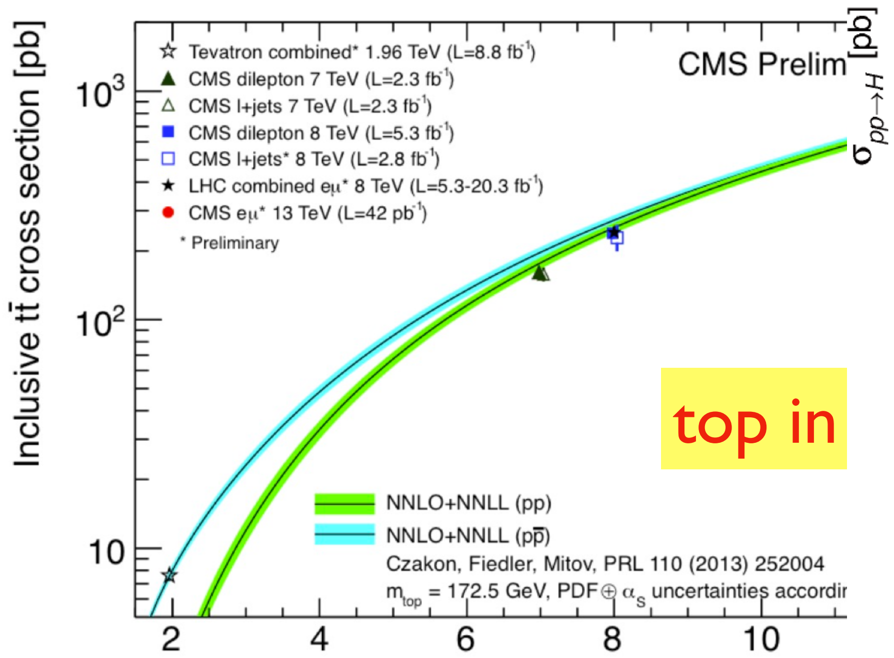

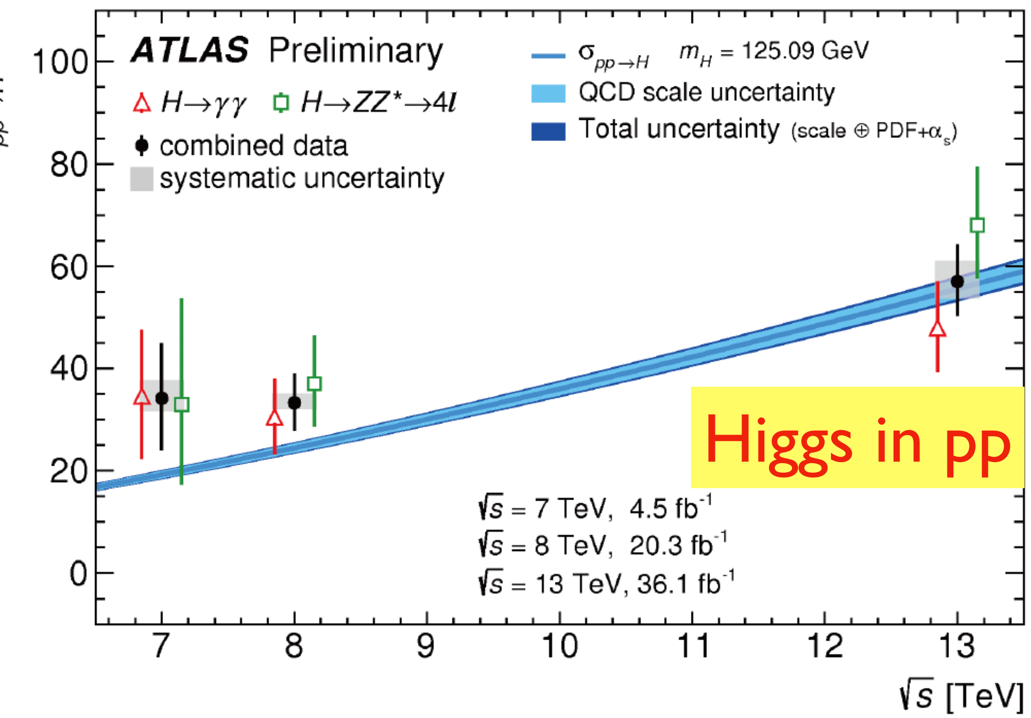

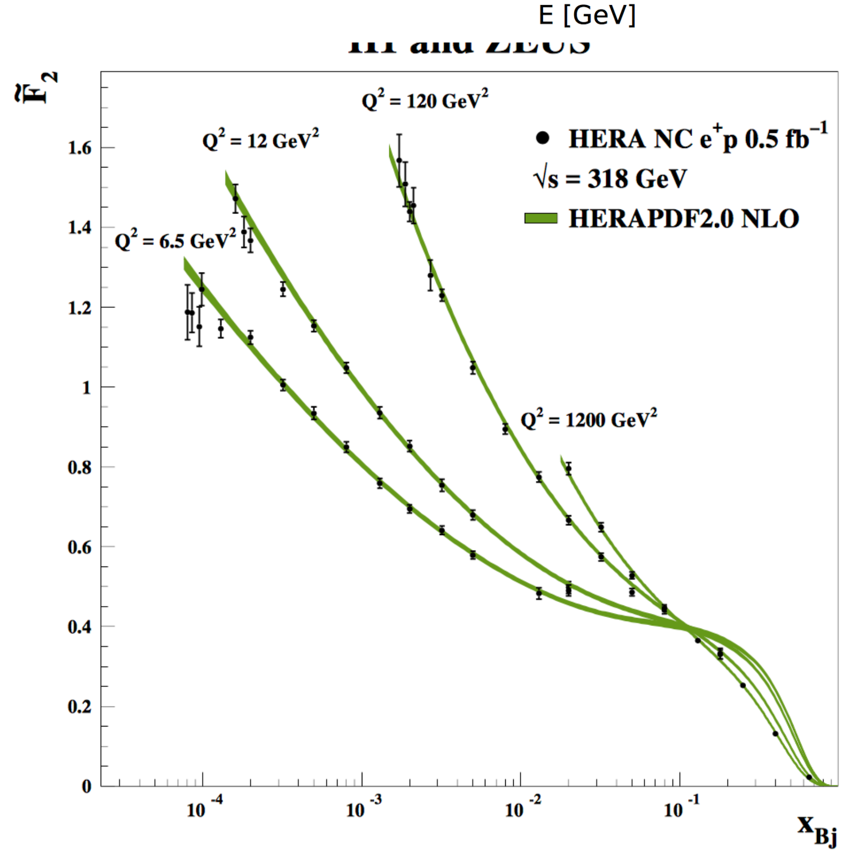

Rise of cross sections

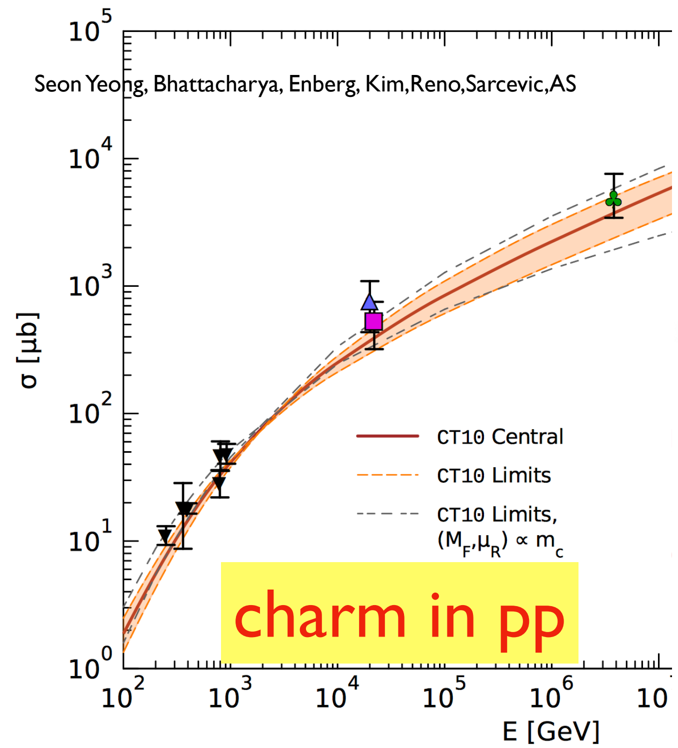

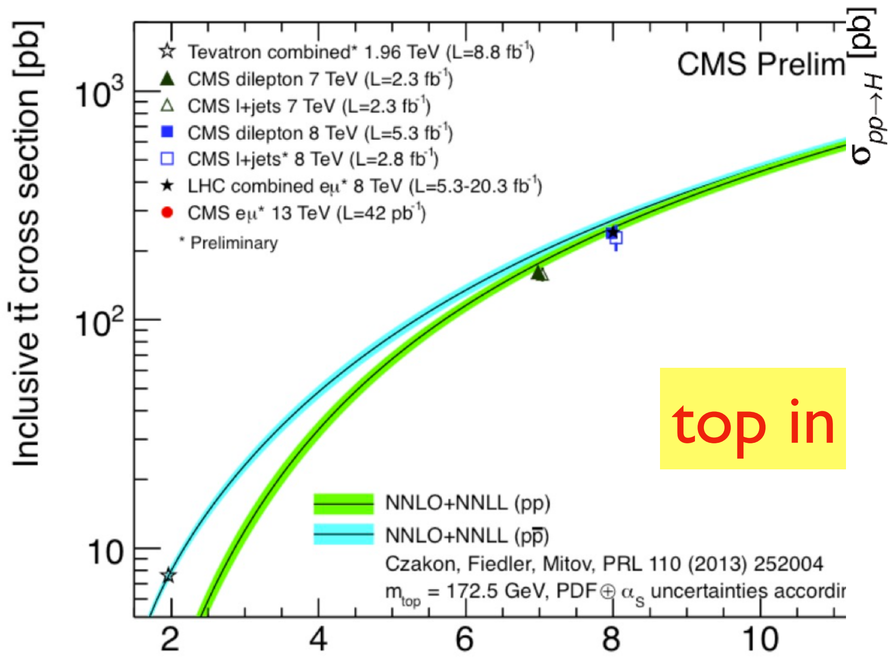

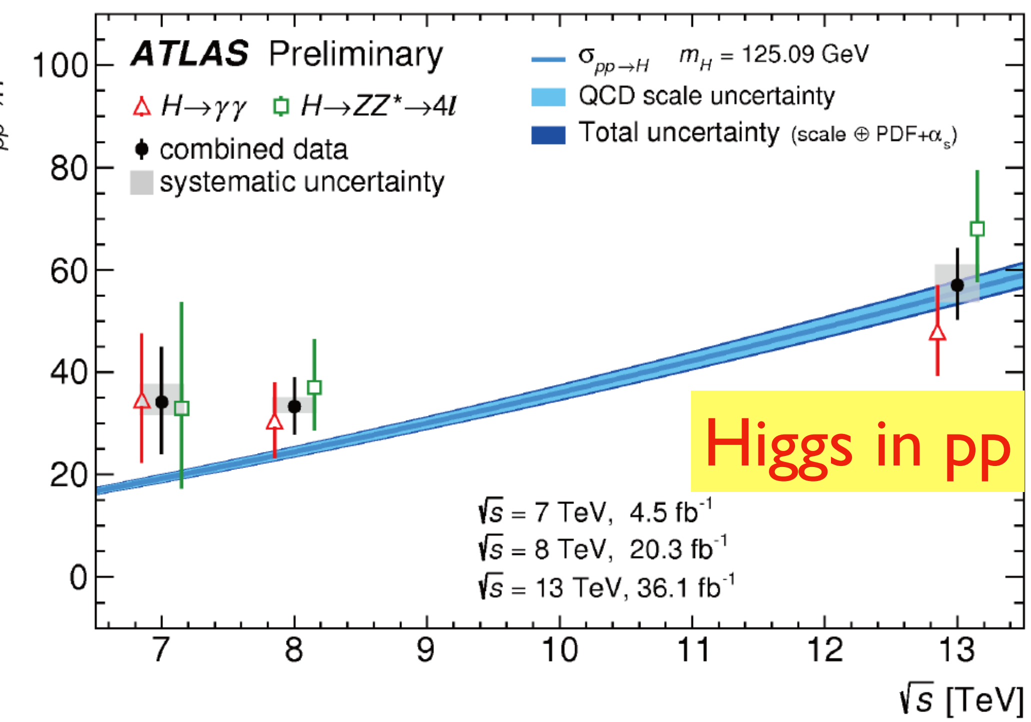

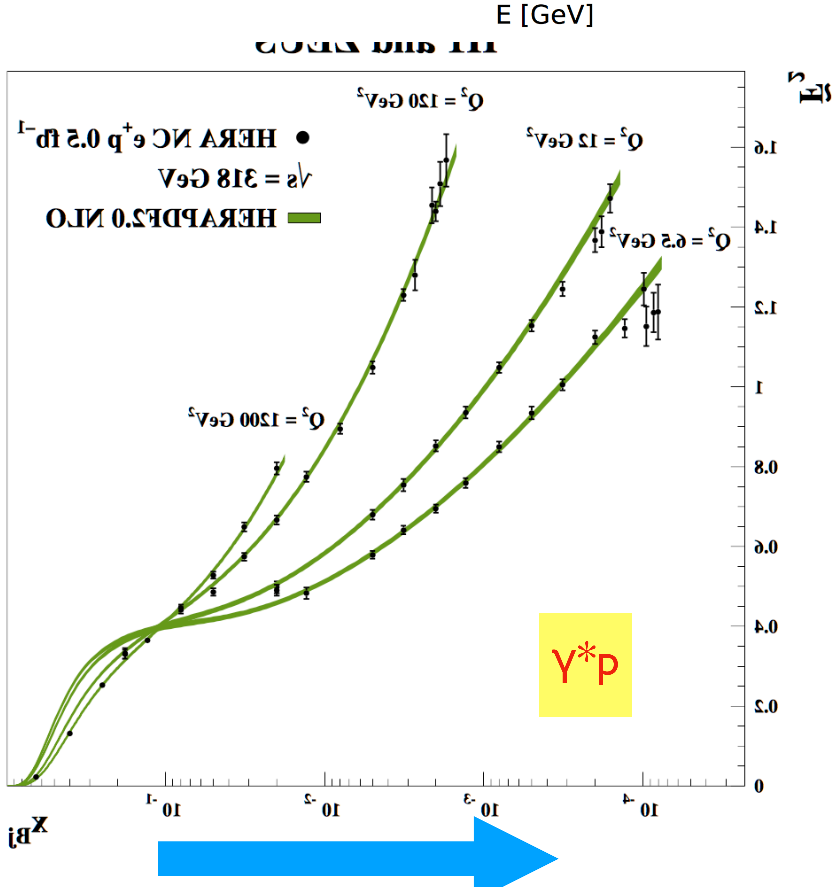

energy

Rise of cross sections

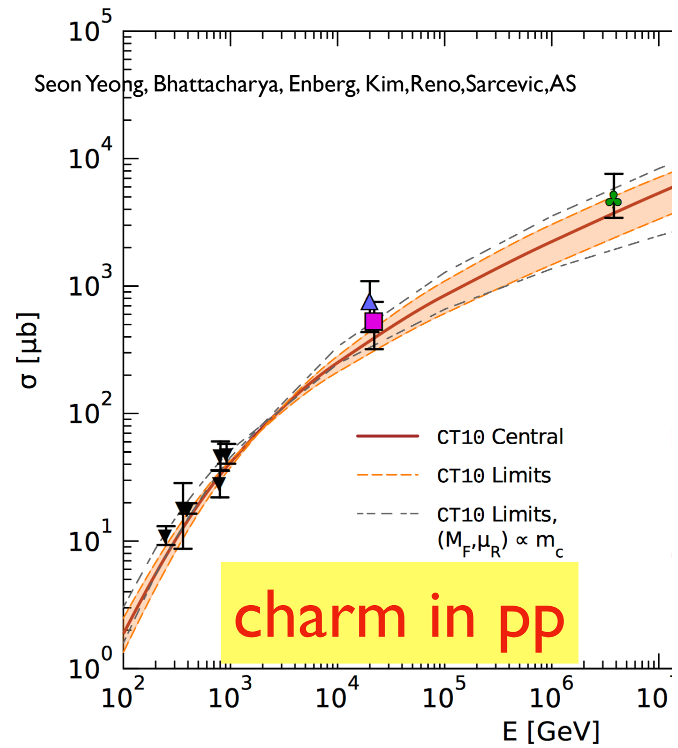

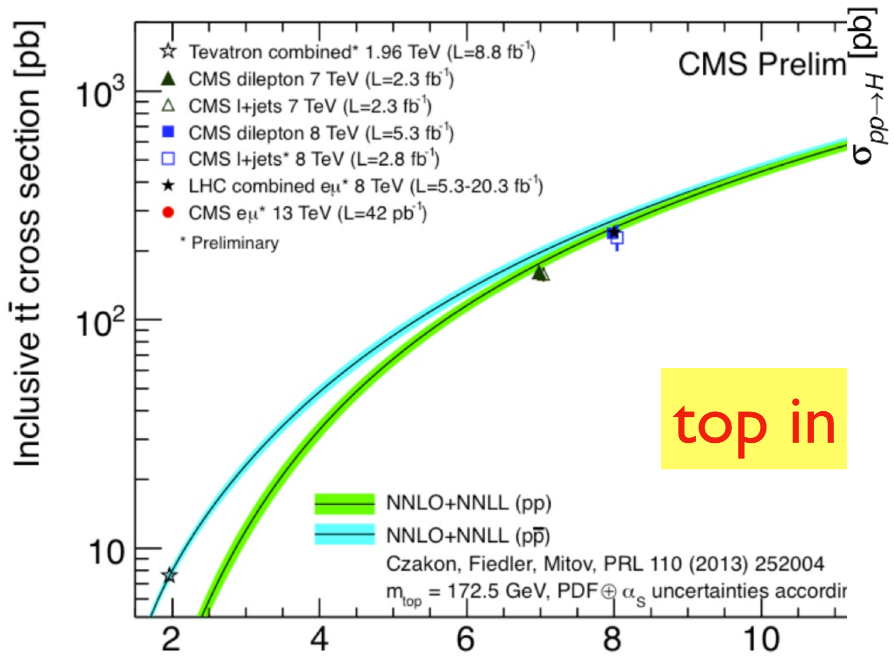

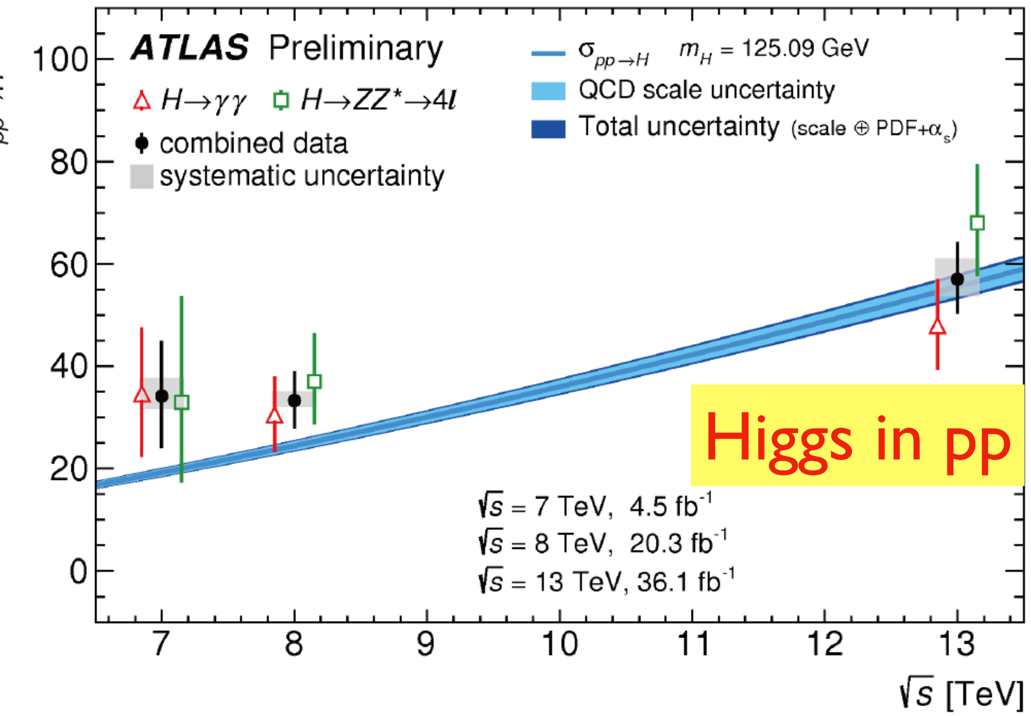

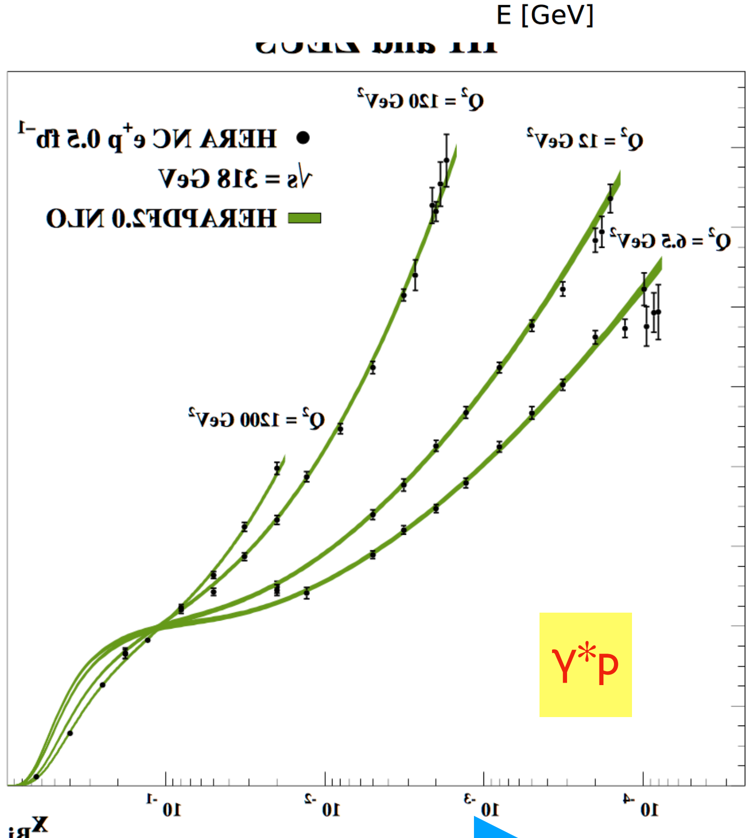

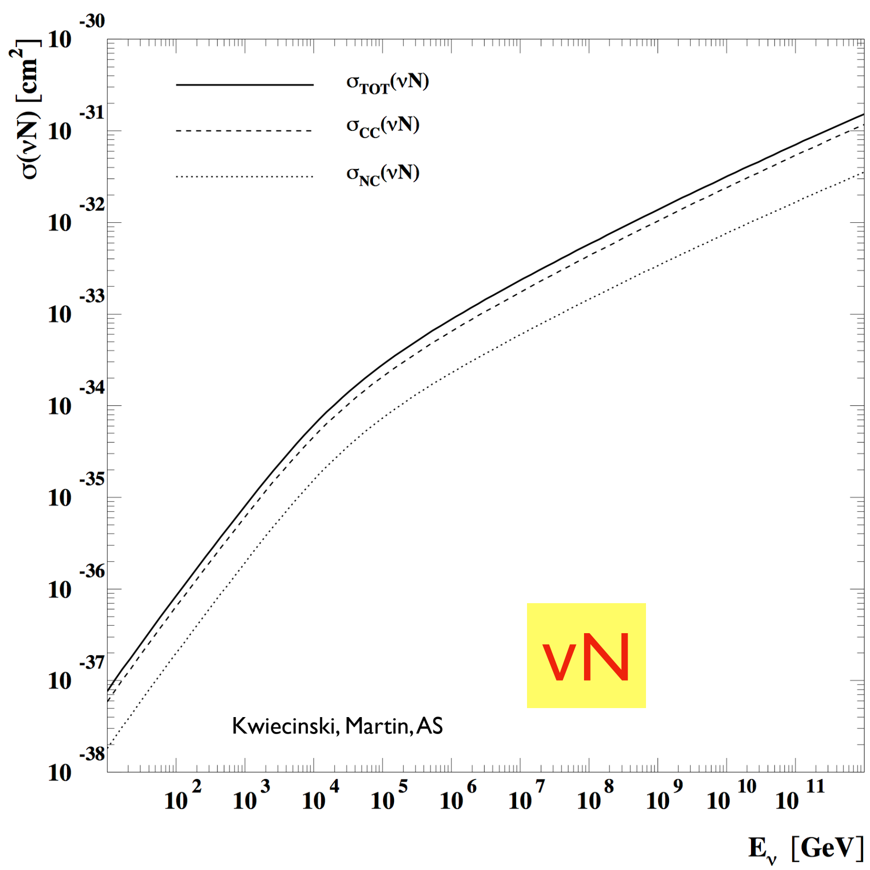

energy

Rise of cross sections

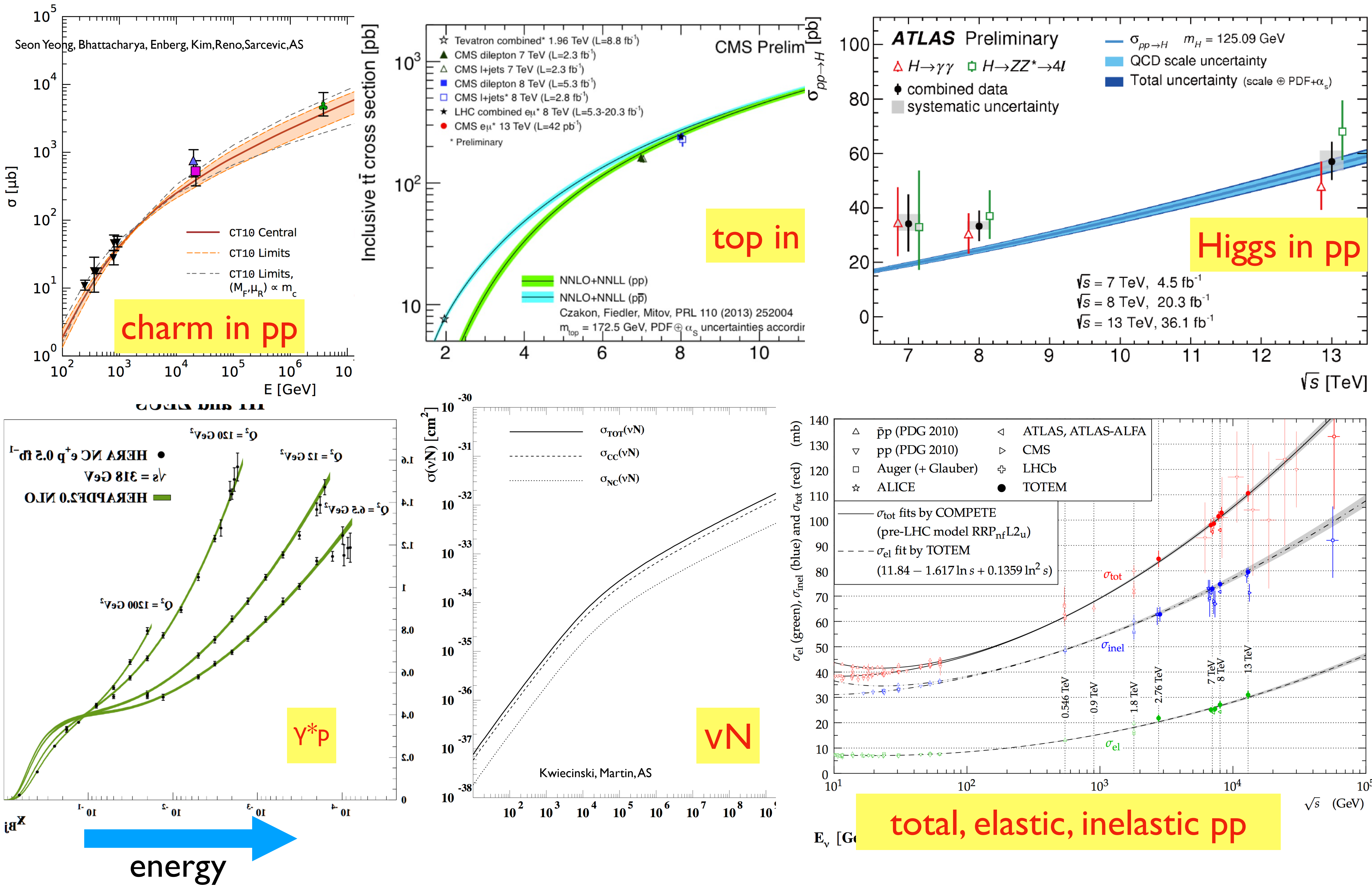

DGLAP evolution

$\gamma^* N$ as a template

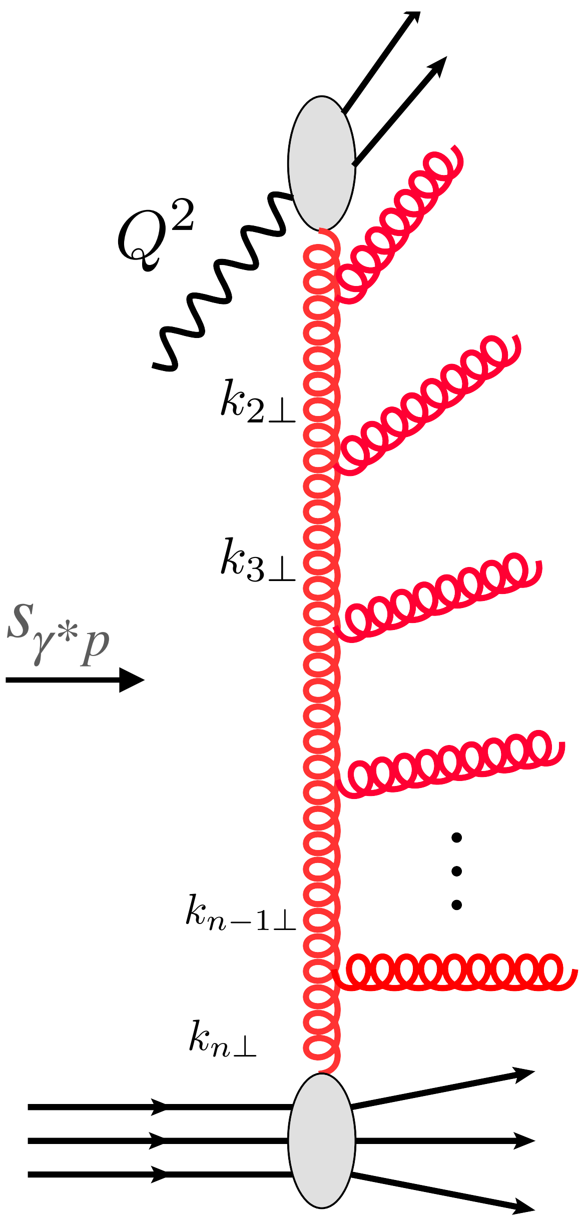

Focusing on gluon emissions

Large parameter

$$Q^2 \to \infty$$

Probing small distances

Strong ordering in transverse momenta

$$Q^2 \gg k_{1\perp}^2 \gg k_{2\perp}^2 \gg k_{3\perp}^2 \cdots \gg k_{n\perp}^2$$

Resummation of large logarithms

$$\int_{\mu_0^2}^{Q^2} \frac{dk_{1\perp}^2}{k_{1\perp}^2} g^2 \int_{\mu_0^2}^{k_{1\perp}^2} \frac{dk_{2\perp}^2}{k_{2\perp}^2} g^2 \int_{\mu_0^2}^{k_{2\perp}^2} \frac{dk_{3\perp}^2}{k_{3\perp}^2} g^2 \cdots \int_{\mu_0^2}^{k_{n-1\perp}^2} \frac{dk_{n\perp}^2}{k_{n\perp}^2} g^2 \simeq \left(g^2 \log \frac{Q^2}{\mu_0^2} \right)^n$$

DGLAP evolution

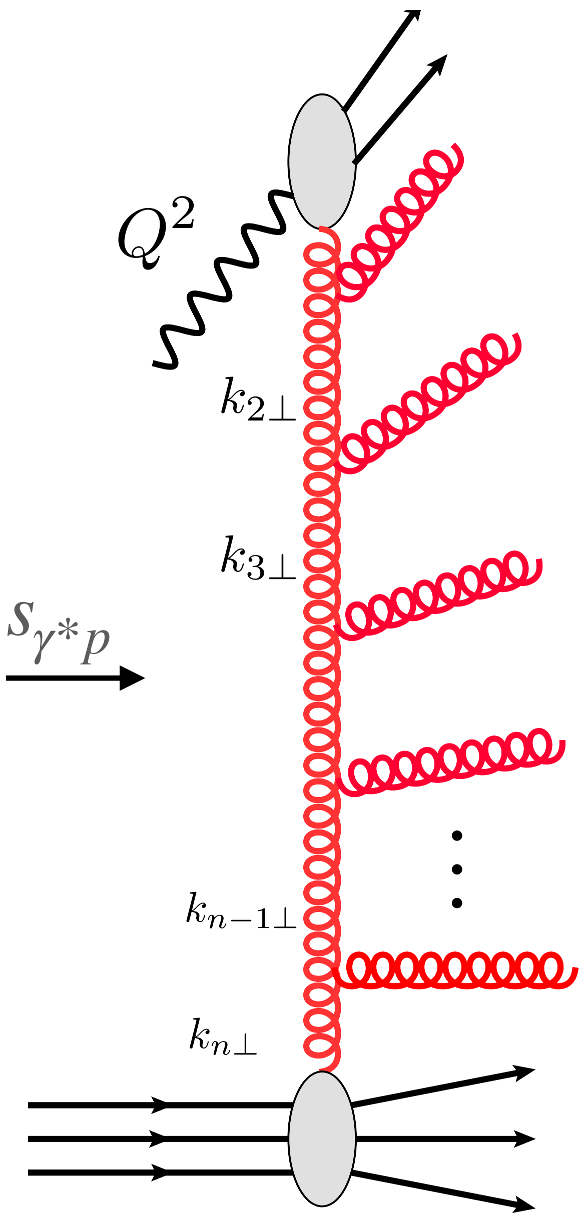

Dokshitzer-Gribov-Lipatov-Altarelli-Parisi

DGLAP evolution equations for parton densities

$$\mu^2 \frac{\partial}{\partial \mu^2} \begin{pmatrix} q_i(x,\mu^2) \\ g(x,\mu^2) \end{pmatrix} = \sum_j \int_x^1 \frac{dz}{z} \begin{pmatrix} P_{q_i q_j}(z,\alpha_s) & P_{q_i g}(z,\alpha_s) \\ P_{g q_j}(z,\alpha_s) & P_{gg}(z,\alpha_s) \end{pmatrix} \begin{pmatrix} q_j(\frac{x}{z},\mu^2) \\ g(\frac{x}{z},\mu^2) \end{pmatrix}$$

q_j : quark density, g : gluon density

Splitting functions calculated perturbatively

$$P_{ab}(z,\alpha_s) \equiv P_{b\to a}(z,\alpha_s) = \frac{\alpha_s}{2\pi} P^{(0)}_{ab}(z) + \left(\frac{\alpha_s}{2\pi}\right)^2 P^{(1)}_{ab}(z) + \left(\frac{\alpha_s}{2\pi}\right)^3 P^{(2)}_{ab}(z) + \ldots$$

LO NLO NNLO

Leading order splitting functions

$$P^{(0)}_{qq}(z) = C_F\left[\frac{1+z^2}{(1-z)_+} + \frac{3}{2}\delta(1-z)\right]$$

$$P^{(0)}_{qg}(z) = T_R\left[z^2 + (1-z)^2\right]$$

$$P^{(0)}_{gq}(z) = C_F\left[\frac{z^2 + (1-z)^2}{z}\right]$$

$$P^{(0)}_{gg}(z) = 2C_A\left[\frac{z}{(1-z)_+} + \frac{1-z}{z} + z(1-z) + \delta(1-z)\frac{11C_A - 4n_f T_R}{6}\right]$$

DGLAP parton densities

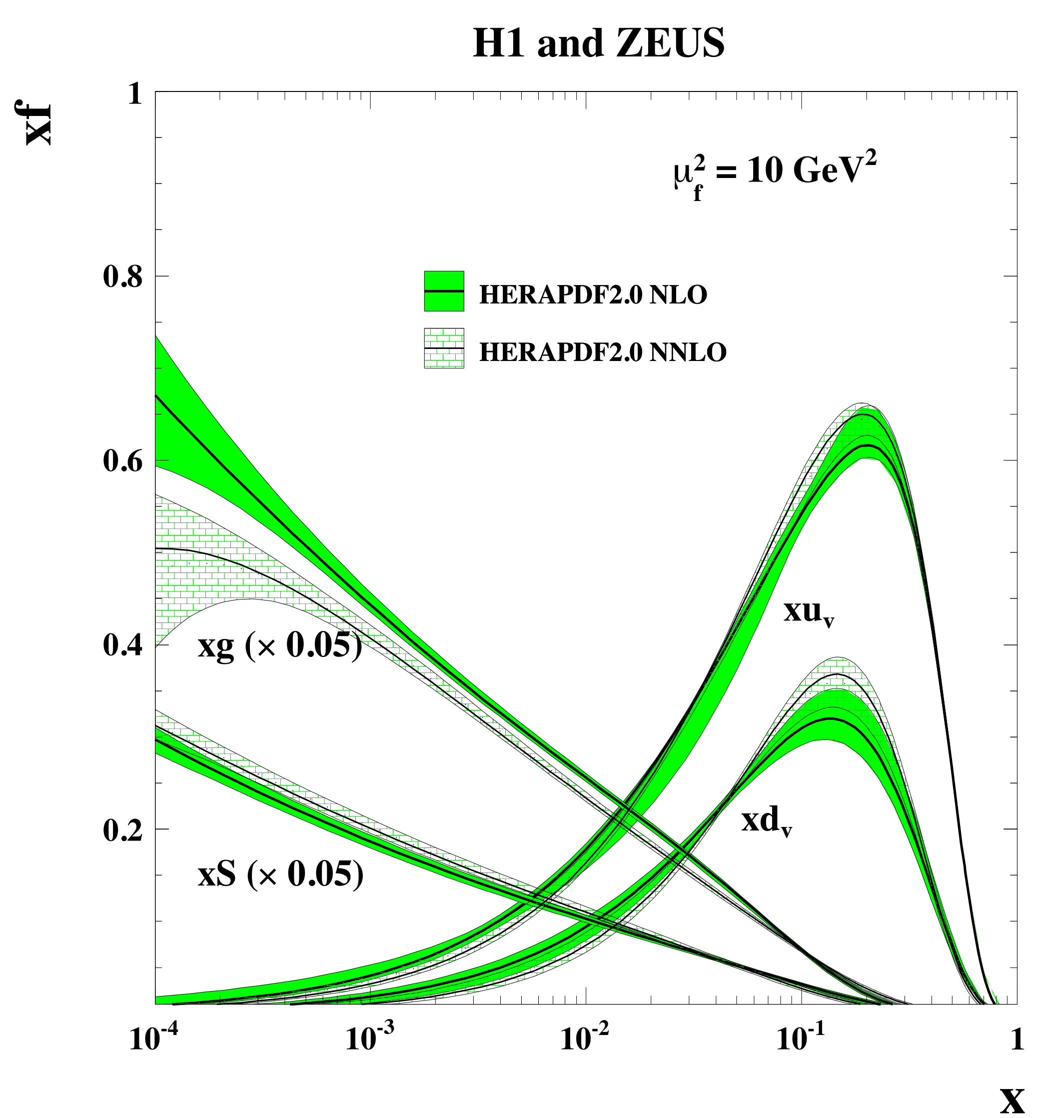

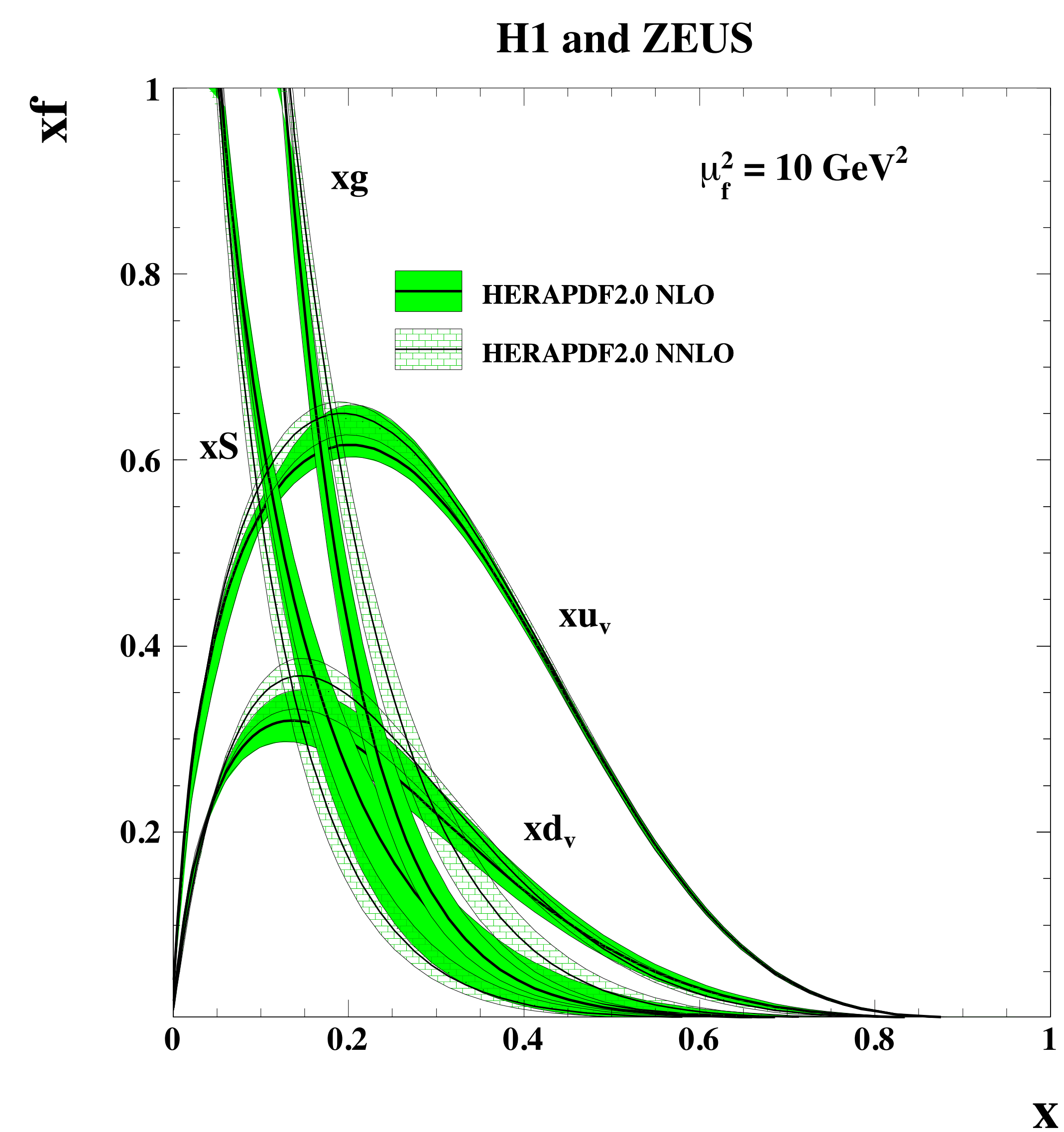

Gluon density dominates at small x

NLO vs NNLO small x behavior

What happens at small x ?

Small x means large energy

$$x = \frac{Q^2}{Q^2 + W^2}$$

$$W^2 = s_{\gamma^* p}$$

Collinear factorization

Given parton density one can compute cross section provided hard scale is present: photon virtuality, transverse momentum of particles, mass of produced particles

Collinear factorization of the cross section

$$d\sigma(x,Q^2) \;=\; \sum_i f_i \otimes d\hat{\sigma}^i \;+\; \mathcal{O}(\Lambda^2/Q^2)$$

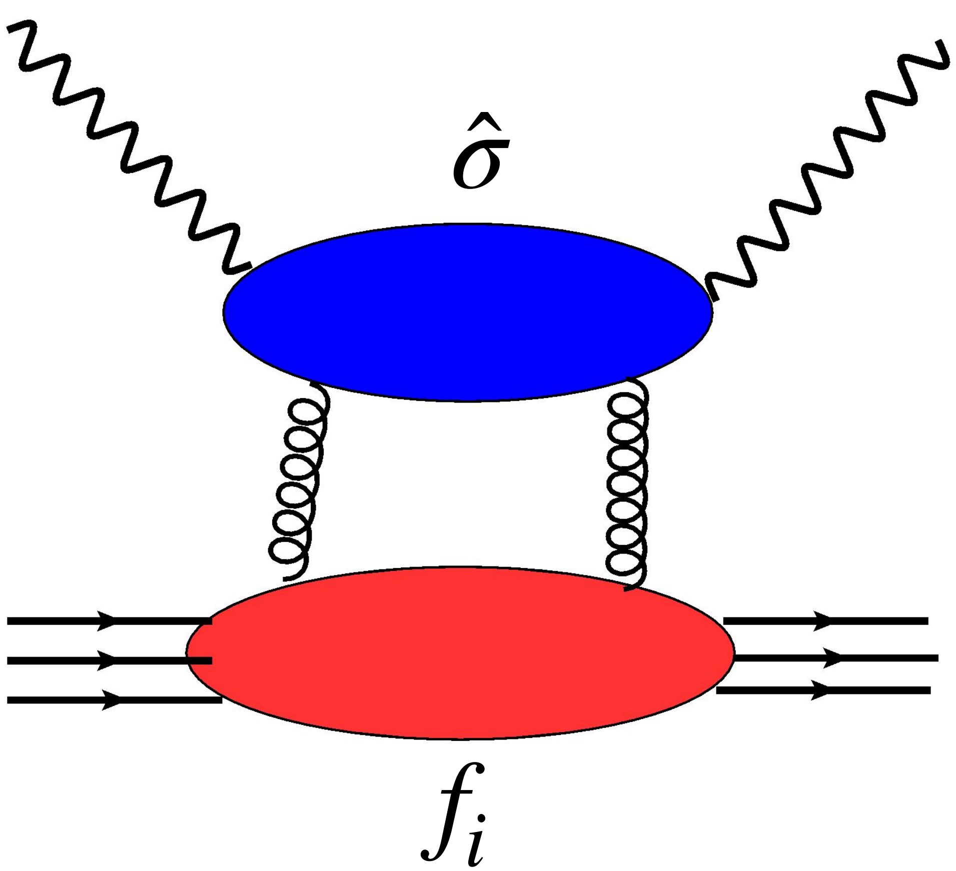

$d\hat{\sigma}^i$ partonic cross section, calculable perturbatively

$f_i(x,Q^2)$ Parton densities:should be universal, can take from process to process

High energy limit

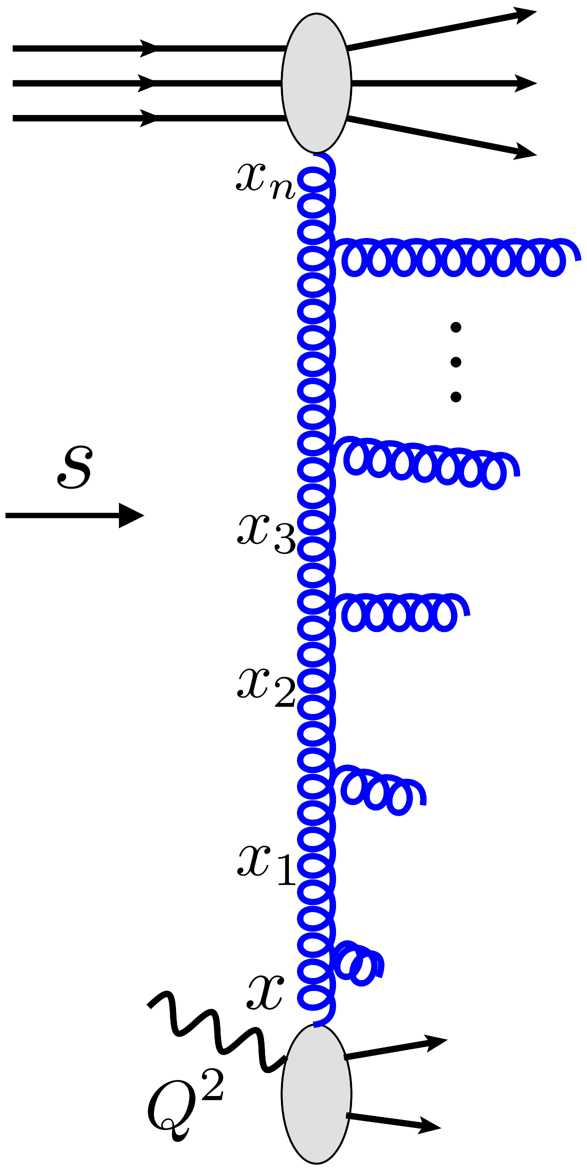

Large parameter

$$s \to \infty$$

Q^2 fixed, perturbative

High energy or Regge limit

$$s \gg Q^2 \gg \Lambda^2$$

High energy limit

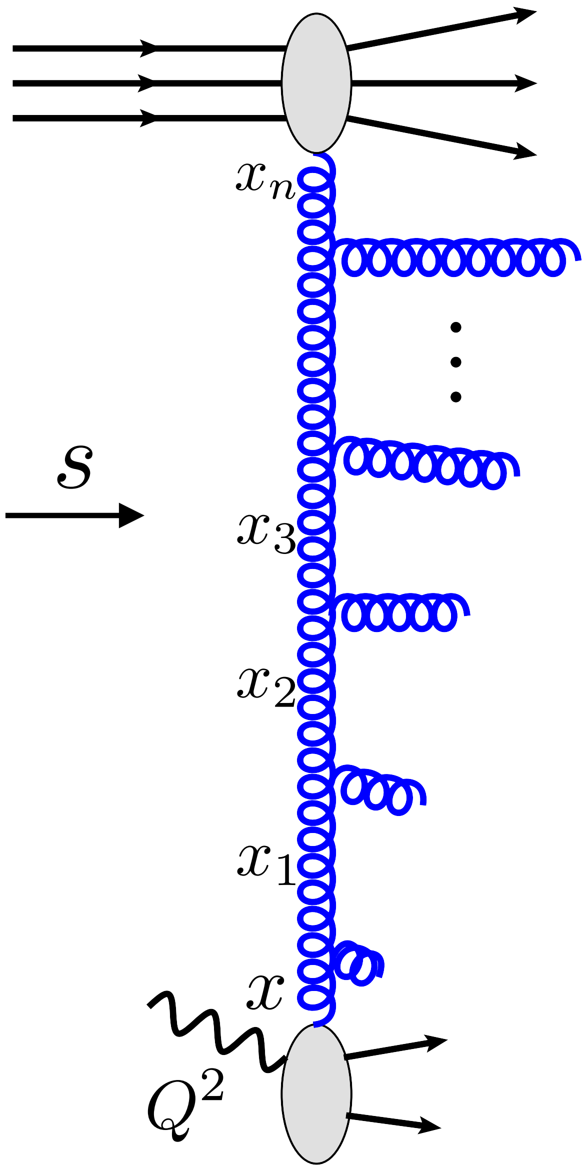

Large parameter

$$s \to \infty$$

High energy or Regge limit

$$s \gg Q^2 \gg \Lambda^2$$

Q^2 fixed, perturbative

Light cone proton momentum

$$p^+ = p^0 + p^z \qquad k_i^+ = x_i p^+$$

Strong ordering in longitudinal momenta

$$x \ll x_1 \ll x_2 \ll \cdots \ll x_n$$

High energy limit

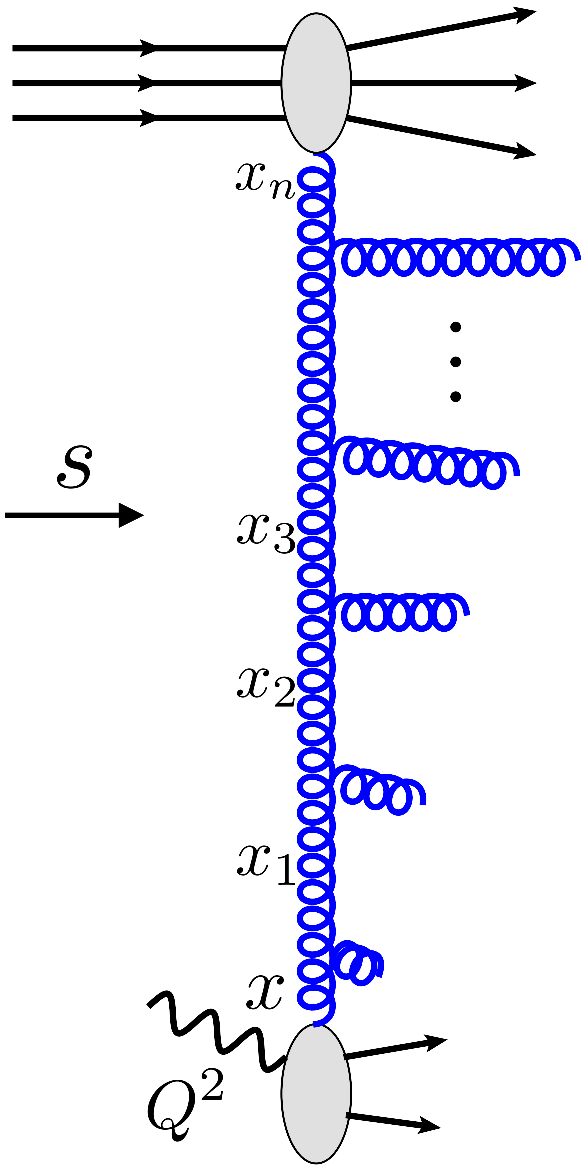

Large parameter

$$s \to \infty$$

High energy or Regge limit

$$s \gg Q^2 \gg \Lambda^2$$

Q^2 fixed, perturbative

Light cone proton momentum

$$p^+ = p^0 + p^z \qquad k_i^+ = x_i p^+$$

Strong ordering in longitudinal momenta

$$x \ll x_1 \ll x_2 \ll \cdots \ll x_n$$

Perturbative coupling but large logarithm

$$\bar{\alpha}_s \ll 1 \qquad \ln\frac{1}{x} \simeq \ln\frac{s}{Q^2} \gg 1$$

High energy limit

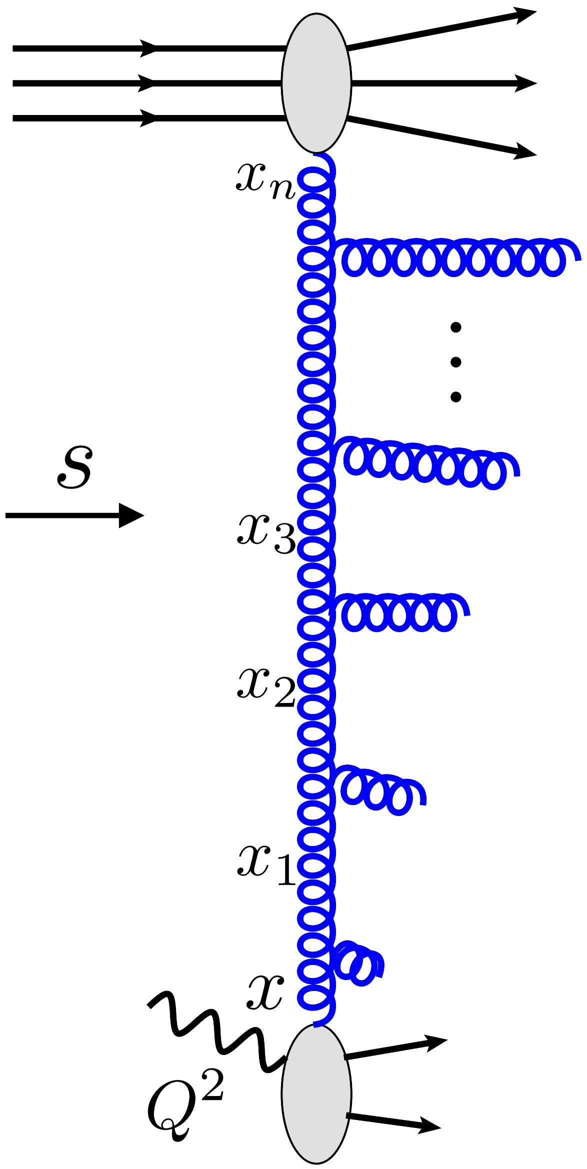

Large parameter

$$s \to \infty$$

Q^2 fixed, perturbative

High energy or Regge limit

$$s \gg Q^2 \gg \Lambda^2$$

Light cone proton momentum

$$p^+ = p^0 + p^z \qquad k_i^+ = x_i p^+$$

Strong ordering in longitudinal momenta

$$x \ll x_1 \ll x_2 \ll \cdots \ll x_n$$

Perturbative coupling but large logarithm

$$\bar{\alpha}_s \ll 1 \qquad \ln \frac{1}{x} \simeq \ln \frac{s}{Q^2} \gg 1$$

Large logarithms

$$\frac{\alpha_s N_c}{\pi} \int_x^1 \frac{dz}{z} = \frac{\alpha_s N_c}{\pi} \ln \frac{1}{x} = \bar{\alpha}_s \ln \frac{1}{x}$$

Leading logarithmic resummation

$$\left(\bar{\alpha}_s \ln \frac{1}{x} \right)^n \qquad \left(\bar{\alpha}_s \ln \frac{s}{s_0} \right)^n$$

High energy limit

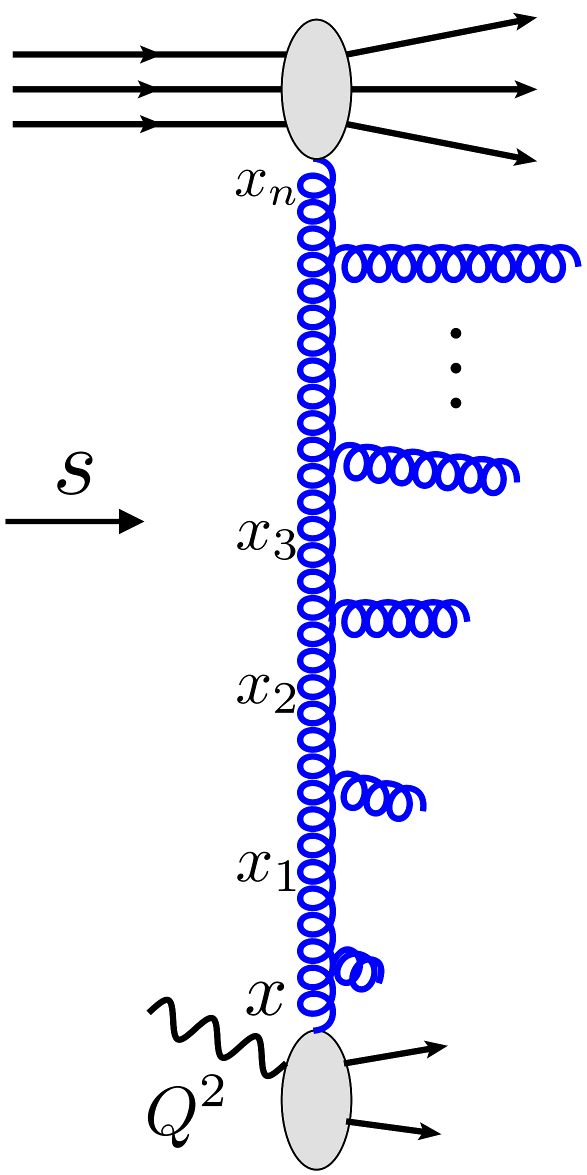

Resummation performed by BFKL evolution equation

$$\frac{\partial \mathcal{F}_g(x,k_T)}{\partial \ln 1/x} = \int d^2k'_T \, \mathcal{K}(k_T,k'_T)\, \mathcal{F}_g(x,k'_T)$$

High energy limit

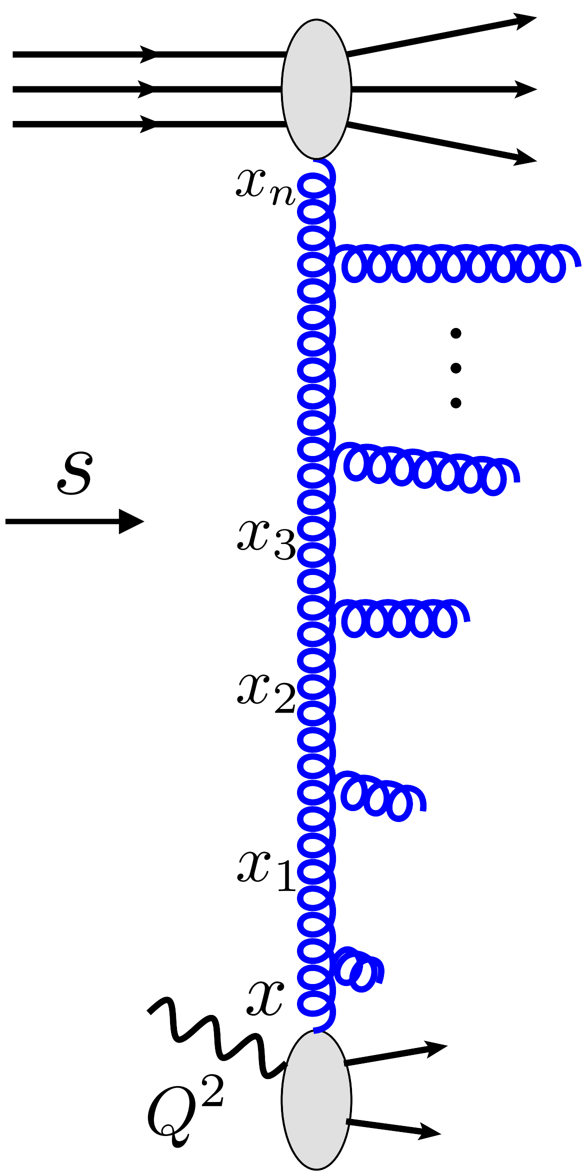

Resummation performed by BFKL evolution equation

$$\frac{\partial \mathcal{F}_g(x,k_T)}{\partial \ln 1/x} = \int d^2k'_T\, \mathcal{K}(k_T,k'_T)\, \mathcal{F}_g(x,k'_T)$$

Branching kernel (perturbative expansion)

$$\mathcal{K} = \bar{\alpha}_s \mathcal{K}^{LLx} + \bar{\alpha}_s^2 \mathcal{K}^{NLLx} + \bar{\alpha}_s^3 \mathcal{K}^{NNLLx} + \dots$$

QCD

N=4 SYM

High energy limit

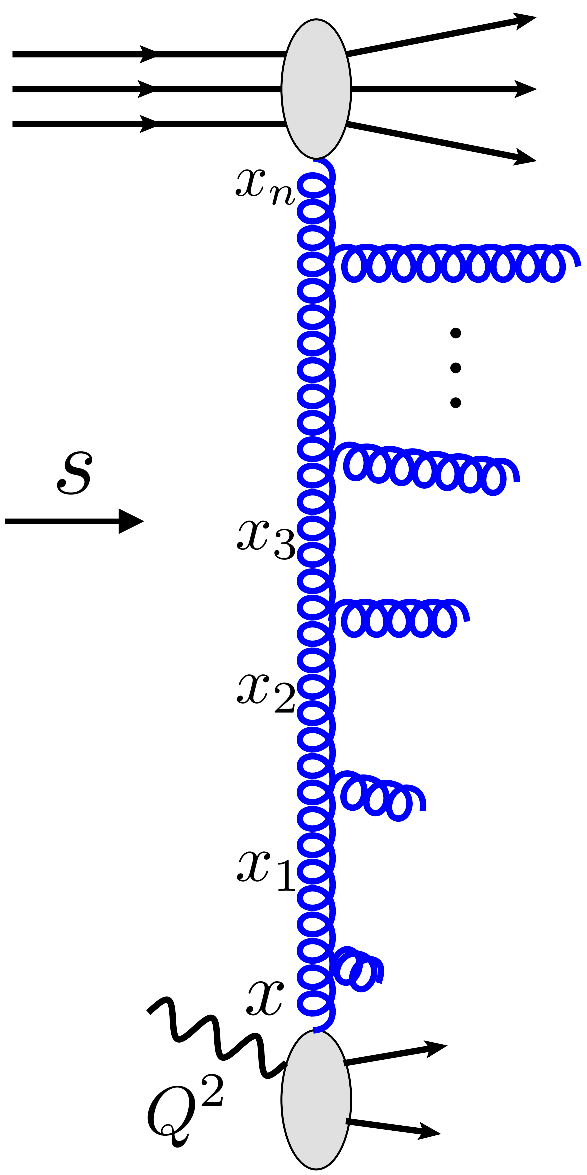

Resummation performed by BFKL evolution equation

$$\frac{\partial \mathcal{F}_g(x,k_T)}{\partial \ln 1/x} = \int d^2k'_T\, \mathcal{K}(k_T,k'_T)\, \mathcal{F}_g(x,k'_T)$$

Branching kernel (perturbative expansion)

$$\mathcal{K} = \bar{\alpha}_s \mathcal{K}^{LLx} + \bar{\alpha}_s^2 \mathcal{K}^{NLLx} + \bar{\alpha}_s^3 \mathcal{K}^{NNLLx} + \dots$$

QCD

N=4 SYM

Unintegrated, (transverse momentum dependent) gluon density

$$\mathcal{F}_g(x,k_T)$$

High energy limit

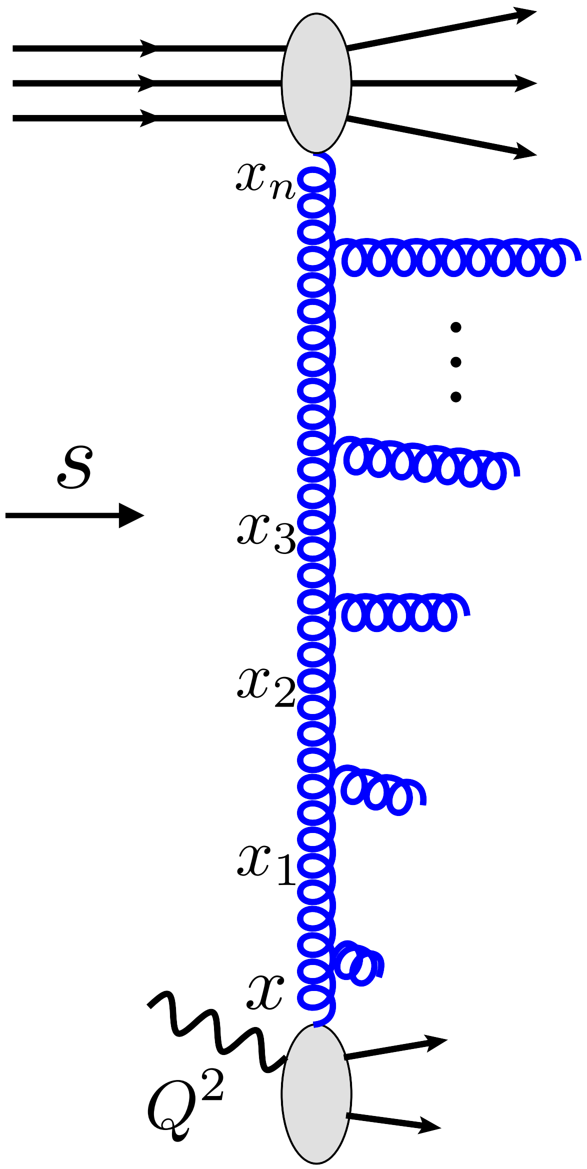

Resummation performed by BFKL evolution equation

$$\frac{\partial \mathcal{F}_g(x,k_T)}{\partial \ln 1/x} = \int d^2k'_T \, \mathcal{K}(k_T,k'_T)\, \mathcal{F}_g(x,k'_T)$$

Branching kernel (perturbative expansion)

$$\mathcal{K} = \bar{\alpha}_s \mathcal{K}^{LLx} + \bar{\alpha}_s^2 \mathcal{K}^{NLLx} + \bar{\alpha}_s^3 \mathcal{K}^{NNLLx} + \dots$$

QCD

N=4 SYM

Unintegrated, (transverse momentum dependent) gluon density

$$\mathcal{F}_g(x,k_T)$$

compare with DGLAP-collinear approach

$$\frac{\partial f_i(x,Q^2)}{\partial \log(Q^2)} = \sum_j \int_x^1 \frac{dz}{z} P_{j\to i}(z) f_j(\frac{x}{z},Q^2)$$

High energy factorization

BFKL evolution equation

$$\frac{\partial \mathcal{F}_g(x, k_T)}{\partial \ln 1/x} = \int d^2 k'_T \, \mathcal{K}(k_T, k'_T) \, \mathcal{F}_g(x, k'_T)$$

Cross sections from high energy factorization

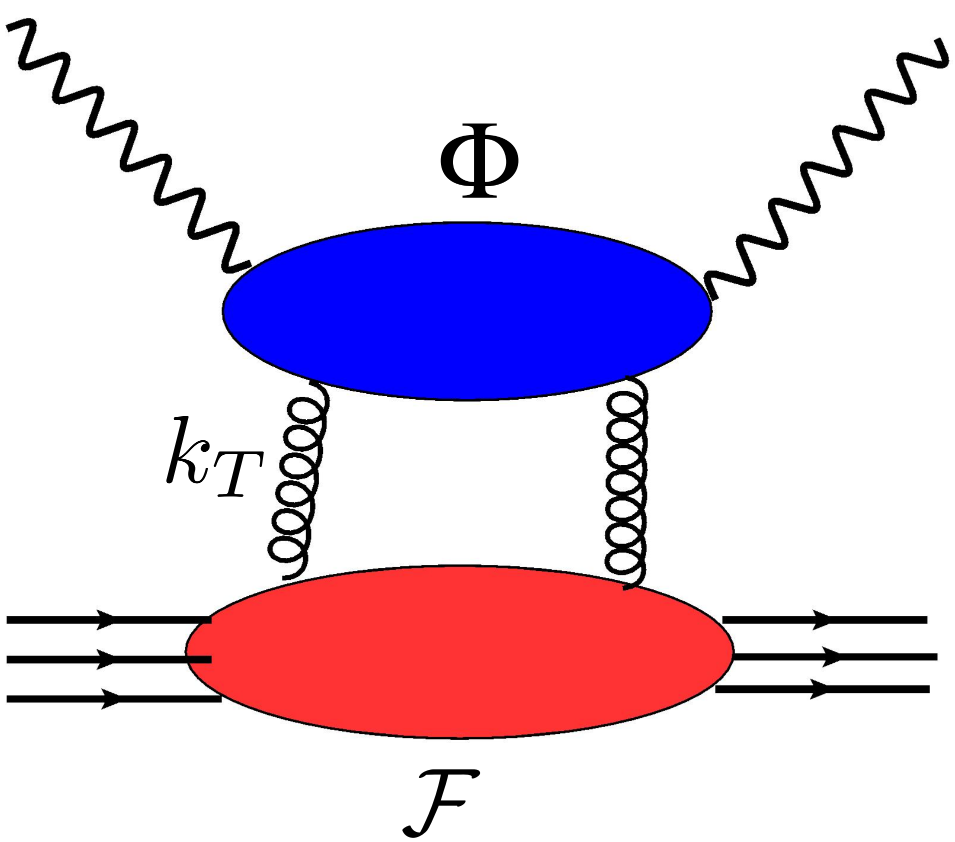

$$d\sigma(x, Q^2) = \Phi \otimes \mathcal{F}$$

Impact factor, perturbatively calculable

$$\Phi(Q, k_T)$$

High energy factorization

BFKL evolution equation

$$\frac{\partial \mathcal{F}_g(x,k_T)}{\partial \ln 1/x} = \int d^2k'_T\, \mathcal{K}(k_T,k'_T)\, \mathcal{F}_g(x,k'_T)$$

Cross sections from high energy factorization

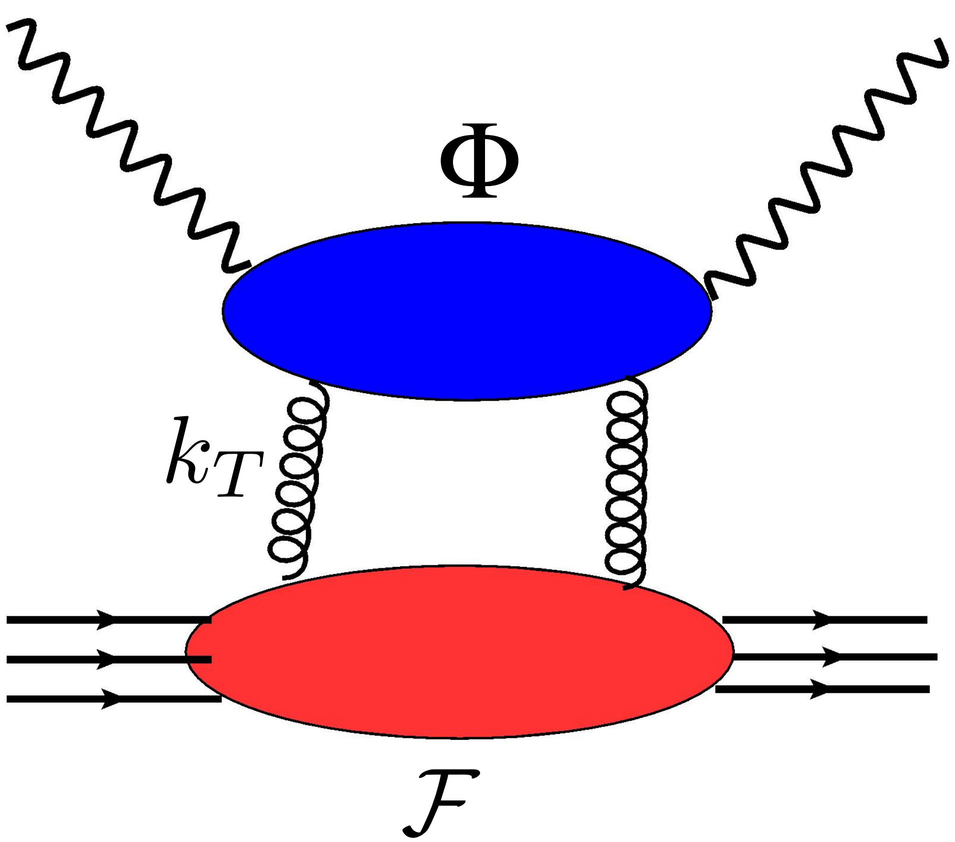

$$d\sigma(x,Q^2) = \Phi \otimes \mathcal{F}$$

Impact factor, perturbatively calculable $\Phi(Q,k_T)$

Unintegrated, (transverse momentum dependent) gluon density $\mathcal{F}_g(x,k_T)$

High energy limit

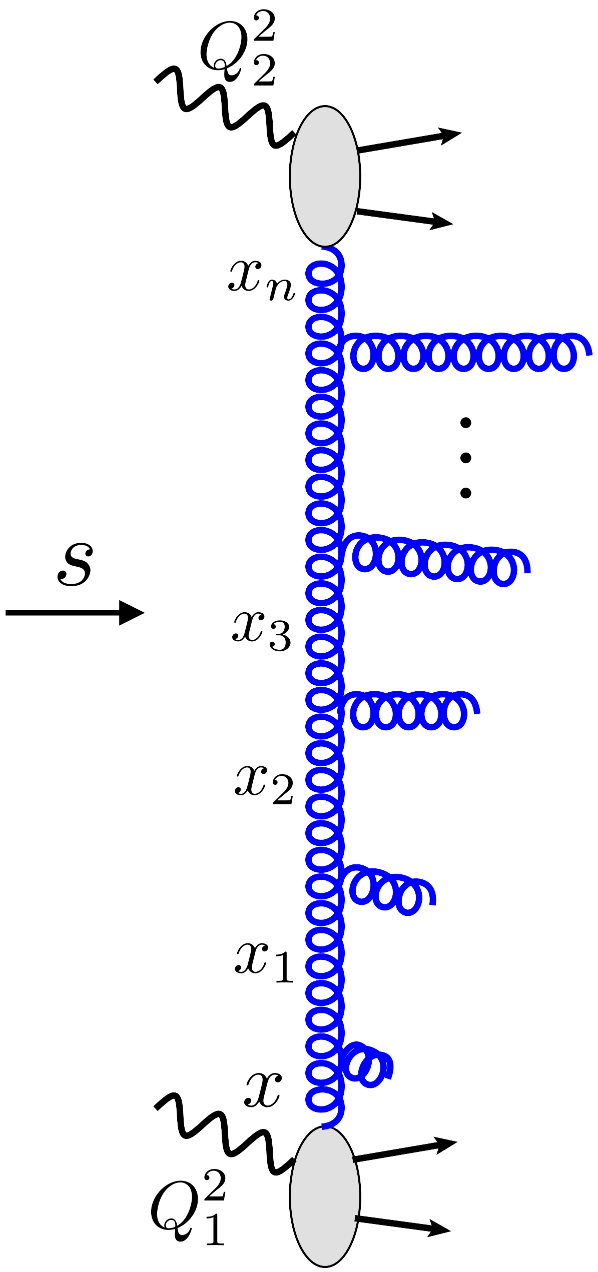

Random walk in transverse momenta

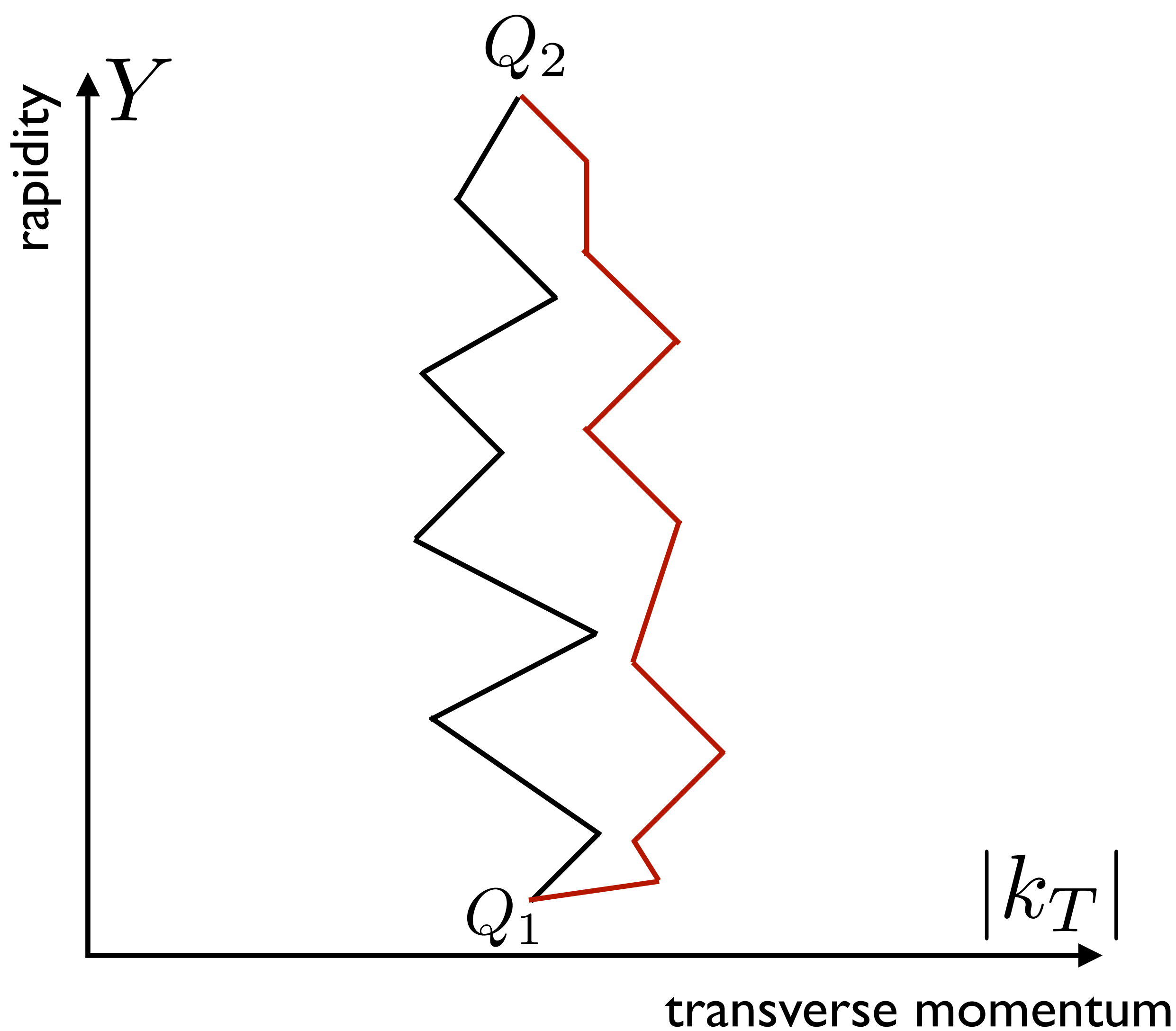

$$Y = \frac{1}{2} \ln \frac{p^+}{p^-}$$

Diffusion of transverse momenta towards IR and UV.
For large energies momenta can diffuse to low scales even when starting from large scales.

High energy limit

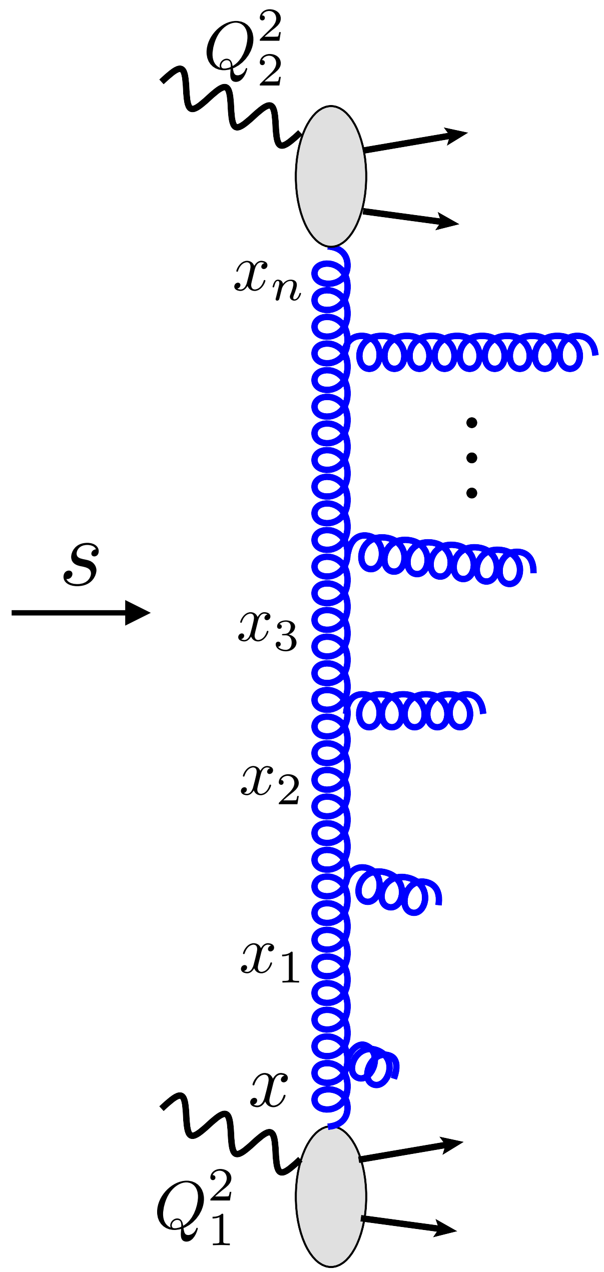

Effects of running coupling:
'pull' towards the infrared region

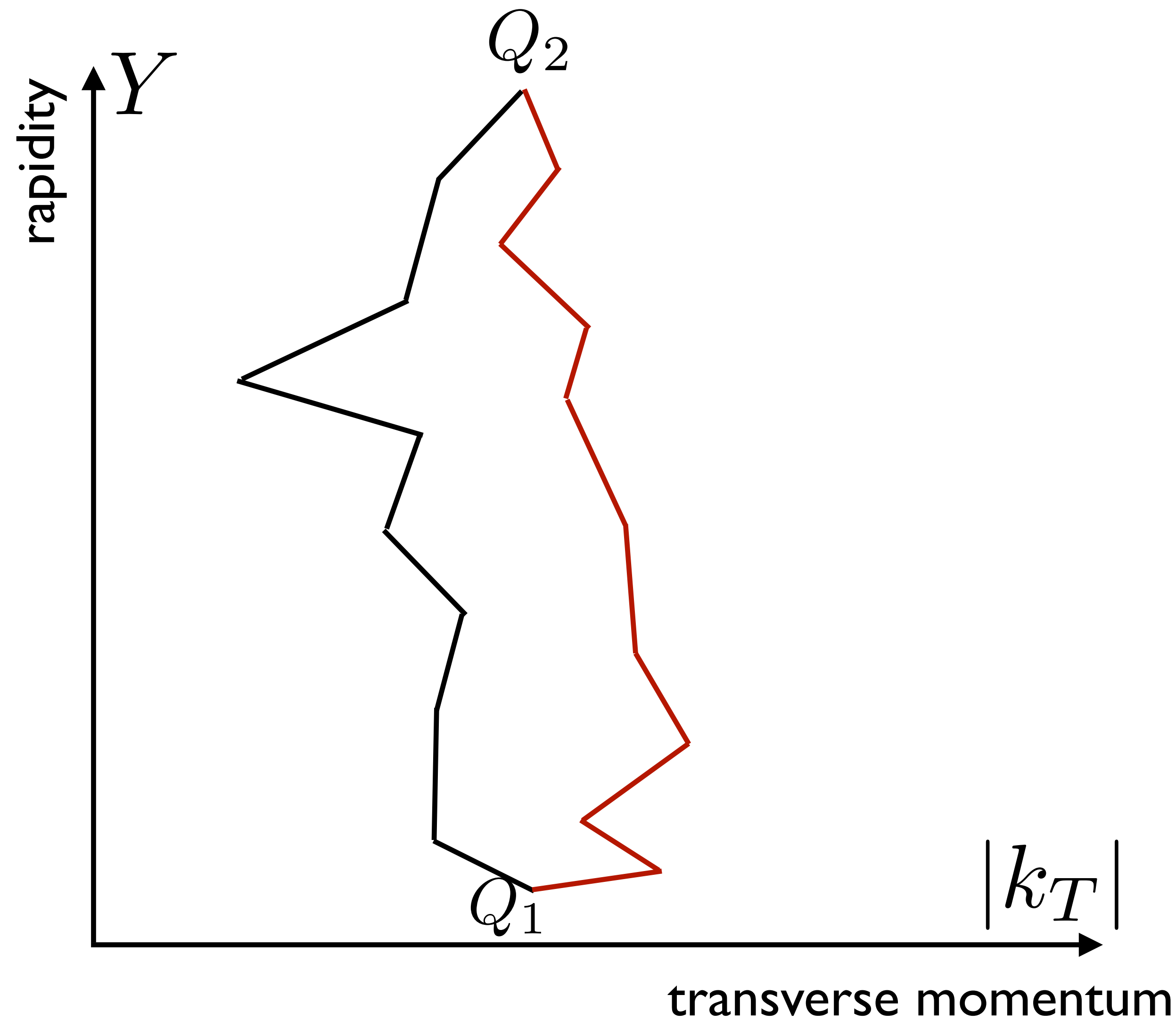

$$Y = \frac{1}{2} \ln \frac{p^+}{p^-}$$

Large non-perturbative effects for large energies.

High energy limit

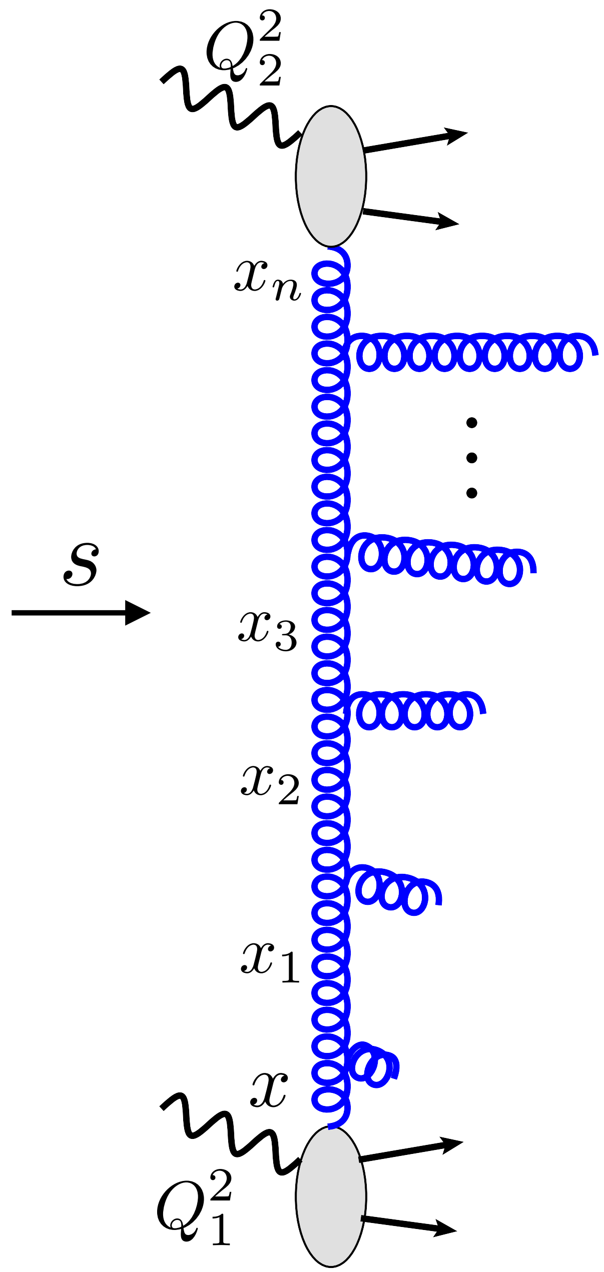

Effects of running coupling:
'pull' towards the infrared region

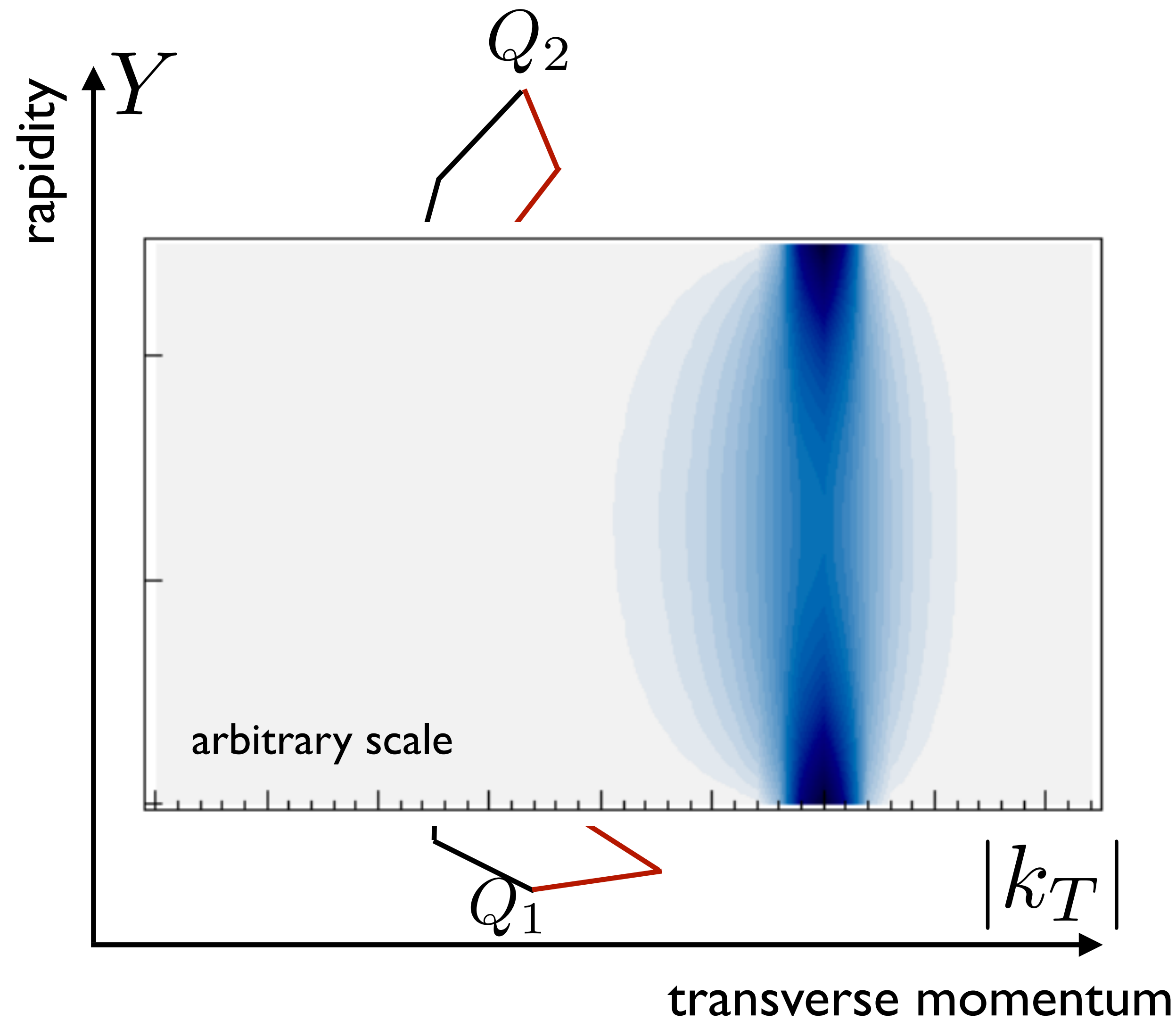

$$Y = \frac{1}{2}\ln\frac{p^+}{p^-}$$

Large non-perturbative effects for large energies.

BFKL solution

BFKL solution

BFKL evolution equation

$$\boxed{\frac{\partial \mathcal{F}_g(x,k_T)}{\partial \ln 1/x} = \int d^2k_T' \, \mathcal{K}(k_T,k_T')\, \mathcal{F}_g(x,k_T')}$$

Solution: $\mathcal{F}_g(x,k_T) \sim x^{-\omega_{IP}}$ Rise of cross sections: $\sigma^{\gamma^* p} \sim s^{\omega_{IP}}$

Pomeron intercept $\omega_{IP}^{LLx} = \bar{\alpha}_s 4 \ln 2$ leading logarithmic

BFKL solution

BFKL evolution equation

$$\frac{\partial \mathcal{F}_g(x,k_T)}{\partial \ln 1/x} = \int d^2k'_T \, \mathcal{K}(k_T,k'_T)\, \mathcal{F}_g(x,k'_T)$$

Solution: $\mathcal{F}_g(x,k_T) \sim x^{-\omega_{IP}}$ Rise of cross sections: $\sigma^{\gamma^* p} \sim s^{\omega_{IP}}$

Pomeron intercept

$\omega_{IP}^{LLx} = \bar{\alpha}_s 4\ln 2$ leading logarithmic

$\omega_{IP}^{NLLx} \simeq \bar{\alpha}_s 4\ln 2(1-6.5\bar{\alpha}_s)$ next-to-leading logarithmic

BFKL solution

BFKL evolution equation

$$\frac{\partial \mathcal{F}_g(x,k_T)}{\partial \ln 1/x} = \int d^2k'_T \, \mathcal{K}(k_T,k'_T) \, \mathcal{F}_g(x,k'_T)$$

Solution: $\mathcal{F}_g(x,k_T) \sim x^{-\omega_{IP}}$ Rise of cross sections: $\sigma^{\gamma^* p} \sim s^{\omega_{IP}}$

Pomeron intercept

$\omega_{IP}^{LLx} = \bar{\alpha}_s 4 \ln 2$ leading logarithmic

$\omega_{IP}^{NLLx} \simeq \bar{\alpha}_s 4 \ln 2 (1 - 6.5\bar{\alpha}_s)$ next-to-leading logarithmic

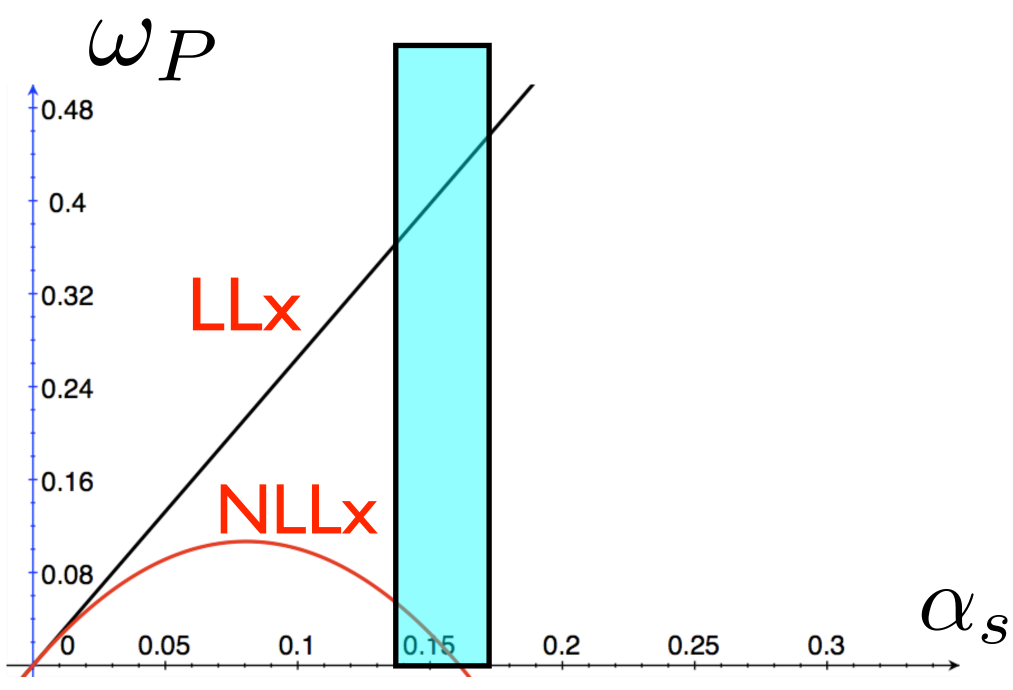

relevant values

BFKL solution

BFKL evolution equation

$$\frac{\partial \mathcal{F}_g(x,k_T)}{\partial \ln 1/x} = \int d^2k'_T\,\mathcal{K}(k_T,k'_T)\,\mathcal{F}_g(x,k'_T)$$

Solution: $\mathcal{F}_g(x,k_T) \sim x^{-\omega_{IP}}$

Rise of cross sections: $\sigma^{\gamma^* p} \sim s^{\omega_{IP}}$

Pomeron intercept

$\omega_{IP}^{LLx} = \bar{\alpha}_s 4\ln 2$ leading logarithmic

$\omega_{IP}^{NLLx} \simeq \bar{\alpha}_s 4\ln 2(1-6.5\bar{\alpha}_s)$ next-to-leading logarithmic

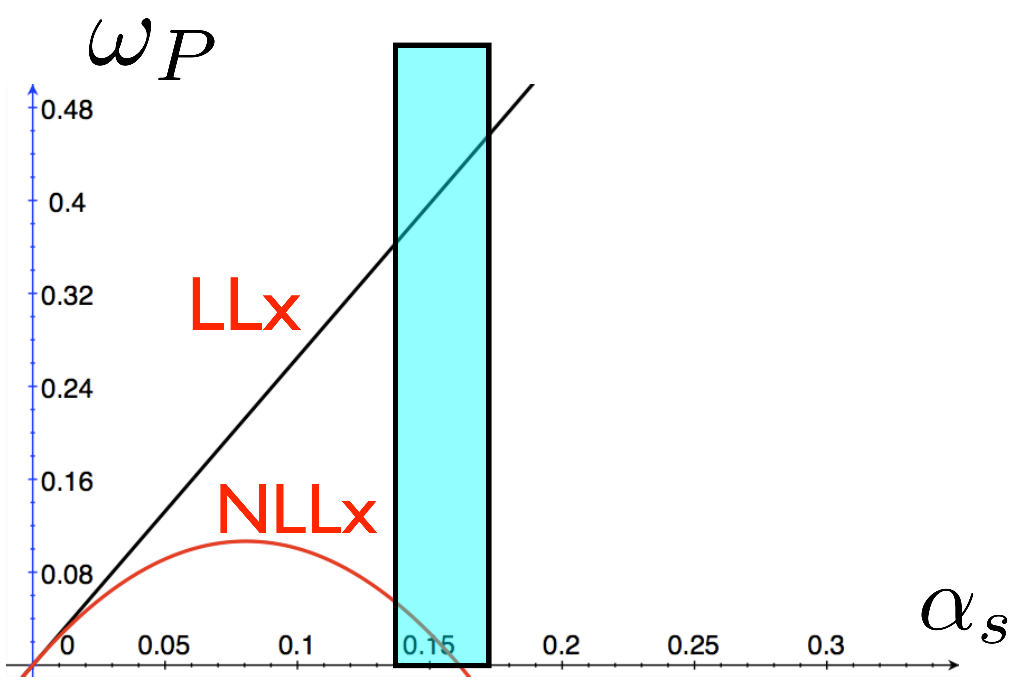

relevant values

LLx vs NLLx BFKL solution for the gluon Green's function

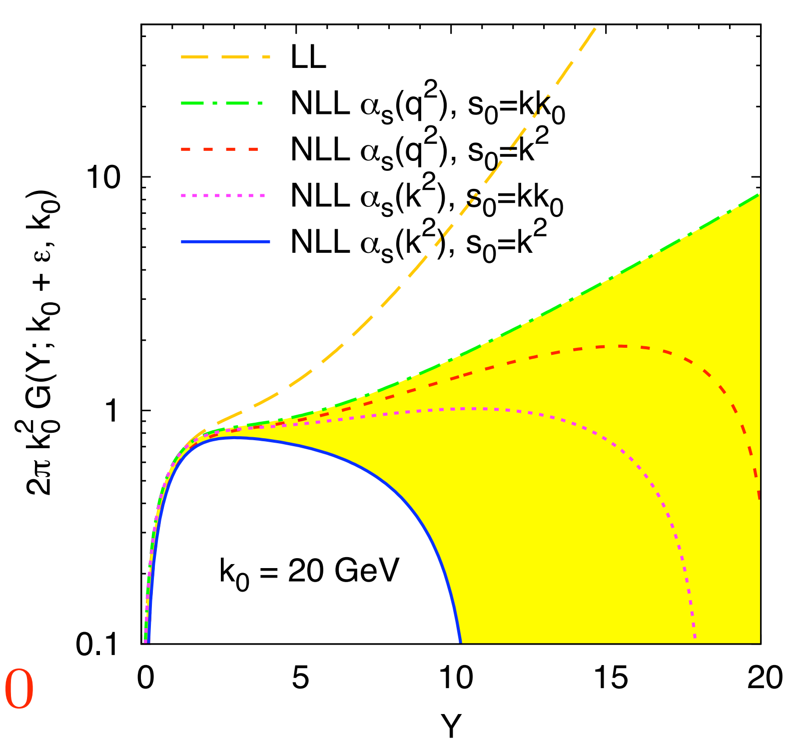

$Y = \ln s/s_0$

BFKL solution

BFKL evolution equation

$$\frac{\partial \mathcal{F}_g(x,k_T)}{\partial \ln 1/x} = \int d^2k'_T\, \mathcal{K}(k_T,k'_T)\, \mathcal{F}_g(x,k'_T)$$

Solution: $\mathcal{F}_g(x,k_T) \sim x^{-\omega_{IP}}$ Rise of cross sections: $\sigma^{\gamma^* p} \sim s^{\omega_{IP}}$

Pomeron intercept

$\omega_{IP}^{LLx} = \bar{\alpha}_s 4 \ln 2$ leading logarithmic

$\omega_{IP}^{NLLx} \simeq \bar{\alpha}_s 4 \ln 2 (1 - 6.5 \bar{\alpha}_s)$ next-to-leading logarithmic

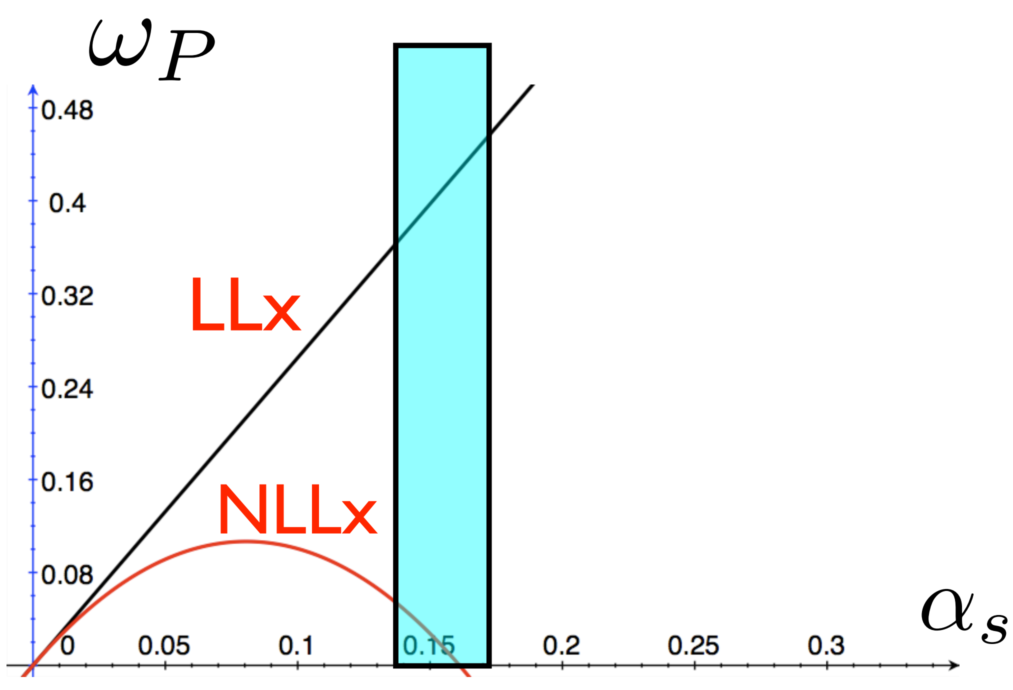

relevant values

LLx vs NLLx BFKL solution for the gluon Green's function

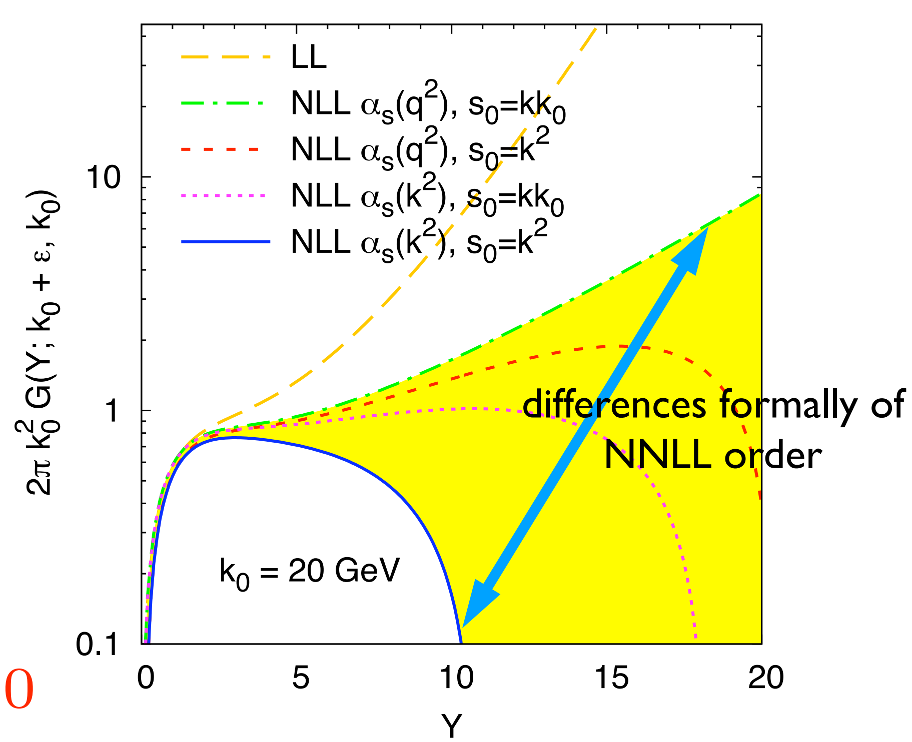

$Y = \ln s/s_0$

BFKL solution

BFKL evolution equation

$$\frac{\partial \mathcal{F}_g(x,k_T)}{\partial \ln 1/x} = \int d^2k'_T\, \mathcal{K}(k_T,k'_T)\, \mathcal{F}_g(x,k'_T)$$

Solution: $\mathcal{F}_g(x,k_T) \sim x^{-\omega_{IP}}$ Rise of cross sections: $\sigma^{\gamma^* p} \sim s^{\omega_{IP}}$

Pomeron intercept

$\omega_{IP}^{LLx} = \bar{\alpha}_s 4 \ln 2$ leading logarithmic

$\omega_{IP}^{NLLx} \simeq \bar{\alpha}_s 4 \ln 2 (1 - 6.5\bar{\alpha}_s)$ next-to-leading logarithmic

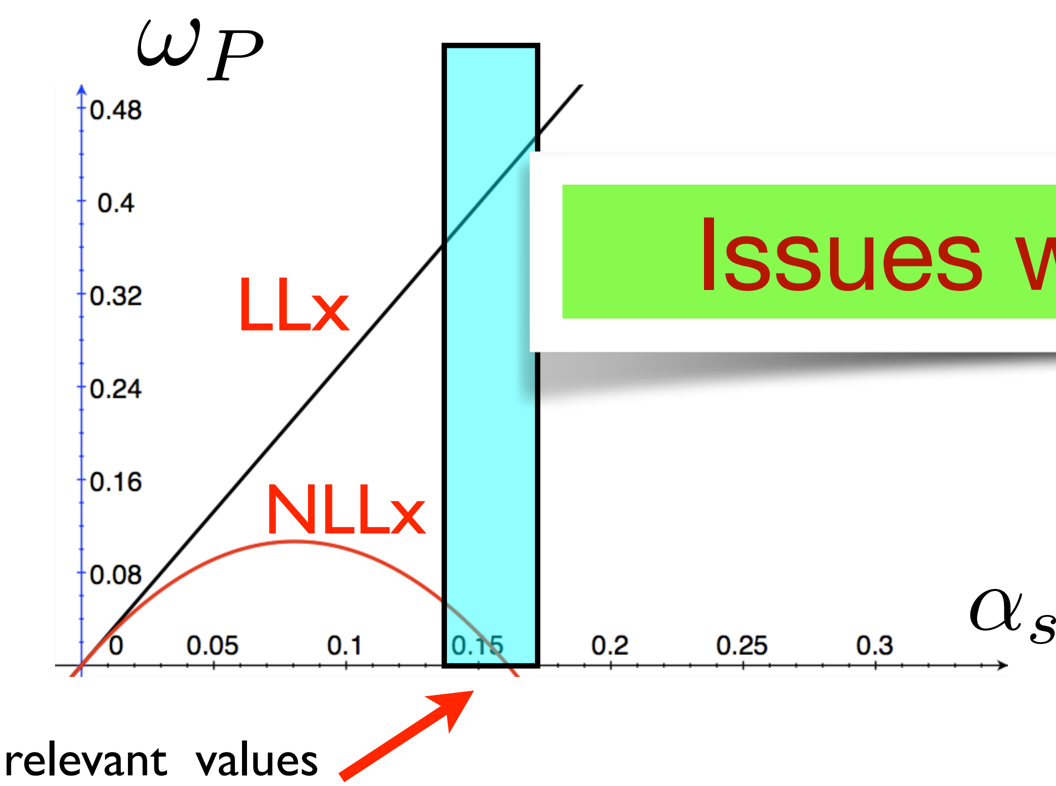

Issues with convergence…

LLx vs NLLx BFKL solution for the gluon Green's function

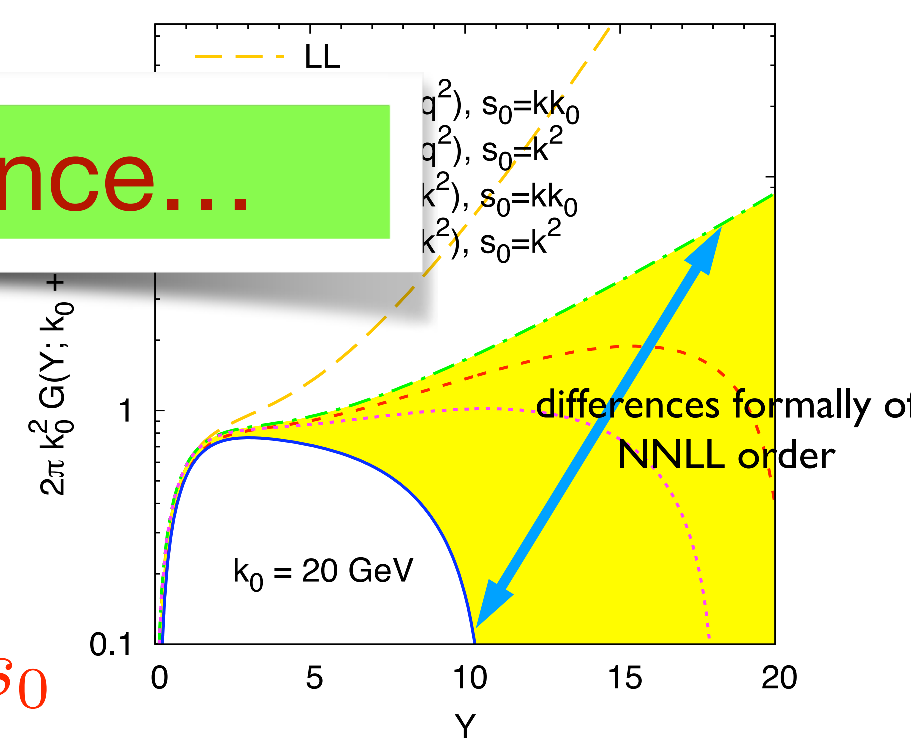

$Y = \ln s/s_0$

Low x resummation

Ciafaloni, Colferai, Salam, AS
Altarelli, Ball, Forte; Thorne; Thorne, White

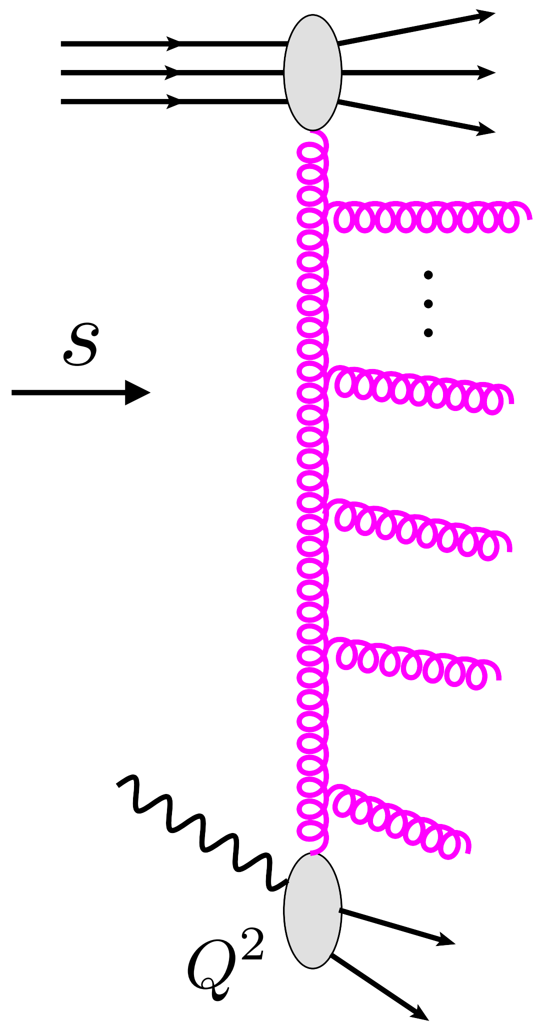

Combine the information from both expansions

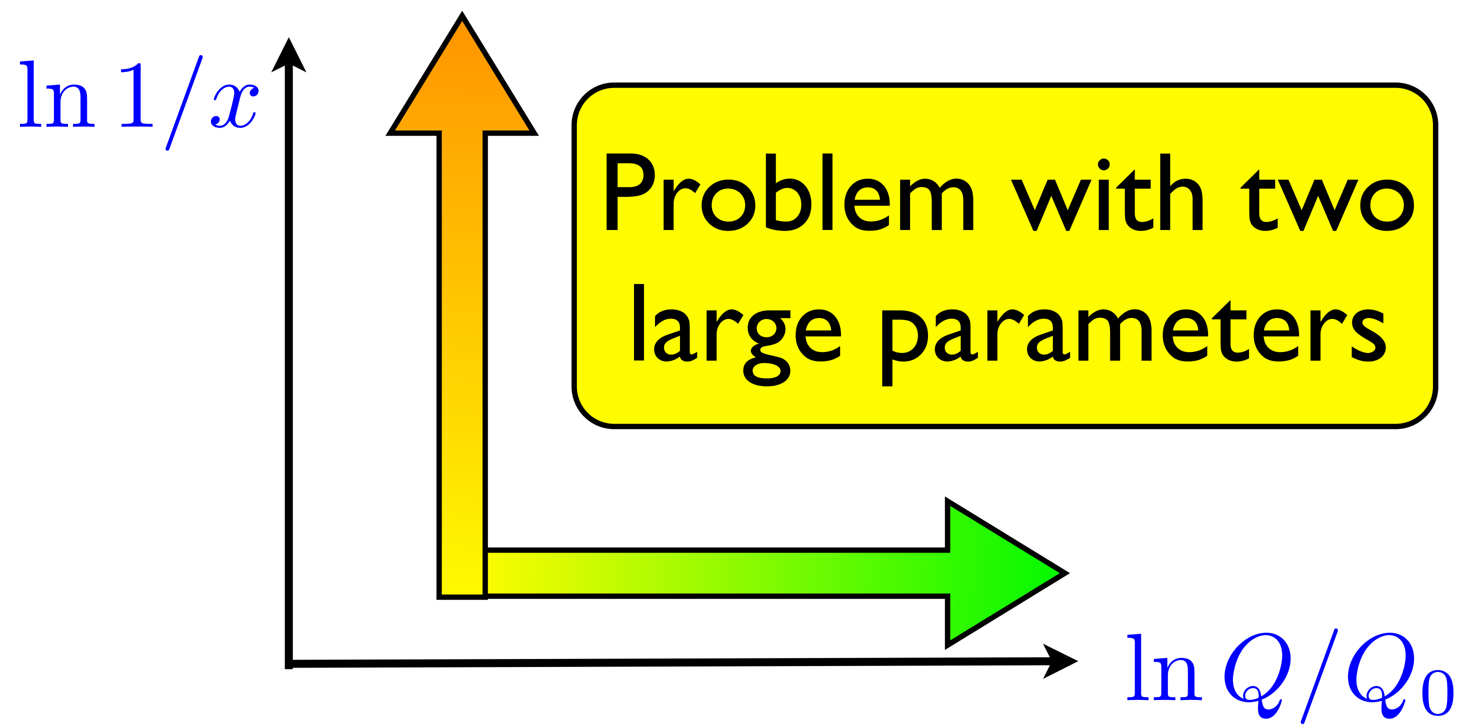

$$\left(\frac{\alpha_s N_c}{\pi} \ln \frac{1}{x}\right)^n$$ logarithms of energy

$$\left(\frac{\alpha_s N_c}{\pi} \ln \frac{Q}{Q_0}\right)^n$$ logarithms of scale (related to transverse momentum)

General setup for resummation

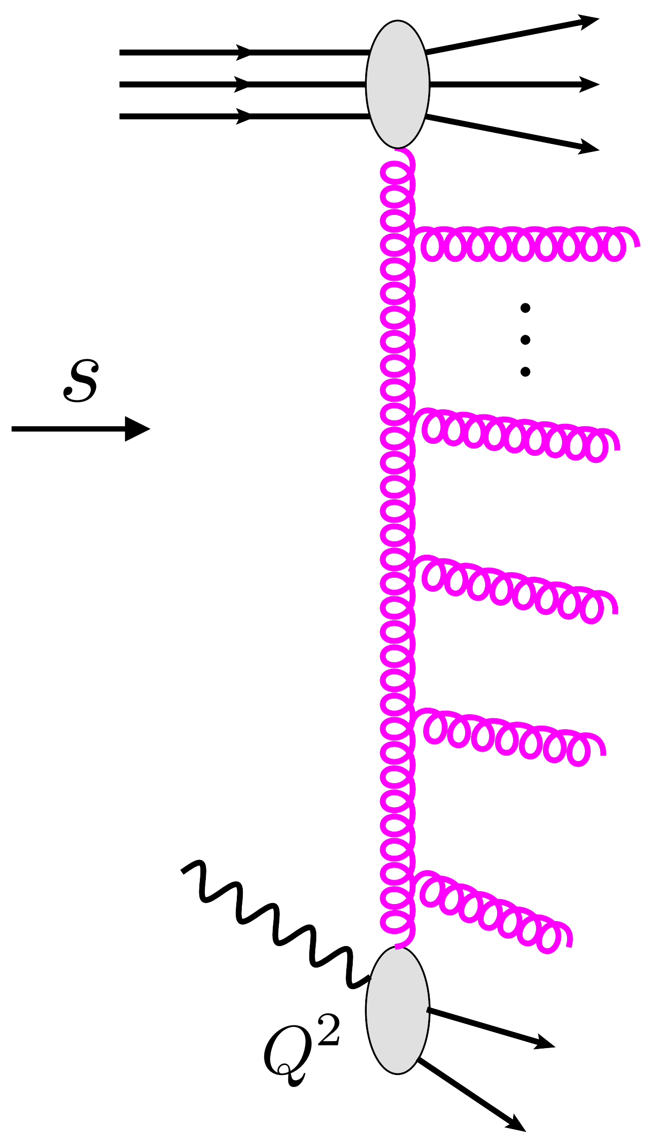

- Kinematical constraints: impose constraints coming from the kinematics by the analysis of individual diagrams.
- DGLAP splitting function recovered at fixed order of large logarithms of scale.
- LLx and NLLx BFKL terms are included.
- Subtraction procedure in order to avoid the double counting.
- Momentum sum rule for the resummed splitting function must be satisfied.
- Running coupling in the BFKL evolution.

Resummation: results

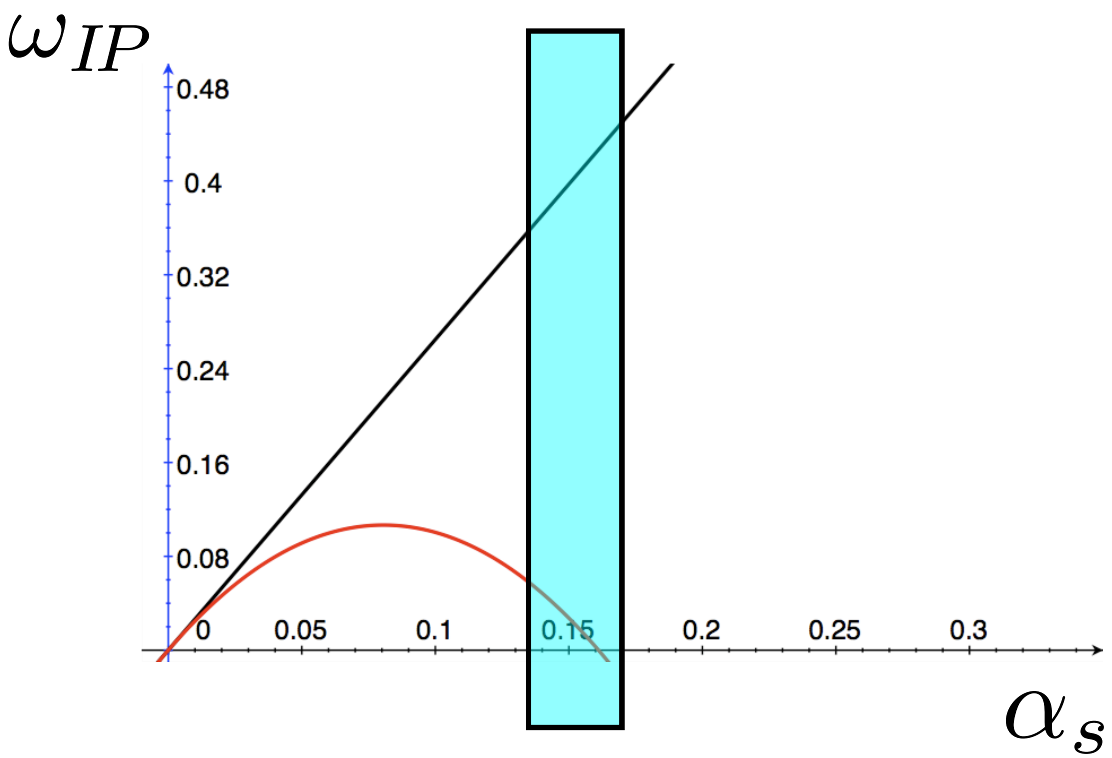

$$\mathcal{F}_g(x, k_T) \sim x^{-\omega_{IP}}$$

$$\sigma^{\gamma^* p} \sim s^{\omega_{IP}}$$

Stable result

$$\omega_{IP} \sim 0.2 - 0.3$$

Significant reduction with respect to LLx

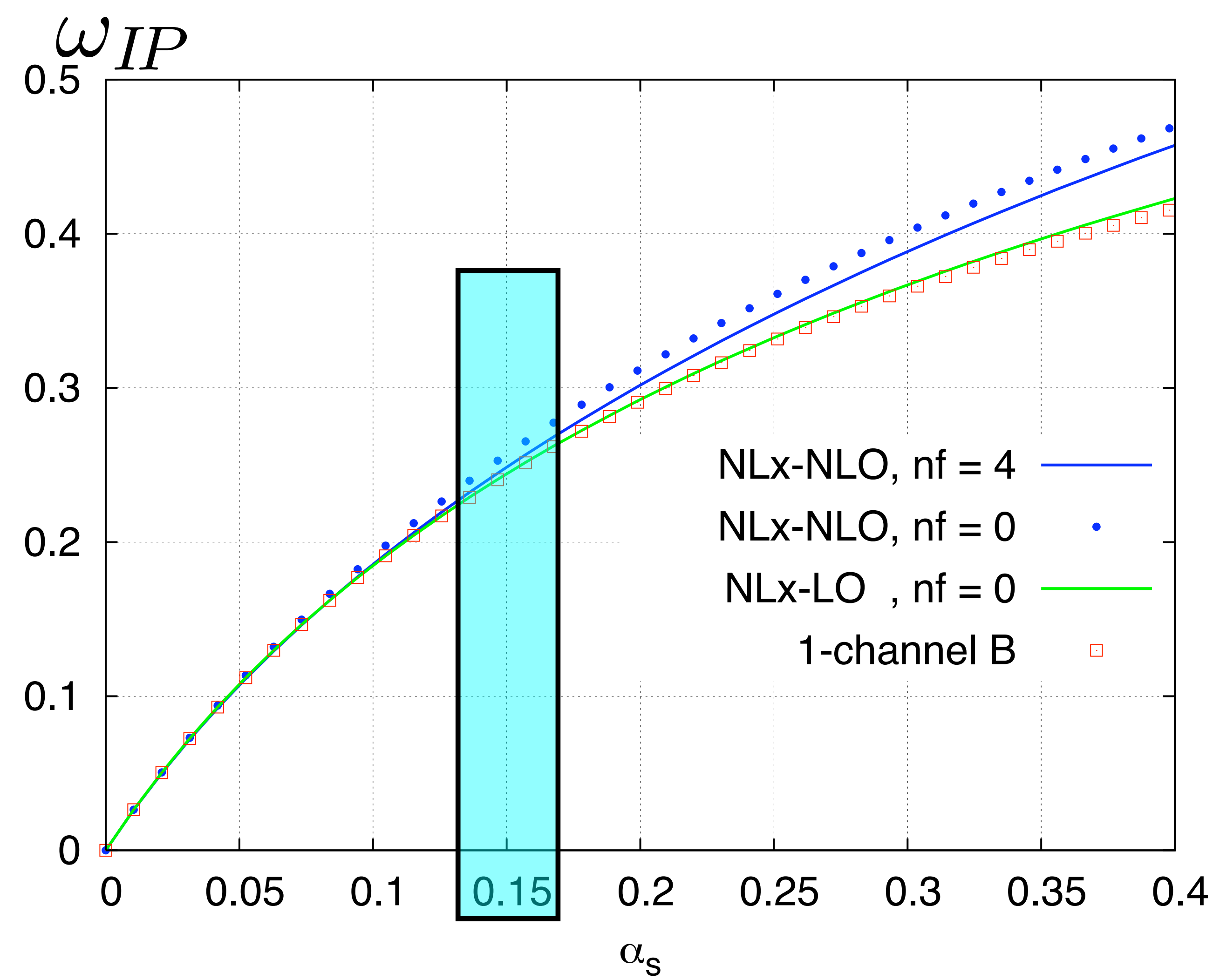

Ciafaloni, Colferai, Salam, AS

Resummation impact on the DIS data

Ball,Bertoni,Bonvini,Marzani,Rojo,Rottoli

move the cutoff to include more data

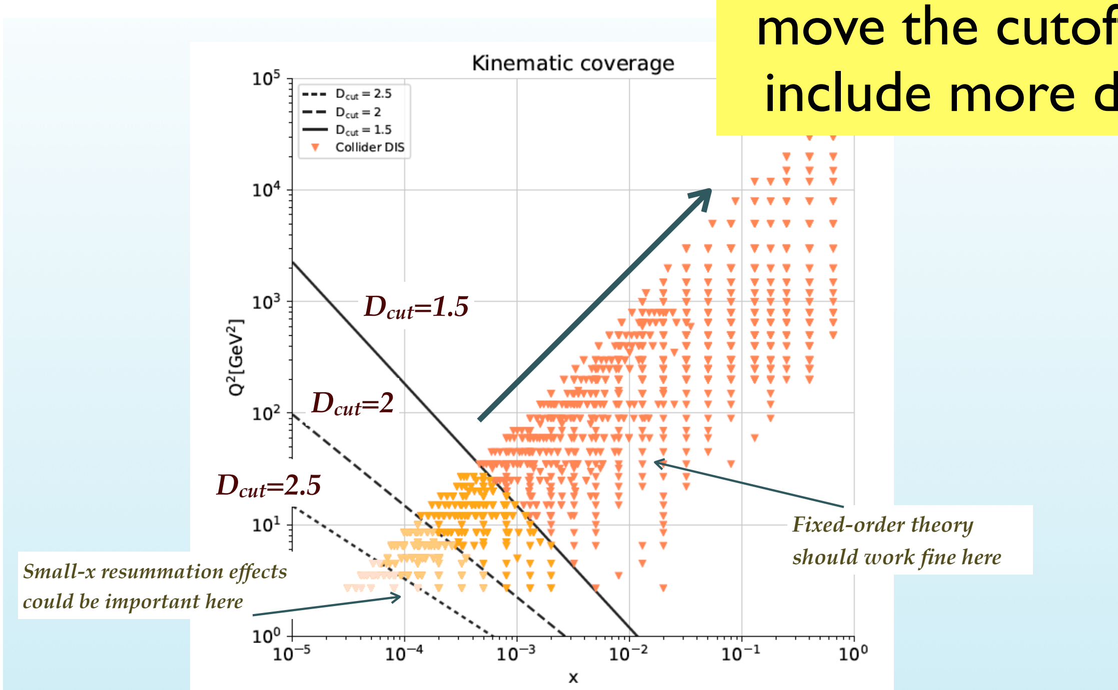

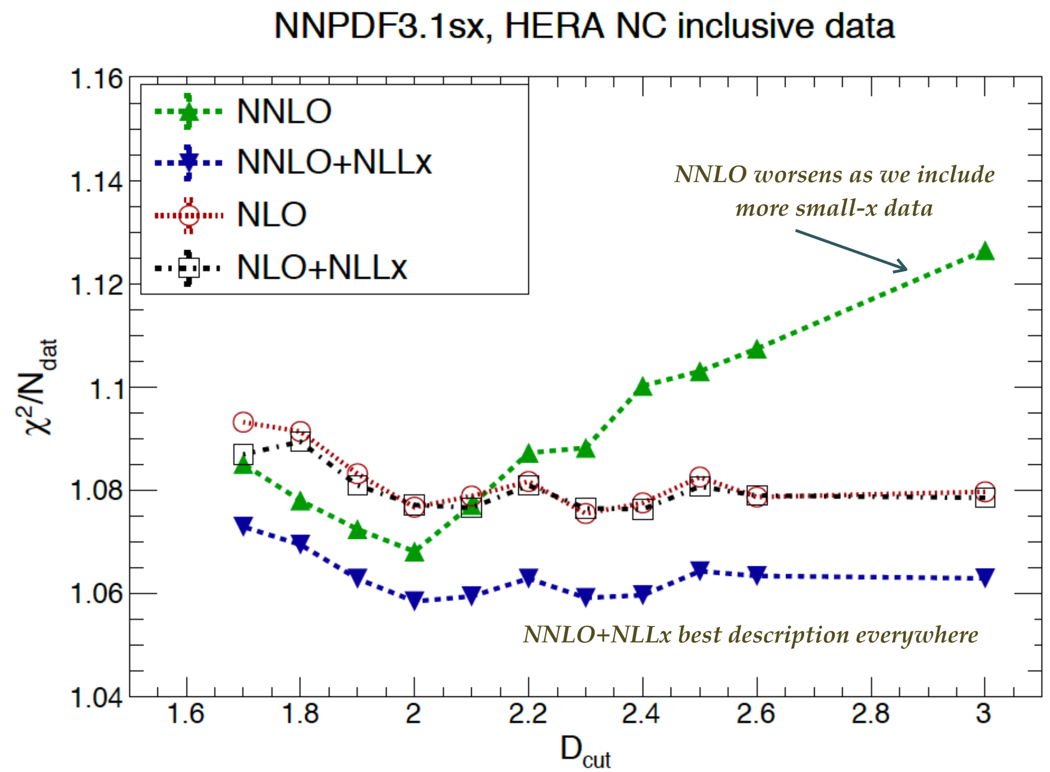

Resummation impact on the DIS data

Ball,Bertoni,Bonvini,Marzani,Rojo,Rottoli

move the cutoff to include more data

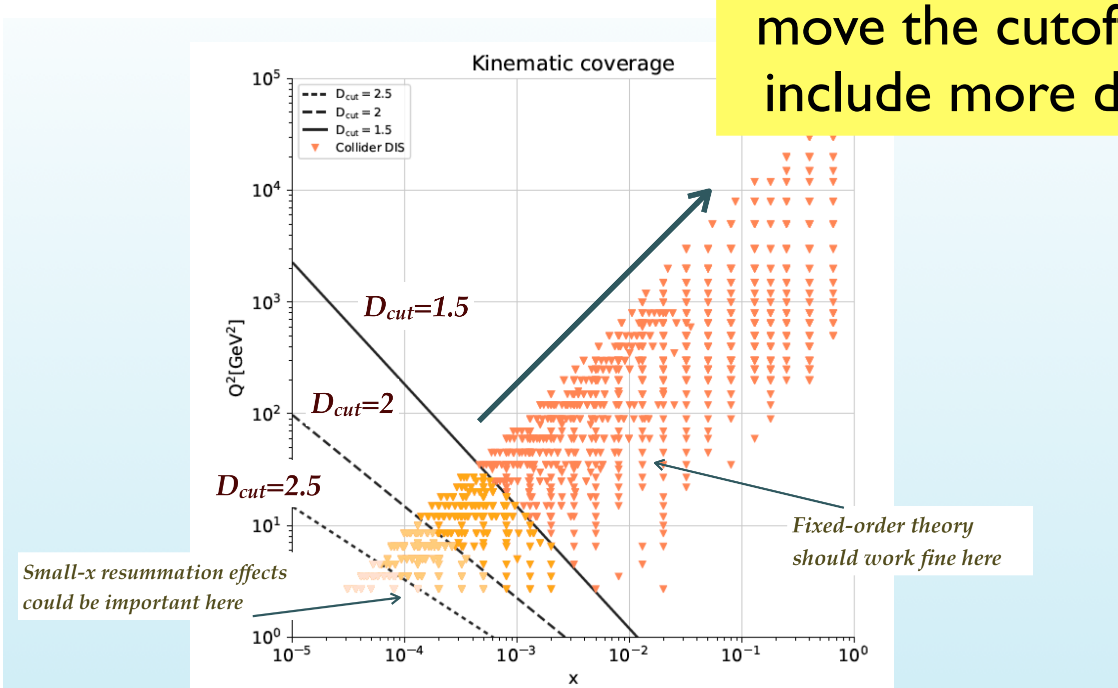

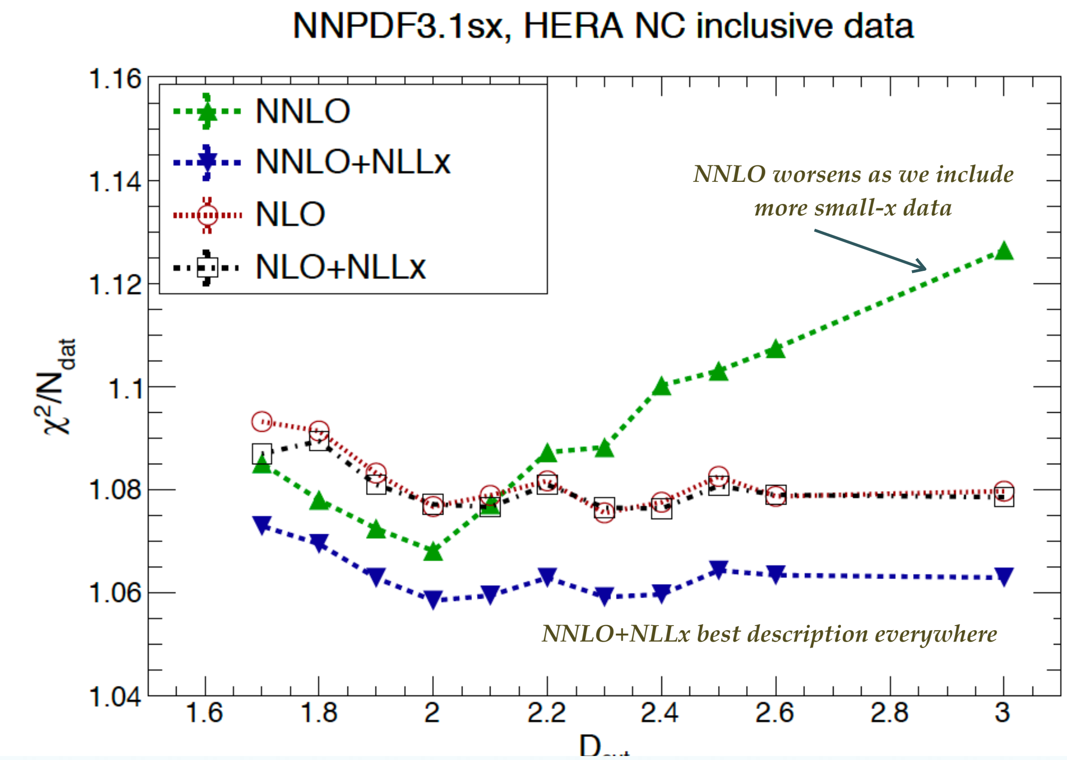

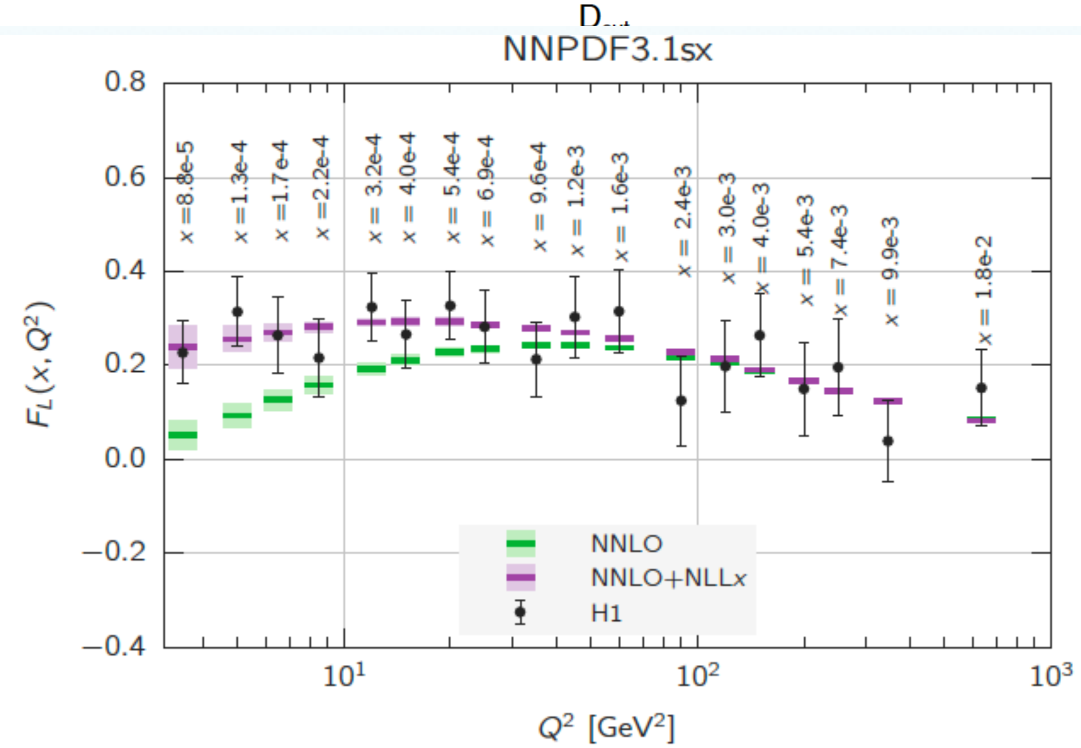

Resummation leads to the improvement the description of the structure function data F_2 for low x and Q.

Better than fixed order NLO, NNLO.

Better description of the longitudinal structure function F_L.

Big 'small x' problem

Gedankenexperiment: proton colliding at high energy with some small probe

Virtual photon is a probe
which fluctuates into
quark-antiquark pair

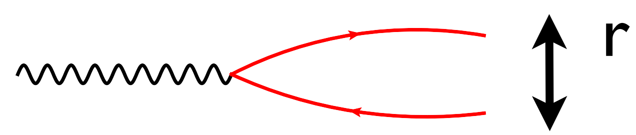

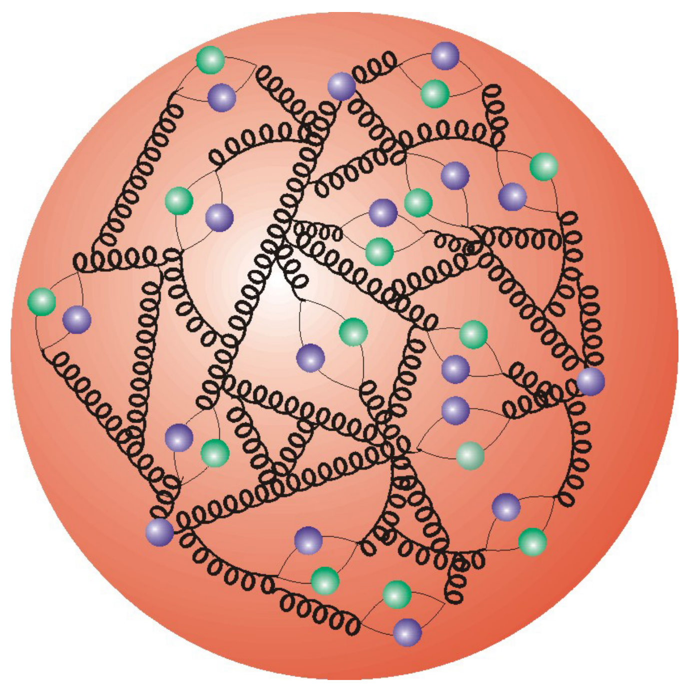

Big 'small x' problem

Gedankenexperiment: proton colliding at high energy with some small probe

Virtual photon is a probe
which fluctuates into
quark-antiquark pair

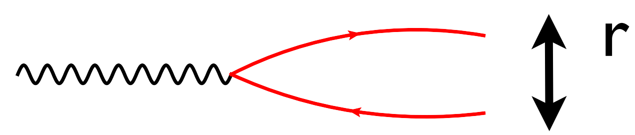

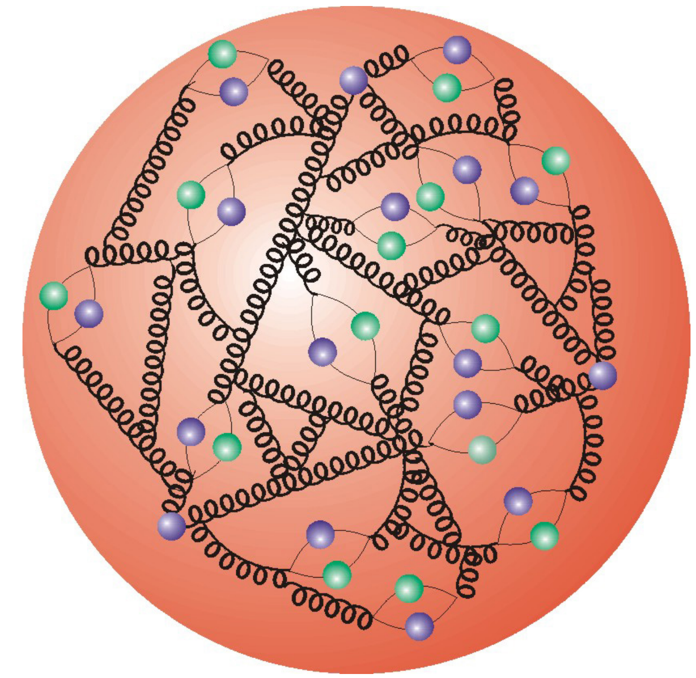

Probability of interaction:

$$P \sim \alpha_s \, r^2 \, x^{-\lambda} \frac{1}{S_T}$$

coupling constant

transverse area (of the probe)

density

Big ‘small x’ problem

Gedankenexperiment: proton colliding at high energy with some small probe

Virtual photon is a probe which fluctuates into quark-antiquark pair

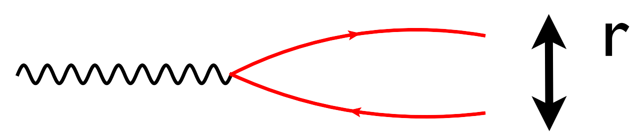

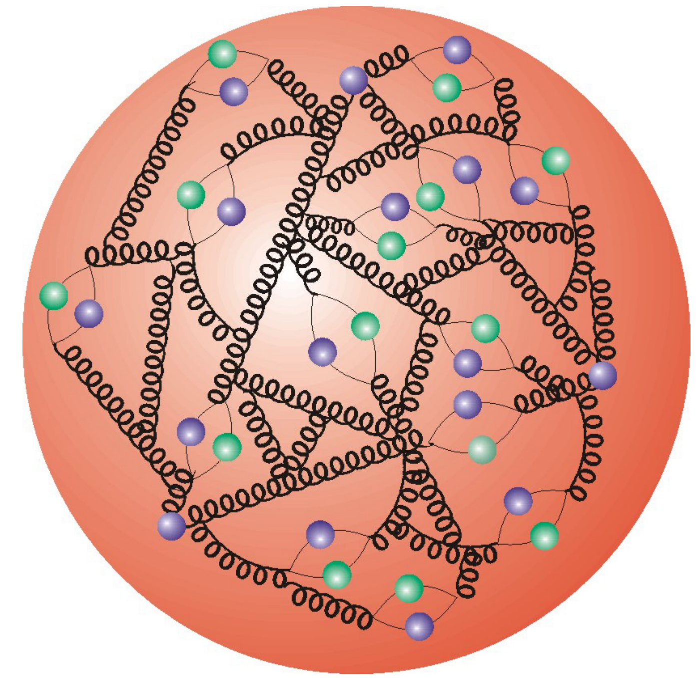

Probability of interaction:

$$P \sim \alpha_s \, r^2 \, x^{-\lambda} \frac{1}{S_T}$$

coupling constant

transverse area (of the probe)

density

$$r^2 \sim \frac{1}{Q^2}$$

Q typical scale in the process

Big 'small x' problem

Gedankenexperiment: proton colliding at high energy with some small probe

Virtual photon is a probe which fluctuates into quark-antiquark pair

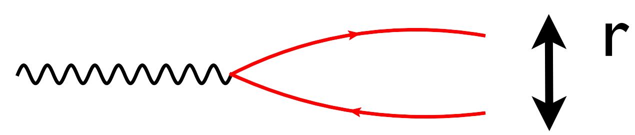

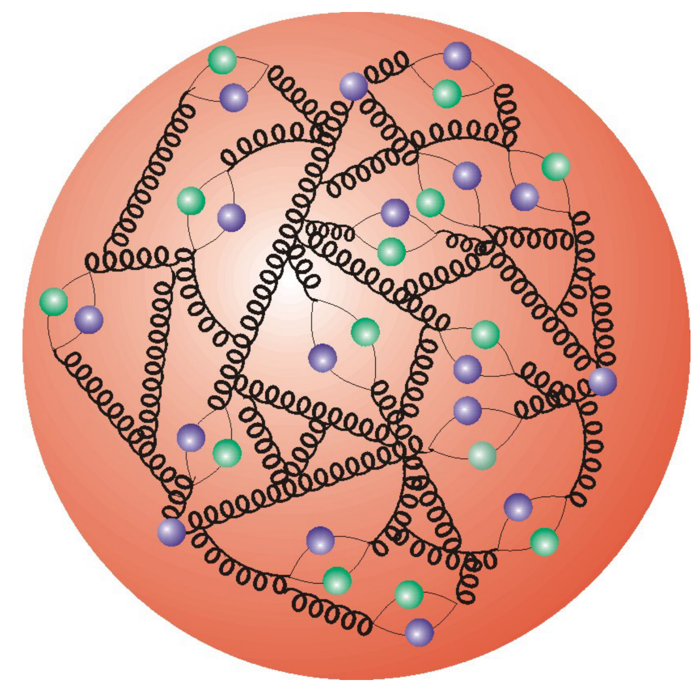

Probability of interaction:

$$P \sim \alpha_s \, r^2 \, x^{-\lambda} \frac{1}{S_T}$$

coupling constant

transverse area (of the probe)

density

$$r^2 \sim \frac{1}{Q^2}$$

Q typical scale in the process

- Probability of interaction becomes very large.
- Totally absorbing target: black disk limit.
- Possible multiple interactions between the probe and the target.
- Possibility of the saturation of the gluon density.

Unitarity and high parton density

Probability of interaction in QCD at high energy

$$\mathcal{P} \sim 1$$

Need to satisfy unitarity of scattering amplitudes

$$SS^\dagger = S^\dagger S = 1$$

Need to take into account contributions from more complicated interactions: two, three, four etc. interactions possible and likely

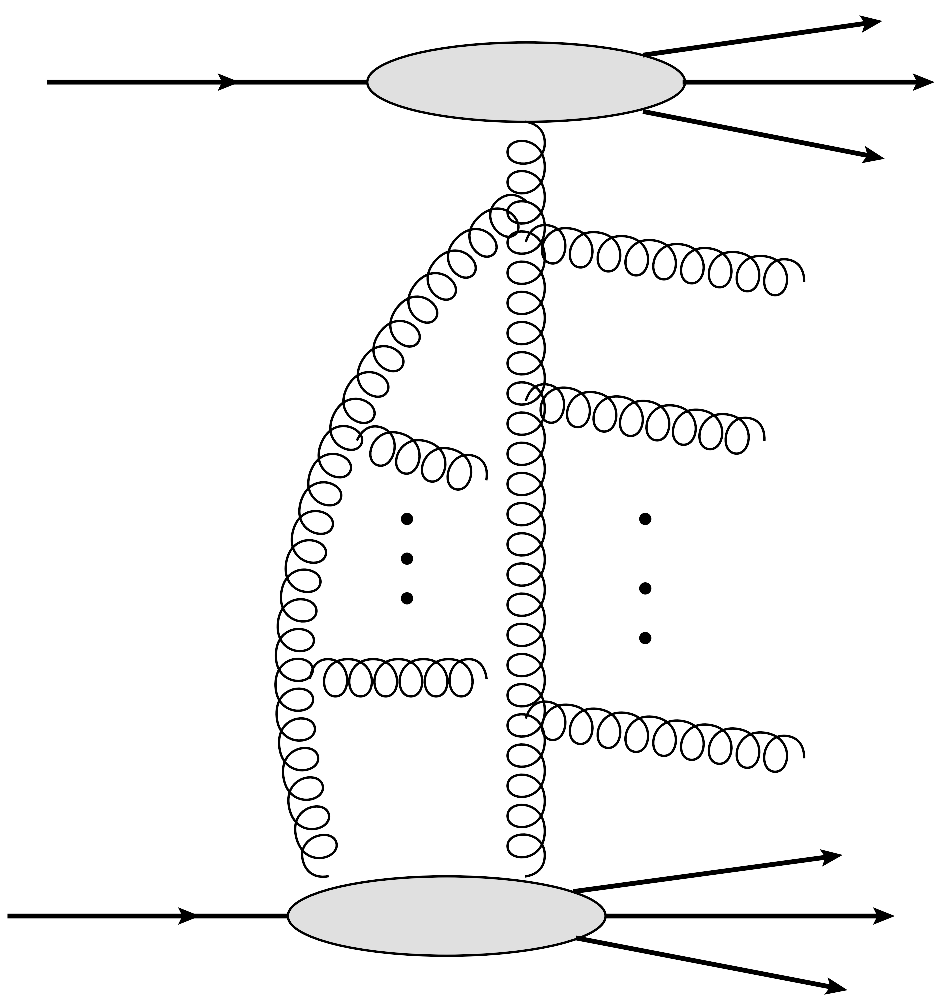

Unitarity and high parton density

Probability of interaction in QCD
at high energy

$$\mathcal{P} \sim 1$$

Need to satisfy unitarity
of scattering amplitudes

$$SS^\dagger = S^\dagger S = 1$$

Need to take into account contributions from more complicated interactions: two, three, four etc. interactions possible and likely

Density or nonlinear effects:

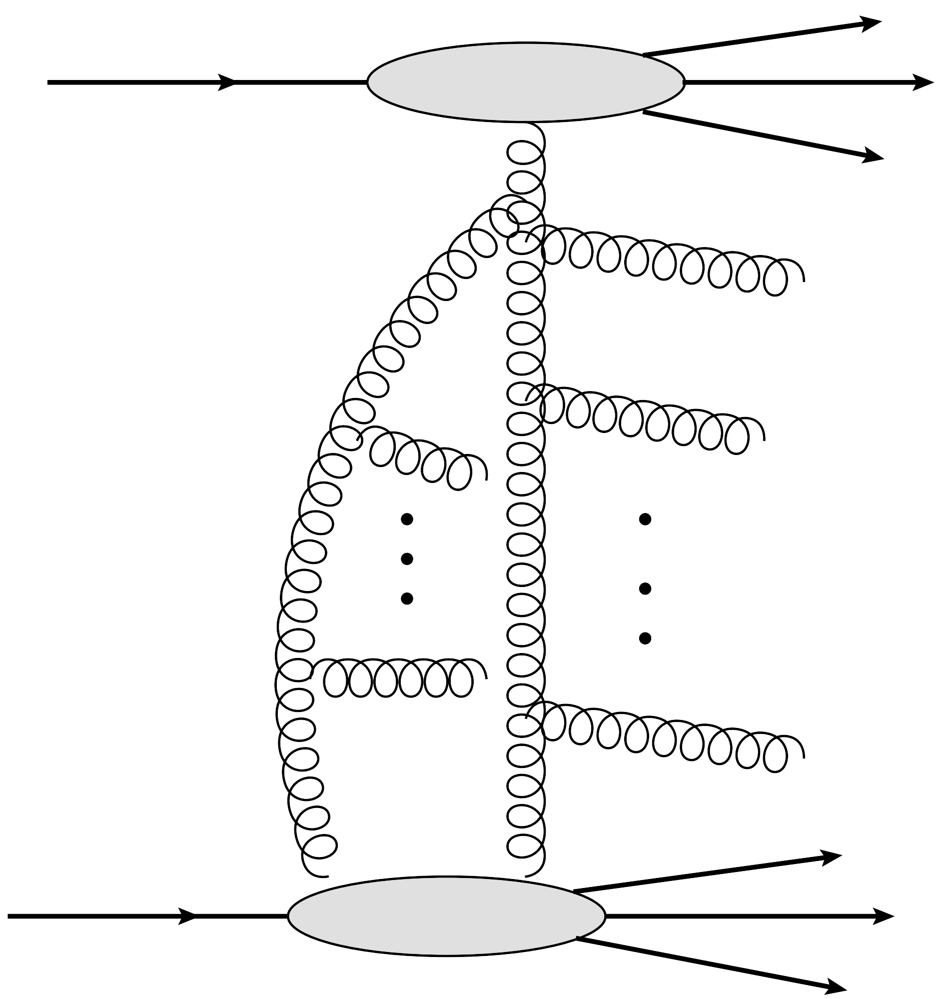

Unitarity and high parton density

Probability of interaction in QCD
at high energy

$$\mathcal{P} \sim 1$$

Need to satisfy unitarity
of scattering amplitudes

$$SS^\dagger = S^\dagger S = 1$$

Need to take into account contributions from more complicated interactions: two, three, four etc. interactions possible and likely

Density or nonlinear effects:

Multi-parton interactions
Gluon saturation

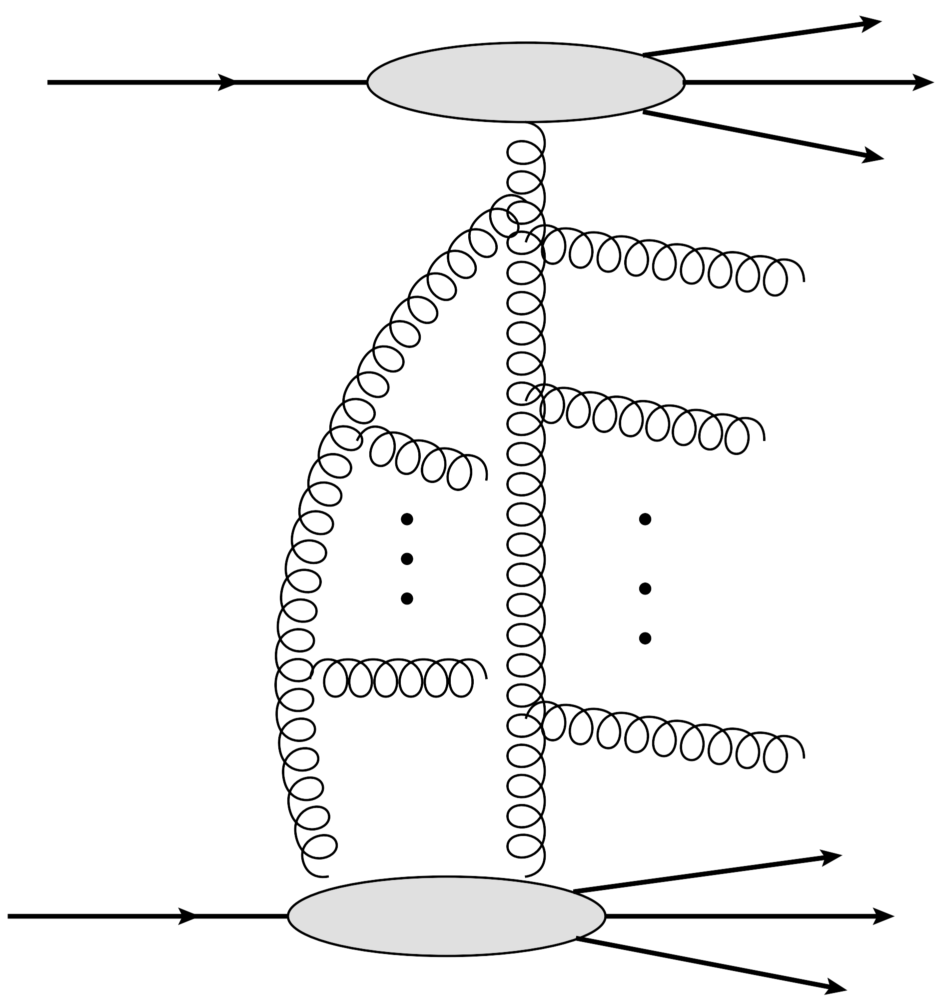

Dipole picture

Dipole picture: suitable for small x physics (related to high energy factorization)

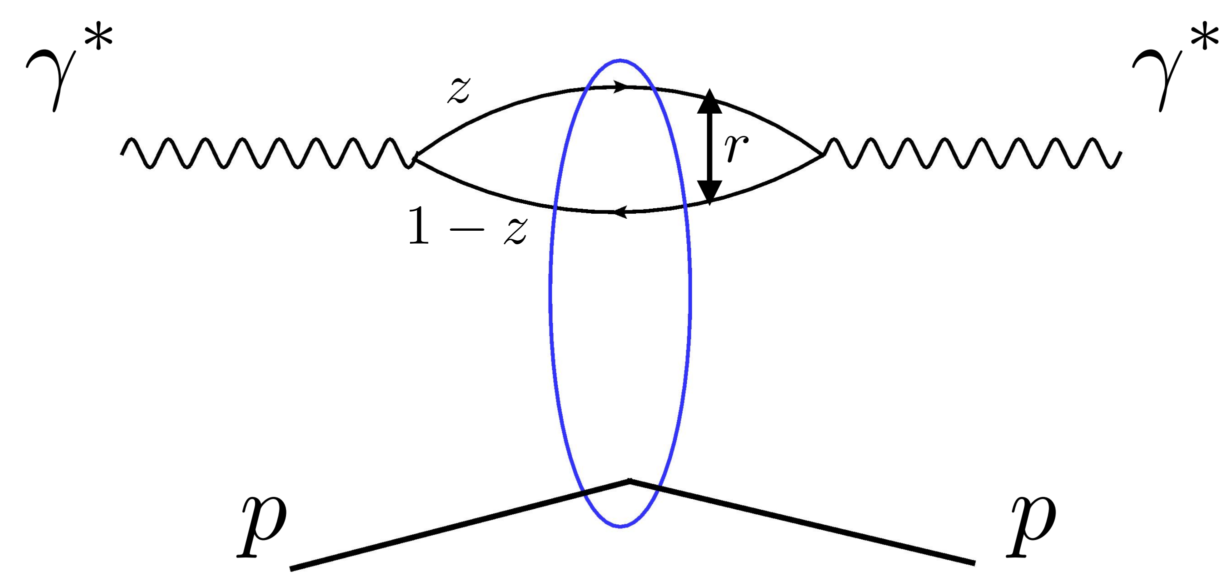

Cross section is calculated from the photon wave function and the dipole amplitude

$$\sigma_{T,L}(x,Q^2) = \int d^2\mathbf{r} \int_0^1 dz \int d^2\mathbf{b} \sum_f |\Psi^f_{T,L}(\mathbf{r},Q^2,z)|^2 2N(x,\mathbf{r},\mathbf{b})$$

z fraction of the lightcone momentum of the photon carried by the quark

$\mathbf{r}$ transverse size of the quark-antiquark dipole

$\mathbf{b}$ impact parameter

Ψ photon wave function

N dipole amplitude

Dipole picture especially suitable to address saturation. Multiple scattering of dipoles on a dense target.

Dipole picture

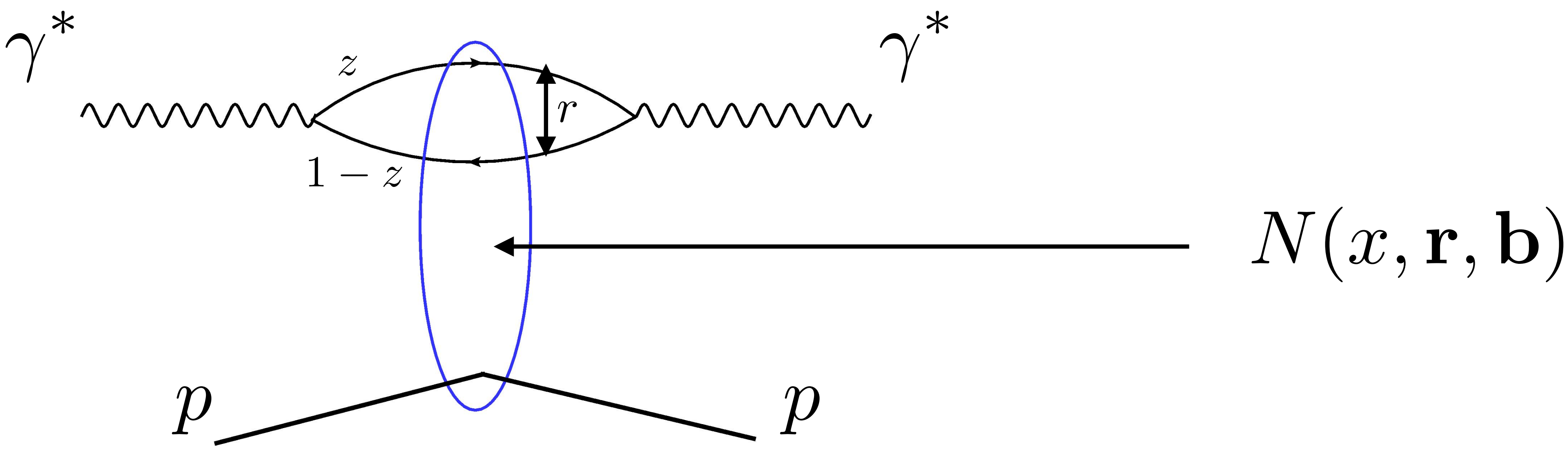

Dipole amplitude contains all the information about the interaction of the dipole with the target

When integrated over the impact parameter one obtains dipole cross section

$$\sigma(x, \mathbf{r}) = 2 \int d^2\mathbf{b}\, N(x, \mathbf{r}, \mathbf{b})$$

Dipole cross section

$$\sigma(x, \mathbf{r})$$

$$\longleftrightarrow$$

Unintegrated gluon density

$$\mathcal{F}_g(x, k_T)$$

How to calculate dipole cross section?

$\sigma(x, \mathbf{r})$

Dipole cross section can be parametrized or obtained from evolution equation (eg. BK)

Dipole model cross sections:

GBW
IP-sat
b-CGC
IIM
MV
FGS
...

QCD equations for dipole cross section(dipole amplitude):

BK equation
JIMWLK equation

Dipole cross section

Modeling dipole cross section $\sigma(x, \mathbf{r})$

Golec-Biernat and Wuesthoff model (GBW model)

$$\sigma(x,r) = \sigma_0 \left(1 - e^{-r^2 Q_s^2(x)/4}\right)$$

Saturation scale

$$Q_s^2(x) = Q_0^2 (x/x_0)^{-\lambda}$$

$\frac{r^2 Q_s^2(x)}{4} \ll 1$

dilute region

$$\sigma(x,r) \simeq \sigma_0 \frac{r^2 Q_s^2(x)}{4} \sim r^2 x^{-\lambda}$$

BFKL - like growth with a power

$\frac{r^2 Q_s^2(x)}{4} \gg 1$

dense region

Saturation

$$\sigma(x,r) \simeq \sigma_0$$

Saturation scale provides boundary between **dense** and *dilute* regions

Dipole cross section: GBW model

Golec-Biernat and Wuesthoff model (GBW model)

$$\sigma(x,r) = \sigma_0 \left(1 - e^{-r^2 Q_s^2(x)/4}\right)$$

Saturation scale

$$Q_s^2(x) = Q_0^2 (x/x_0)^{-\lambda}$$

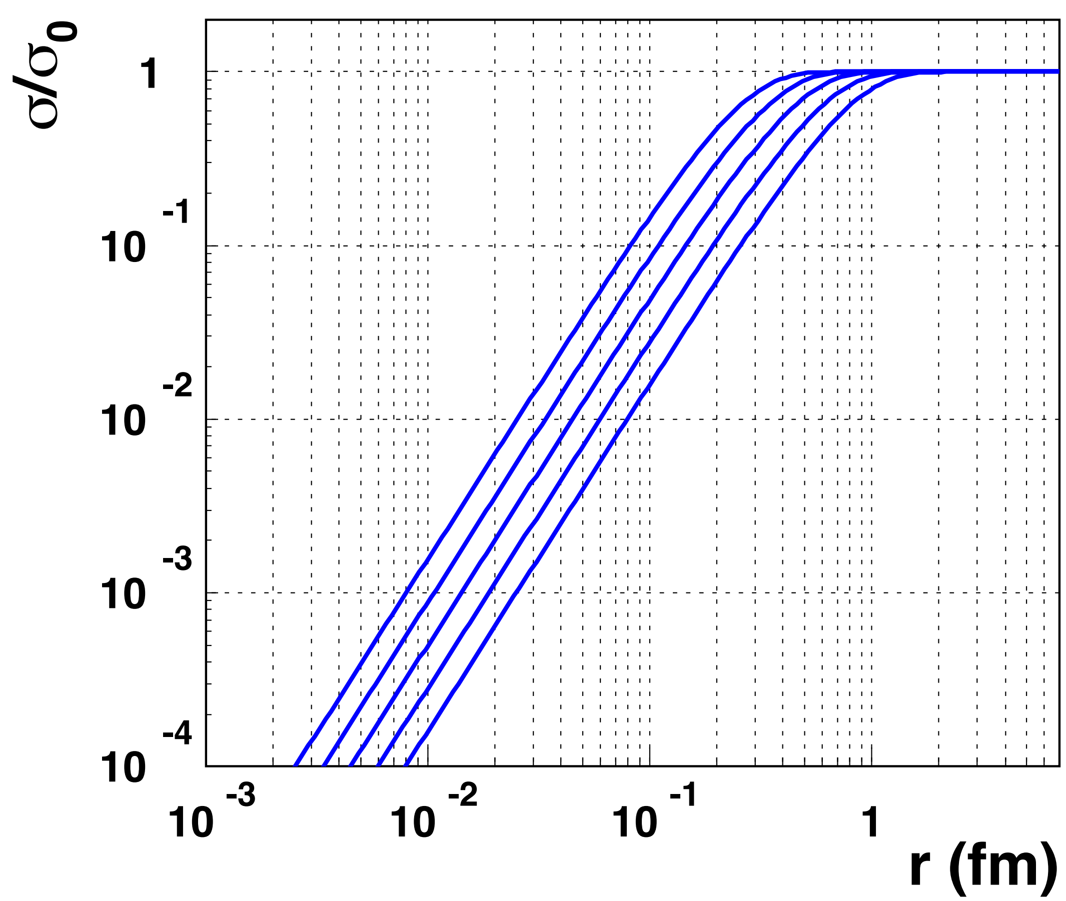

$$\lambda \simeq 0.27 - 0.28$$

$$Q_0 = 1\,\mathrm{GeV}$$

$$x_0 = 0.4 - 2.2 \times 10^{-4}$$

$$\sigma_0 = 23 - 30 \text{ mb}$$

curves from left to right

$$x = 10^{-6}, 10^{-5}, 10^{-4}, 10^{-3}, 10^{-2}$$

Dipole cross section: GBW model

Golec-Biernat and Wuesthoff model (GBW model)

$$\sigma(x,r) = \sigma_0 \left(1 - e^{-r^2 Q_s^2(x)/4}\right)$$

Effectively function of one combined variable

$$\sigma(x,r) = \sigma(rQ_s(x))$$

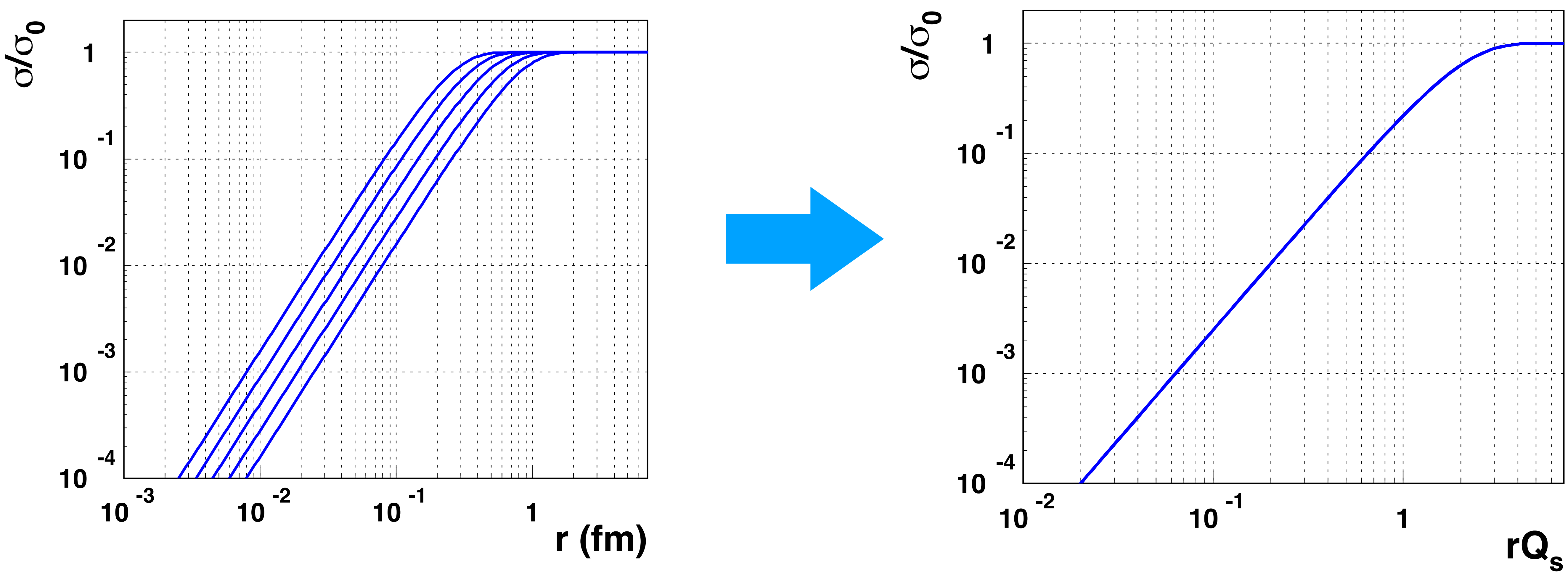

Geometric scaling: dependence on the combination of $rQ_s(x)$

GBW model: description of HERA data

Description of the data in the original GBW model (1998)

$$\sigma^{\gamma^* p}(x,Q^2) = \frac{4\pi^2 \alpha_{em}}{Q^2} F_2(x,Q^2)$$

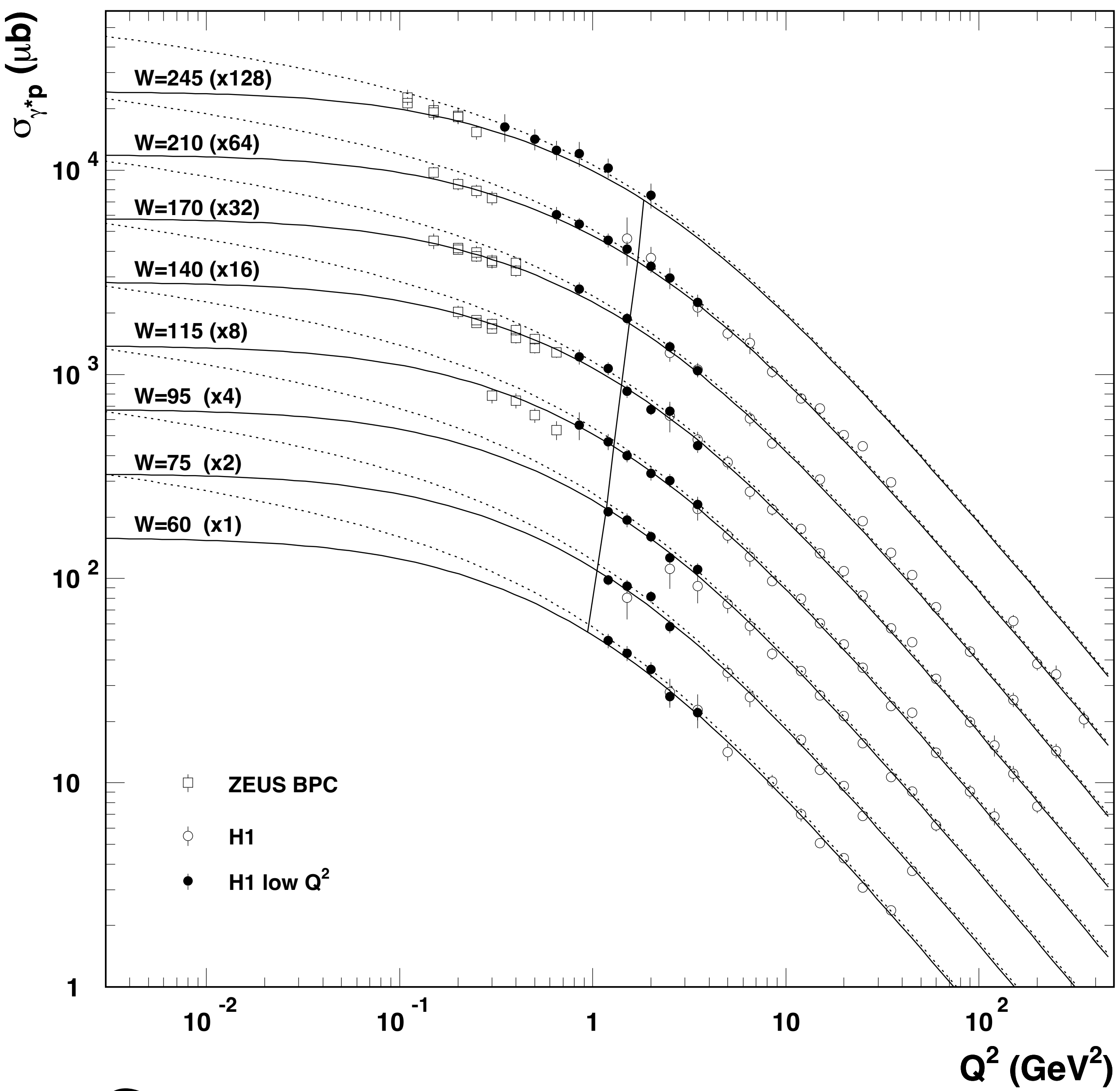

Cross section

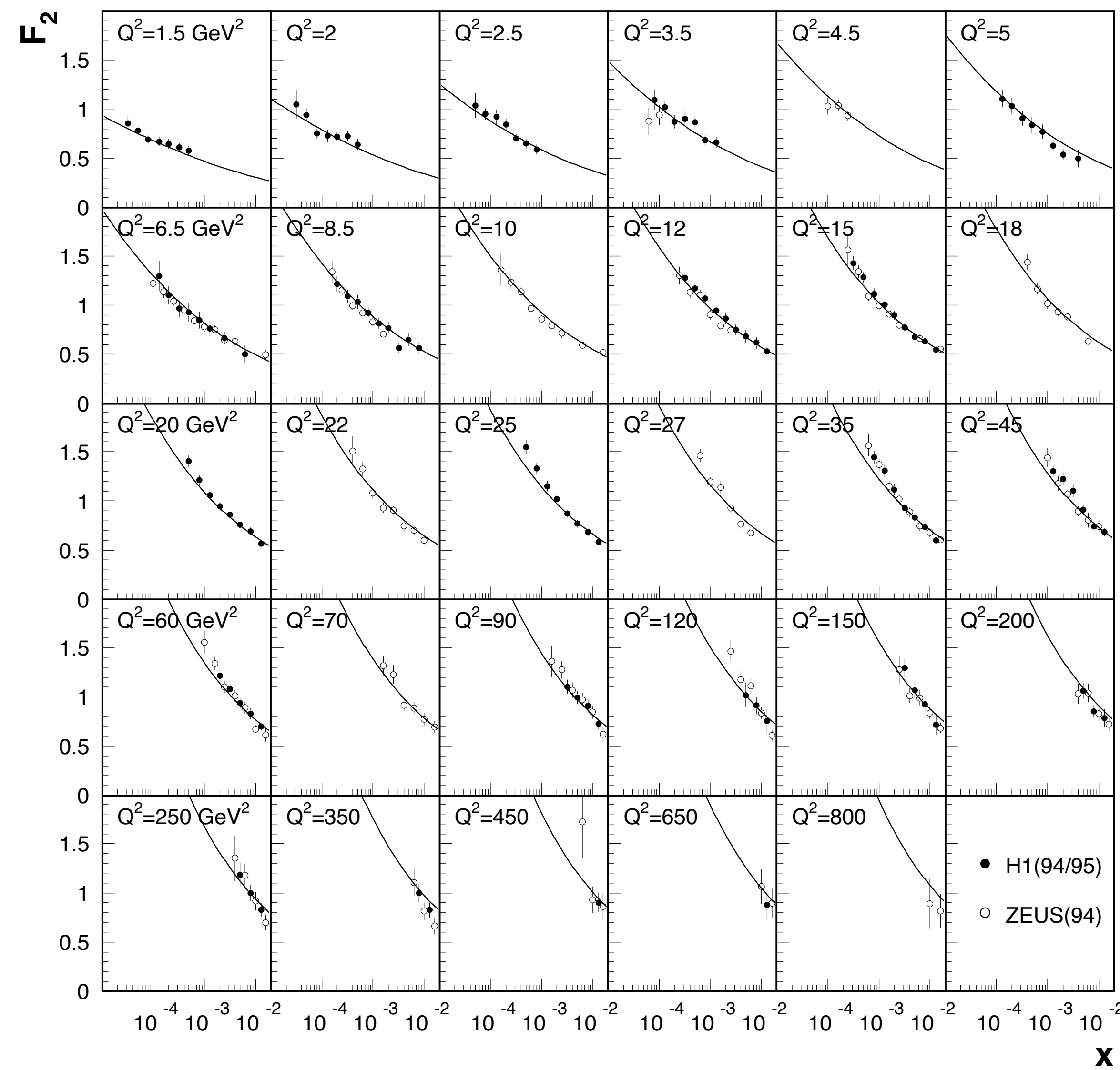

Structure function F_2

Description of the data at low Q^2 require non-zero quark masses

GBW model: update and DGLAP evolution

GBW model does not contain DGLAP evolution, necessary for high Q^2

DGLAP improved saturation model

$$\sigma_{\rm dip}(r,x) = \sigma_0 \left\{ 1 - \exp\left(-\frac{\pi^2 r^2 \, \alpha_s(\mu^2) \, xg(x,\mu^2)}{3\sigma_0} \right) \right\}$$

Gluon density satisfies DGLAP evolution

$$\frac{\partial g(x,\mu^2)}{\partial \ln \mu^2} = \frac{\alpha_s(\mu^2)}{2\pi} \int_x^1 \frac{dz}{z} \, P_{gg}(x) \, g(x/z,\mu^2)$$

Scale

$$\mu^2 = \frac{C}{r^2} + \mu_0^2$$

Dipole cross section for small dipole sizes

$$\sigma_{\rm dip} \approx \frac{\pi^2}{3} r^2 \alpha_s(C/r^2) \, xg(x, C/r^2)$$

Color transparency and connection to QCD result (DGLAP logarithms)

GBW model: update and DGLAP evolution

blue: GBW
red: GBW+DGLAP

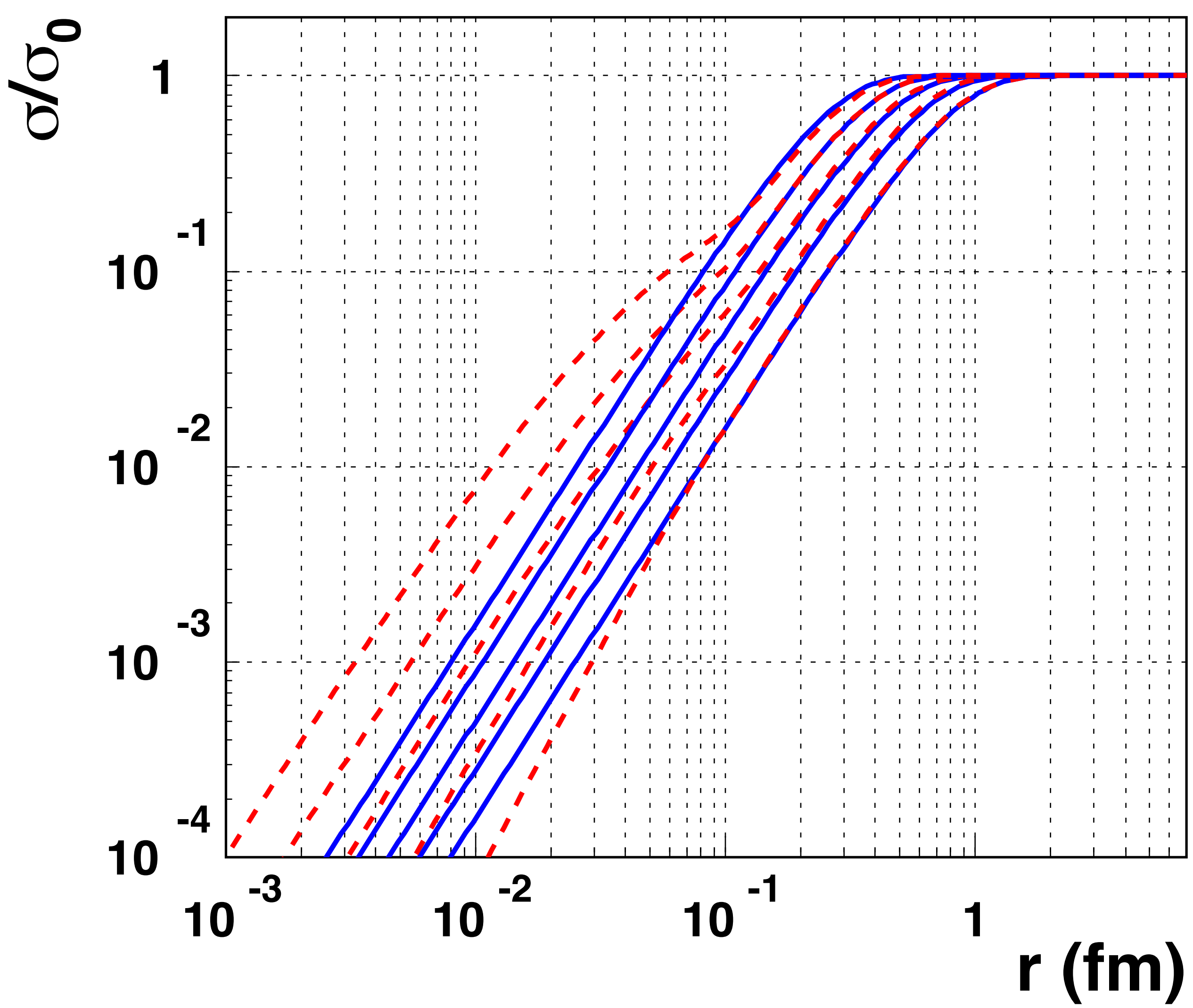

saturation scale

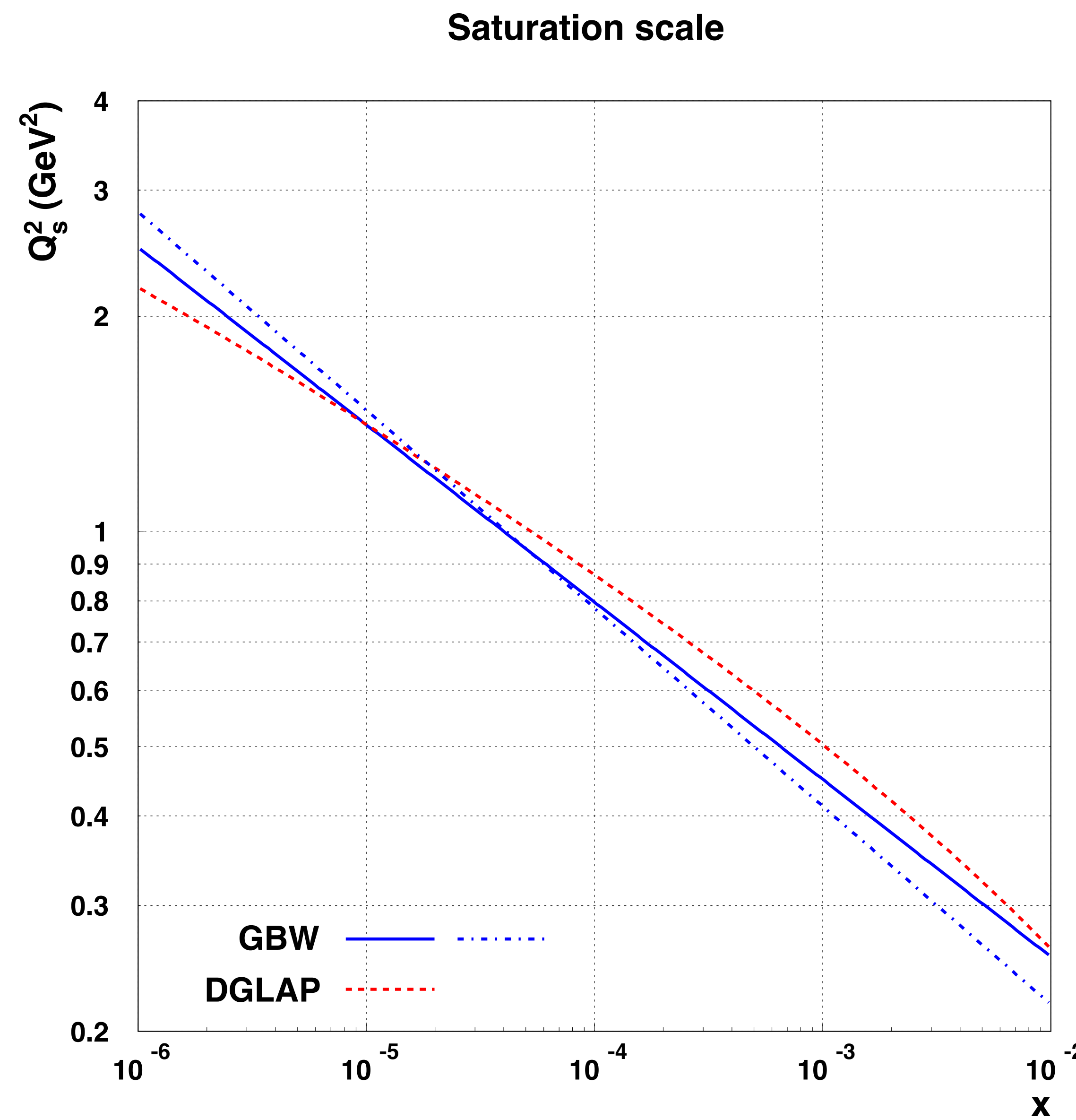

saturation scale in GBW model

$$Q_s^2(x) = Q_0^2(x/x_0)^{-\lambda}$$

saturation scale in GBW+DGLAP model

$$Q_s^2(x) = \frac{4\pi^2}{3\sigma_0}\,\alpha_s(\mu_0^2)\,xg(x,\mu_0^2)$$

GBW model: update and DGLAP evolution

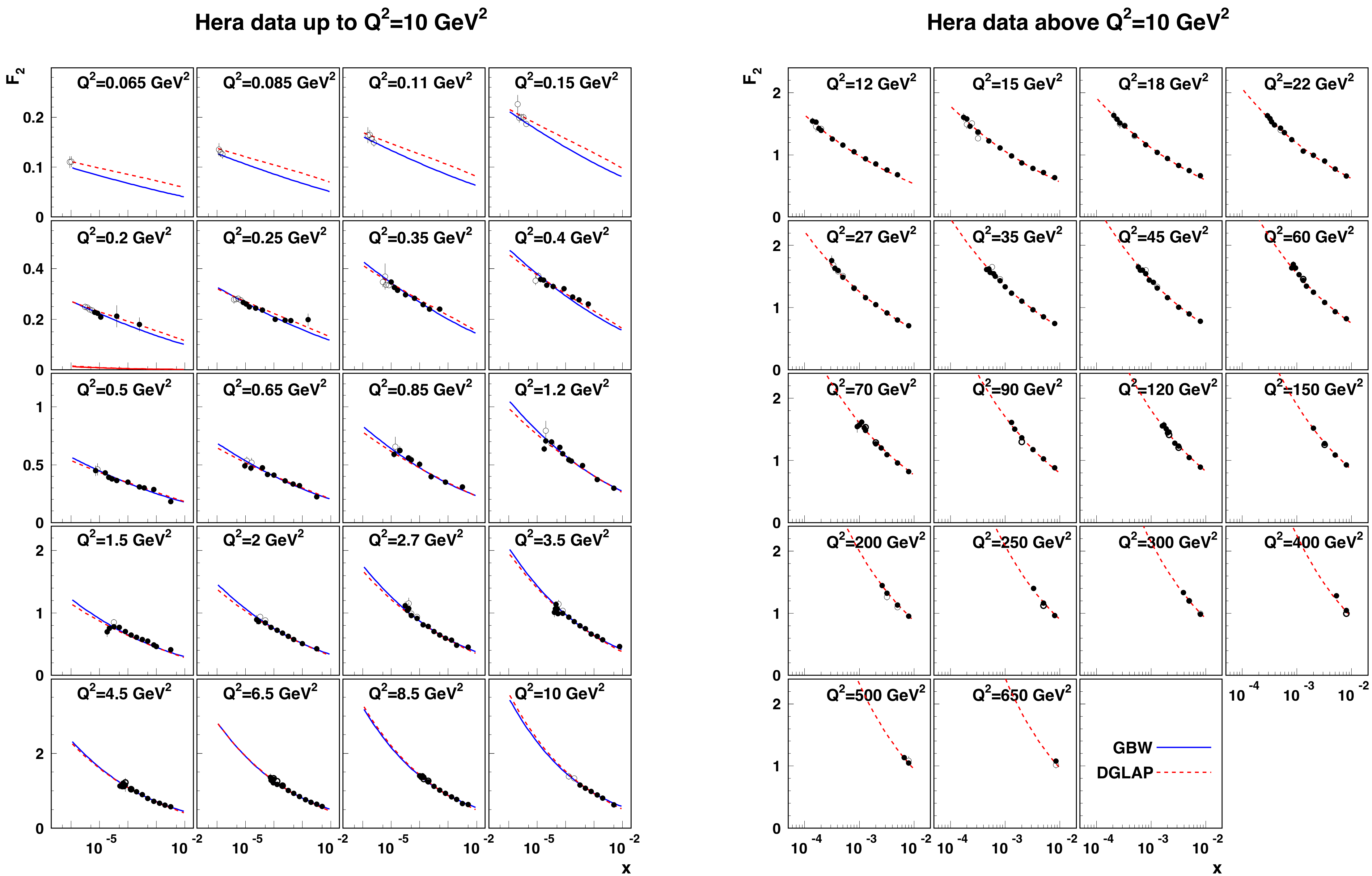

Good description in both models for data at $Q^2 < 10\ \mathrm{GeV}^2$

Above that DGLAP needed, GBW model not shown since not fitted there

BK nonlinear evolution equation

Dipole amplitude from the QCD evolution equation

quark-antiquark pair: dipole

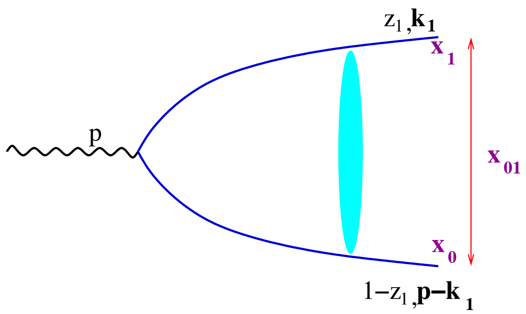

dipole splitting model *A.H.Mueller*

one (soft) gluon emission

dipole splitting

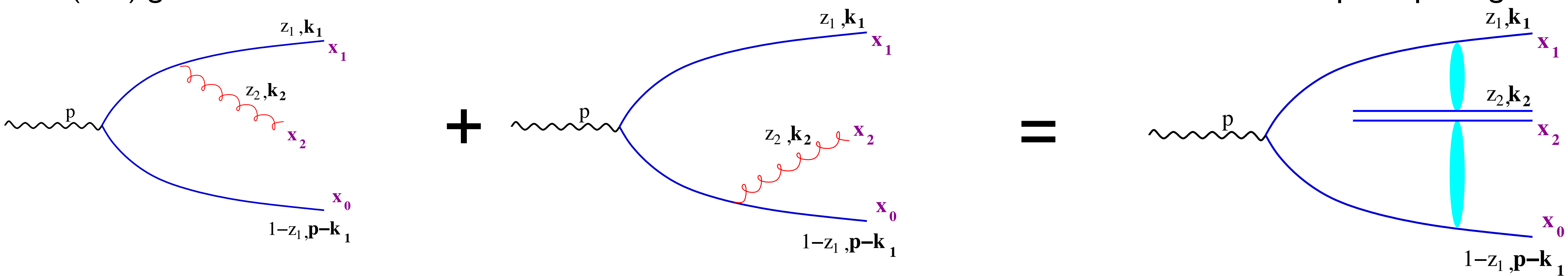

Need to construct the amplitude for scattering of dipoles on target.

One scattering

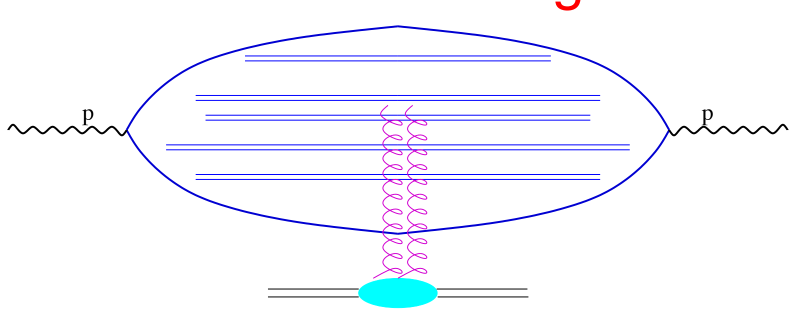

Linear evolution

Multiple scatterings

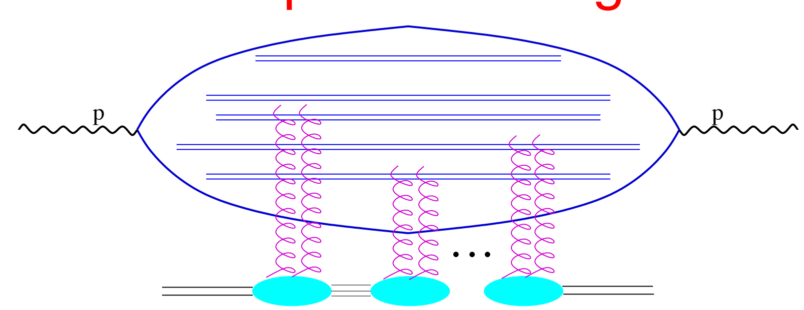

Nonlinear evolution

A.H.Mueller, Y. Kovchegov

BK nonlinear evolution equation

$$N(x, \mathbf{r}, \mathbf{b}) \to N(Y, \mathbf{x}_0, \mathbf{x}_1)$$ dipole scattering amplitude

$\mathbf{x}_0, \mathbf{x}_1$ coordinates of the dipole in the transverse space

dipole size

$$\mathbf{r} = \mathbf{x}_0 - \mathbf{x}_1$$

impact parameter

$$\mathbf{b} = \frac{\mathbf{x}_0 + \mathbf{x}_1}{2}$$

$$Y = \ln \frac{1}{x}$$ rapidity difference between the dipole and the target

BK nonlinear evolution at leading logarithmic (in ln1/x) order:

$$\frac{\partial N_{\mathbf{x}_0 \mathbf{x}_1}}{\partial Y} = \overline{\alpha}_s \int \frac{d^2 \mathbf{x}_2}{2\pi} \frac{(\mathbf{x}_0 - \mathbf{x}_1)^2}{(\mathbf{x}_0 - \mathbf{x}_2)^2 (\mathbf{x}_1 - \mathbf{x}_2)^2} [N_{\mathbf{x}_0 \mathbf{x}_2} + N_{\mathbf{x}_1 \mathbf{x}_2} - N_{\mathbf{x}_0 \mathbf{x}_1} - N_{\mathbf{x}_0 \mathbf{x}_2} N_{\mathbf{x}_1 \mathbf{x}_2}]$$

linear part: equivalent to LLx BFKL

nonlinear part

Note that N=1 solves the equation, which is the black disk limit.

Balitsky, Kovchegov

Solution to BK equation

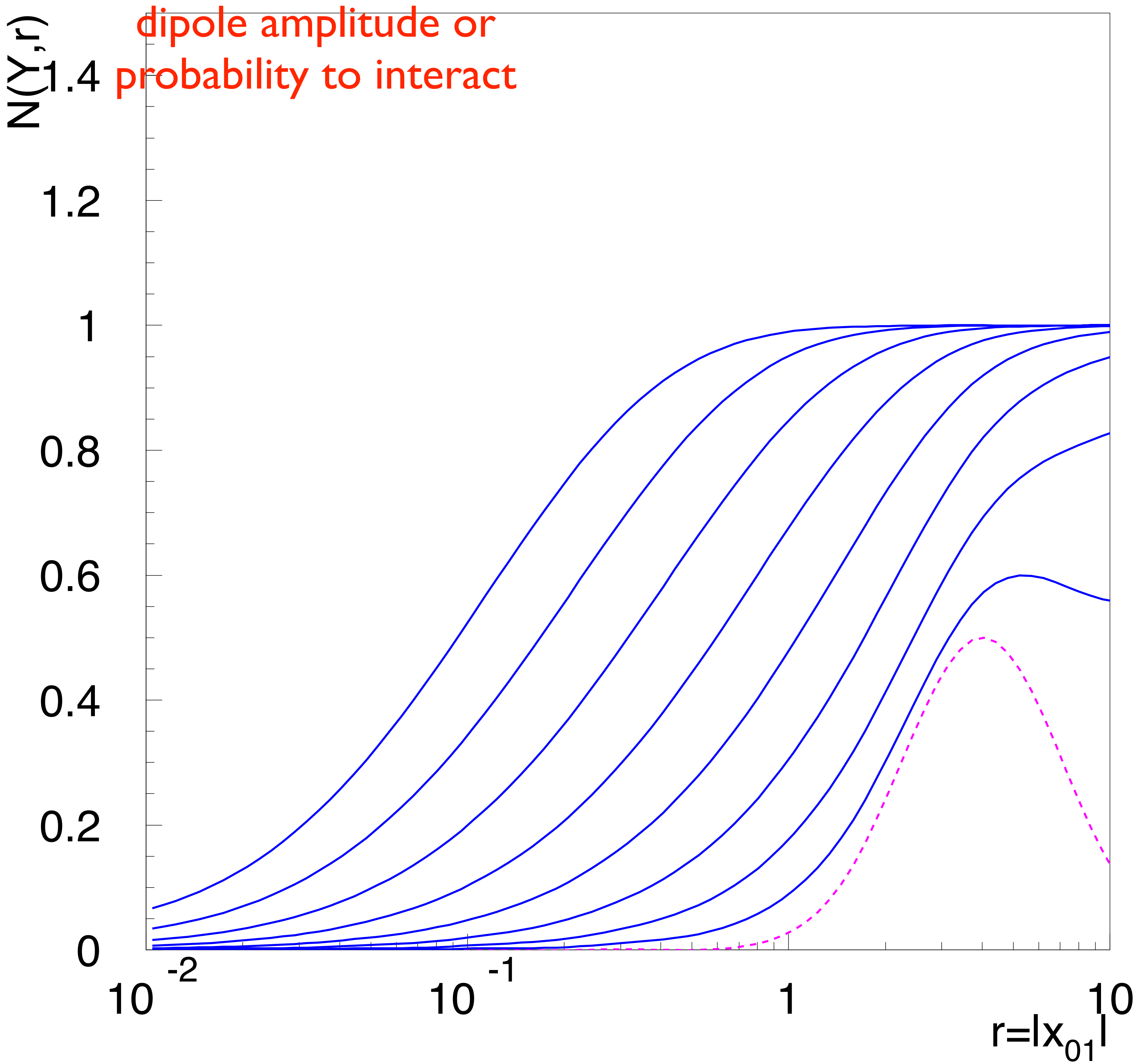

Solution to BK equation

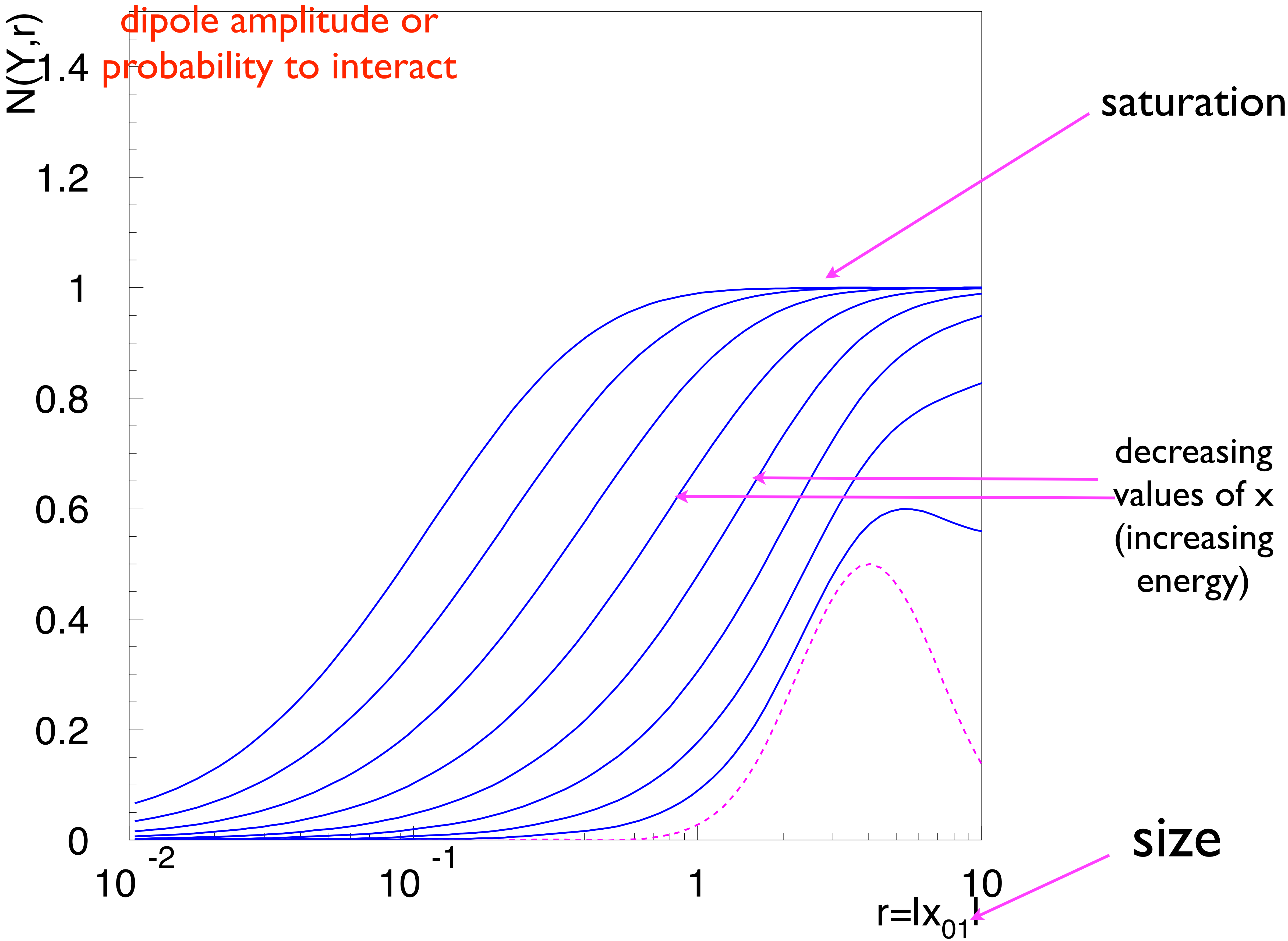

Solution to BK equation

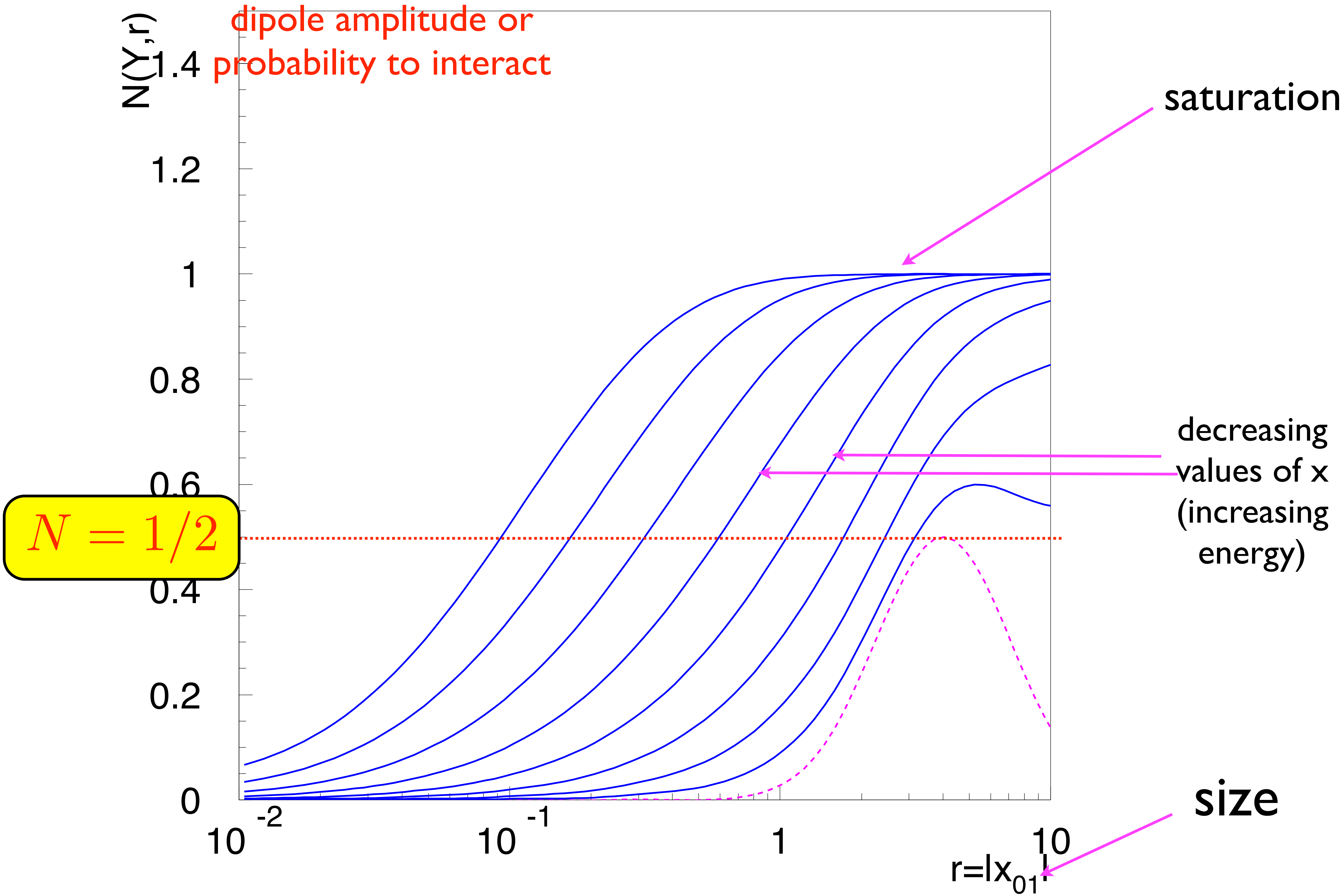

Solution to BK equation

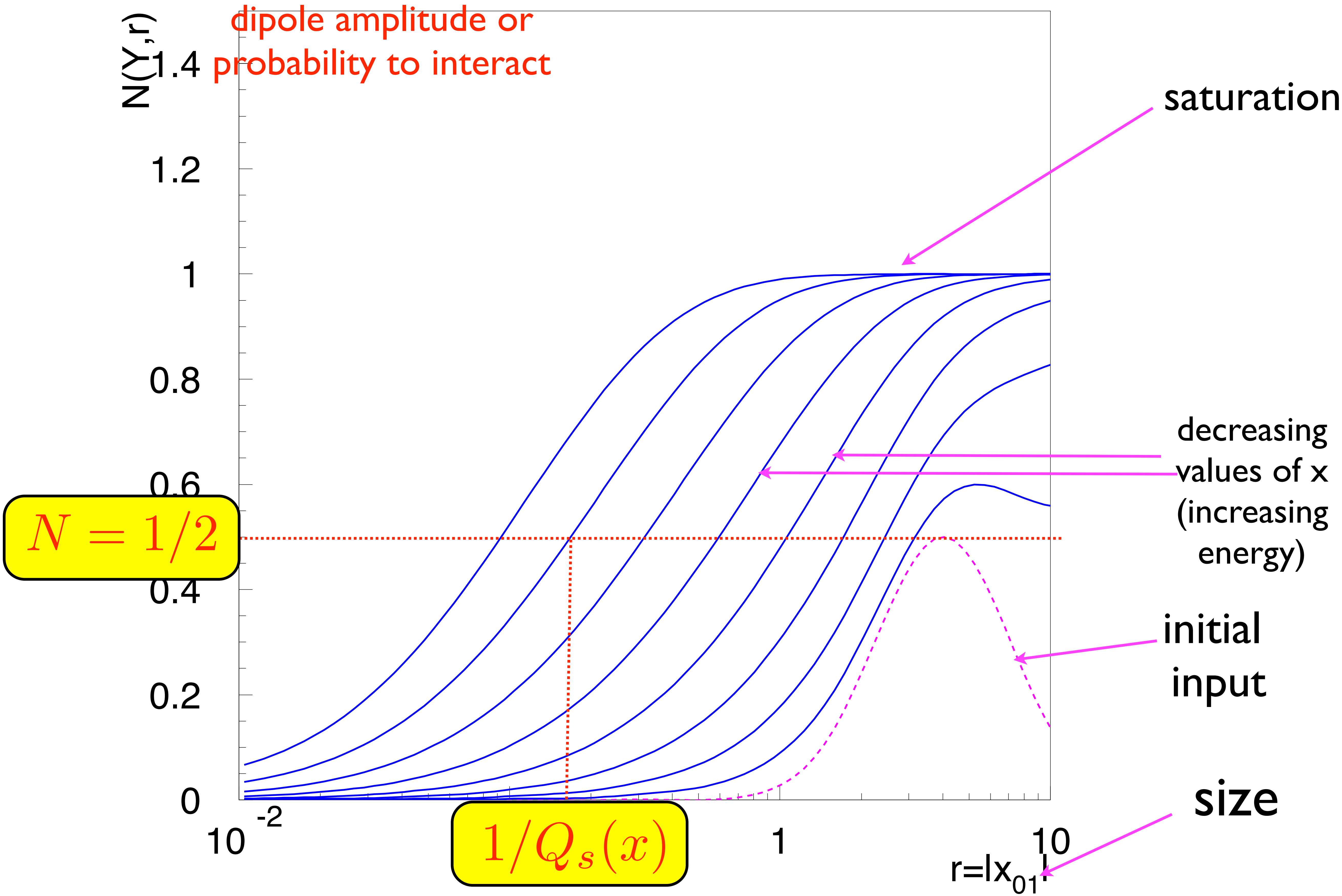

Saturation scale

Solution to nonlinear evolution equation generates the characteristic scale: saturation scale which divides the dense and dilute region.

$$\boxed{Q_s(x)^2 \simeq Q_0^2 x^{-\lambda_s}}$$

λ_s related to (but not exactly equal) to the BFKL Pomeron intercept

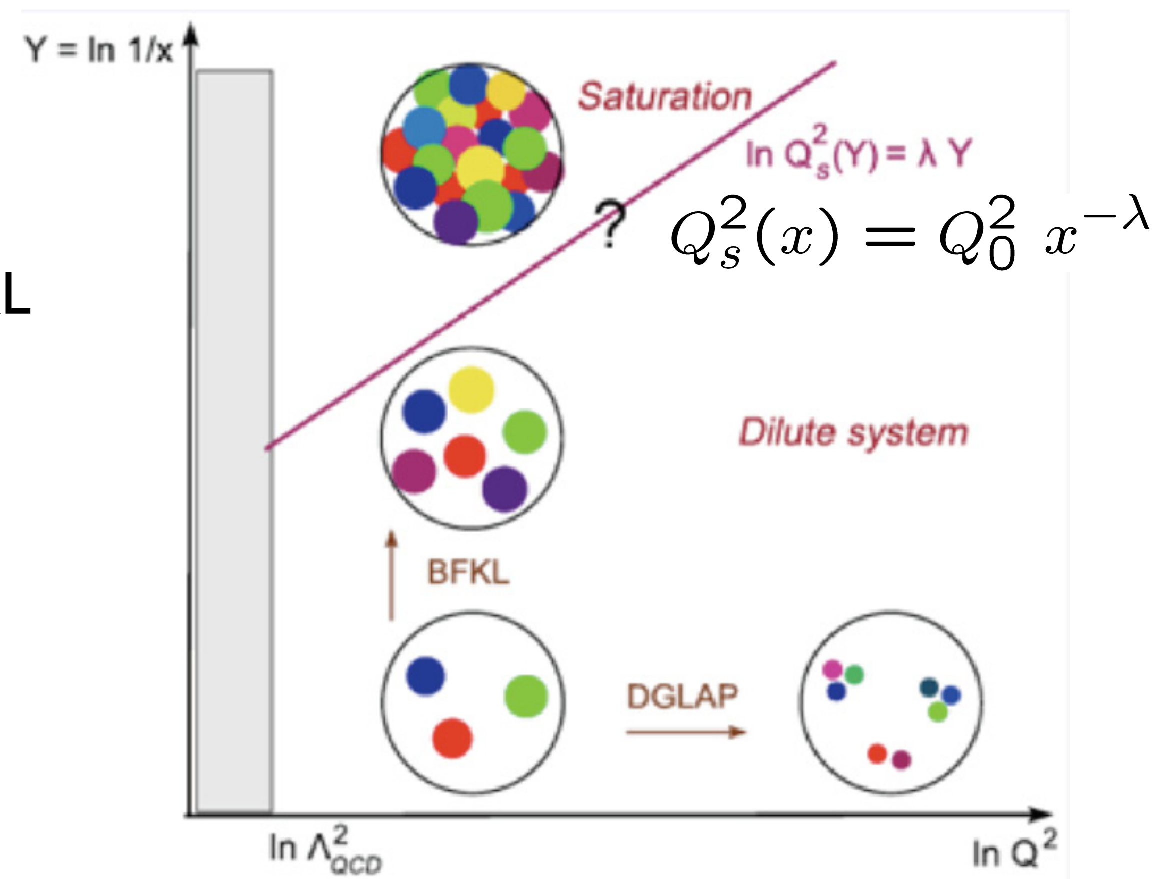

If the target is nucleus, there is additional enhancement due to nuclear number A:

$$\boxed{Q_s(x)^2 \simeq A^{1/3} Q_0^2 x^{-\lambda_s}}$$

The normalization of the saturation scale cannot be computed analytically, it is determined by the initial condition. In practice it is fitted parameter.

Diffusion properties of BFKL and BK

Investigate the solution in the momentum space

$$\phi(k,Y) := \int_0^\infty \frac{dr}{r} J_0(k\,r)\,N(r,Y)$$

BK equation in momentum space (LO):

$$\frac{d\phi(k,Y)}{dY} = \bar{\alpha}_s \int \frac{dk'}{k'} \mathcal{K}(k,k')\,\phi(k',Y) - \bar{\alpha}_s \phi^2(k,Y)$$

Solution to the linear-BFKL equation

$$k\phi(k,Y) = \frac{1}{\sqrt{\pi \bar{\alpha}_s \chi''(0) Y}} \exp(\bar{\alpha}_s \chi(0) Y) \exp\left(-\frac{\ln^2(k^2/k_0^2)}{2\bar{\alpha}_s \chi''(0) Y}\right)$$

Diffusion into infrared (small k) region of transverse momenta

BFKL kernel eigenfunction (LO)

$$\chi(\gamma) = 2\psi(1) - \psi(\gamma) - \psi(1-\gamma)$$

Diffusion properties of BFKL

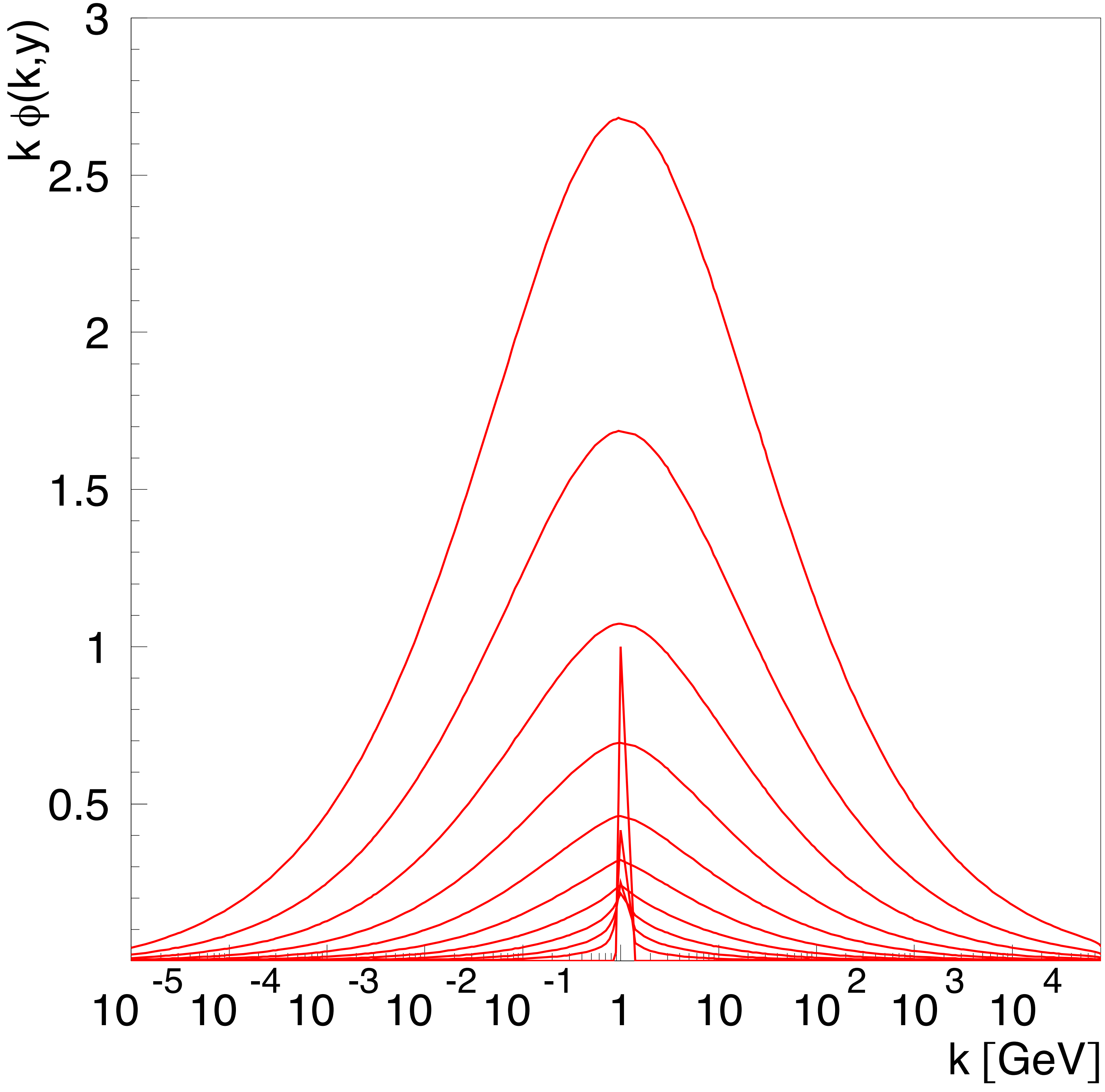

$$k\phi^{(\mathrm{lin})}(k,Y) \sim e^{\bar{\alpha}_s \chi(0) Y} \, e^{\left(-\frac{\ln^2(k^2/k_0^2)}{2\bar{\alpha}_s \chi''(0) Y}\right)}$$

Distribution in log of momentum
Diffusion clearly visible

Diffusion suppression in BK equation

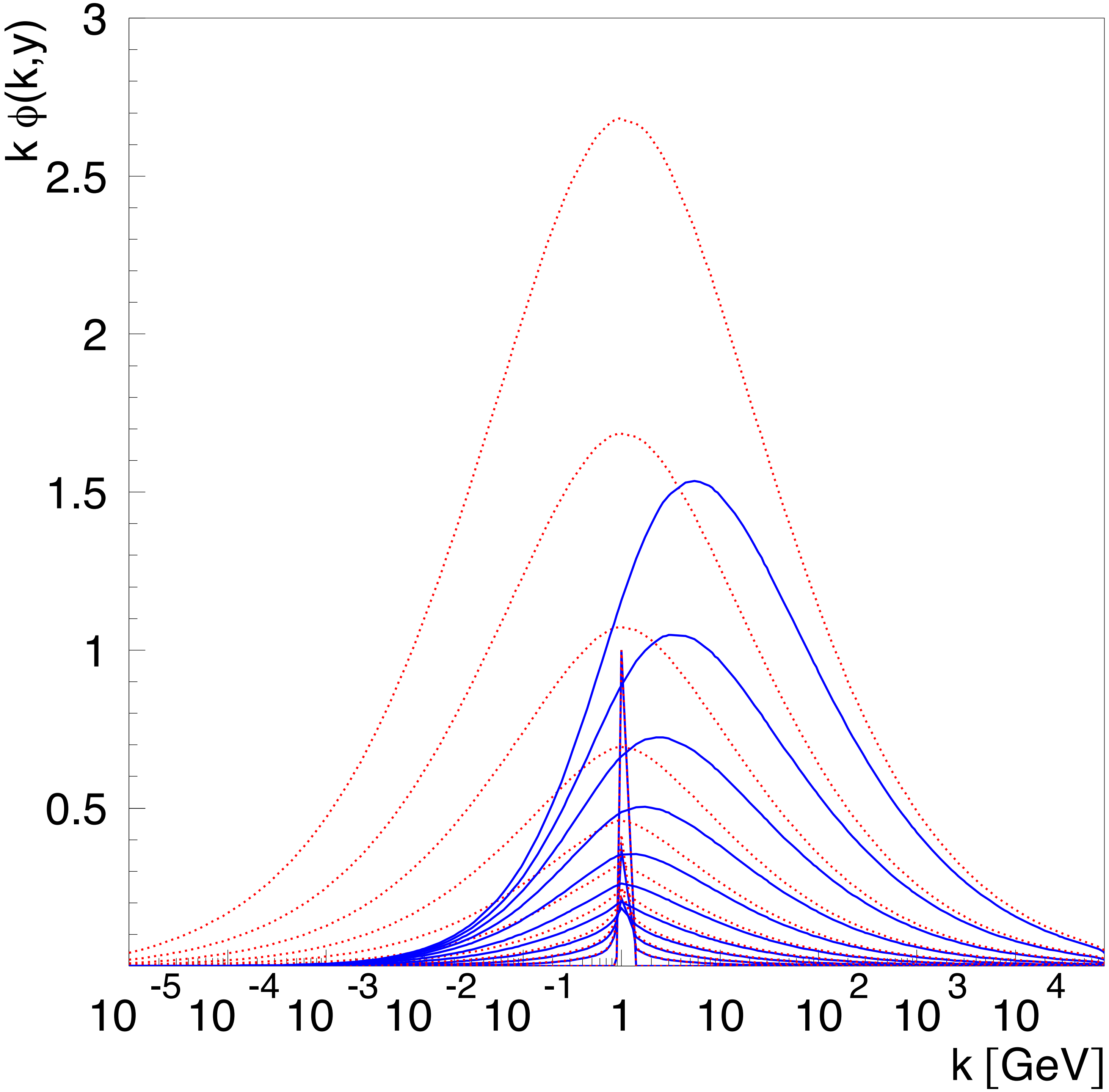

Red : BFKL
Blue: BK

Suppression of diffusion into infrared for nonlinear solution

Peak moves from initial k_0 towards large k with increasing Y

Can define saturation scale as the position of the maximum

$$Q_s(Y) = k_{\max}(Y)$$

Diffusion suppression in BK equation

Renormalized distribution

$$\Psi(k,Y) \;=\; \frac{k\phi(k,Y)}{k_{\max}(Y)\phi(k_{\max}(Y),Y)}$$

Linear

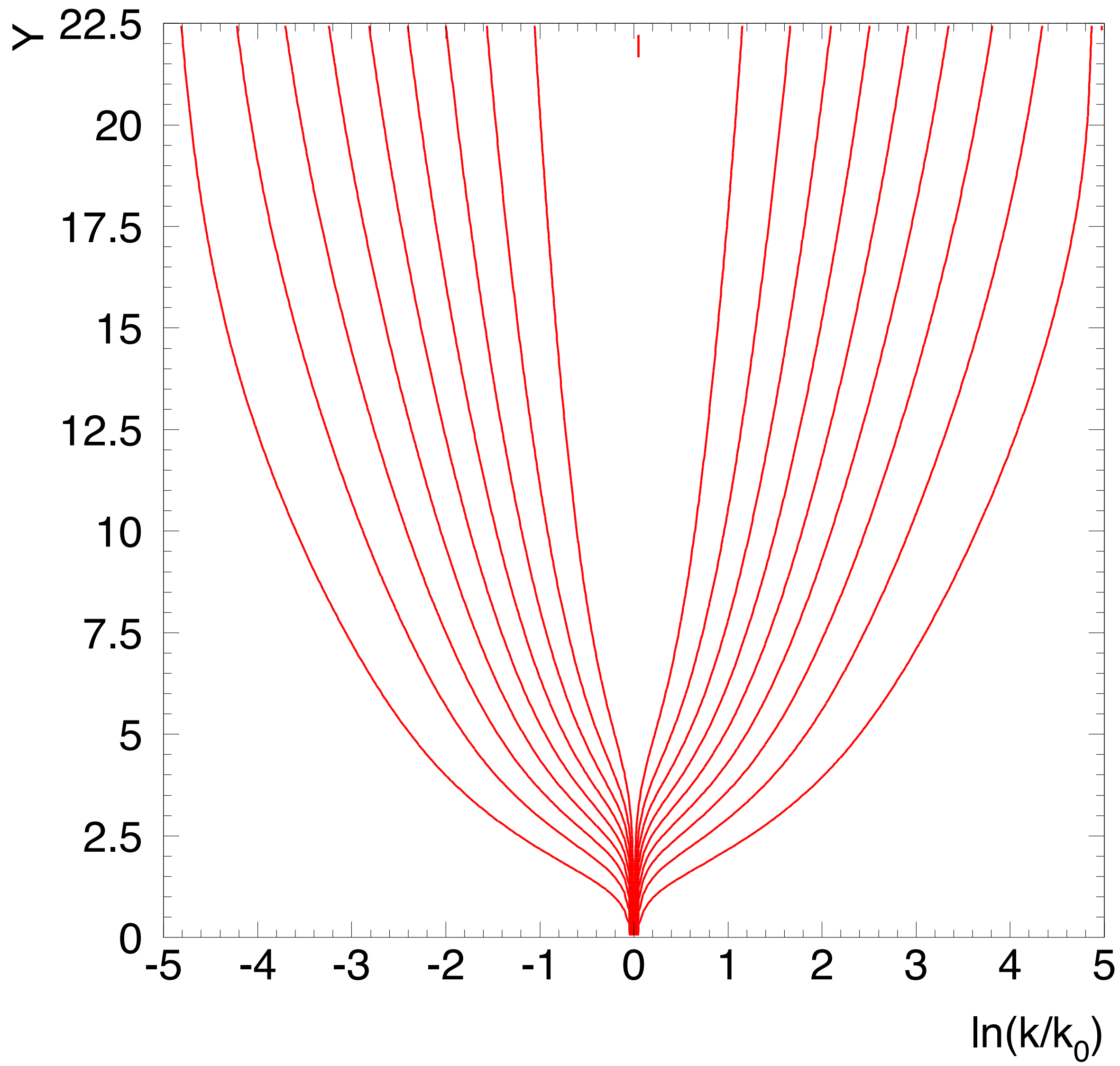

Nonlinear

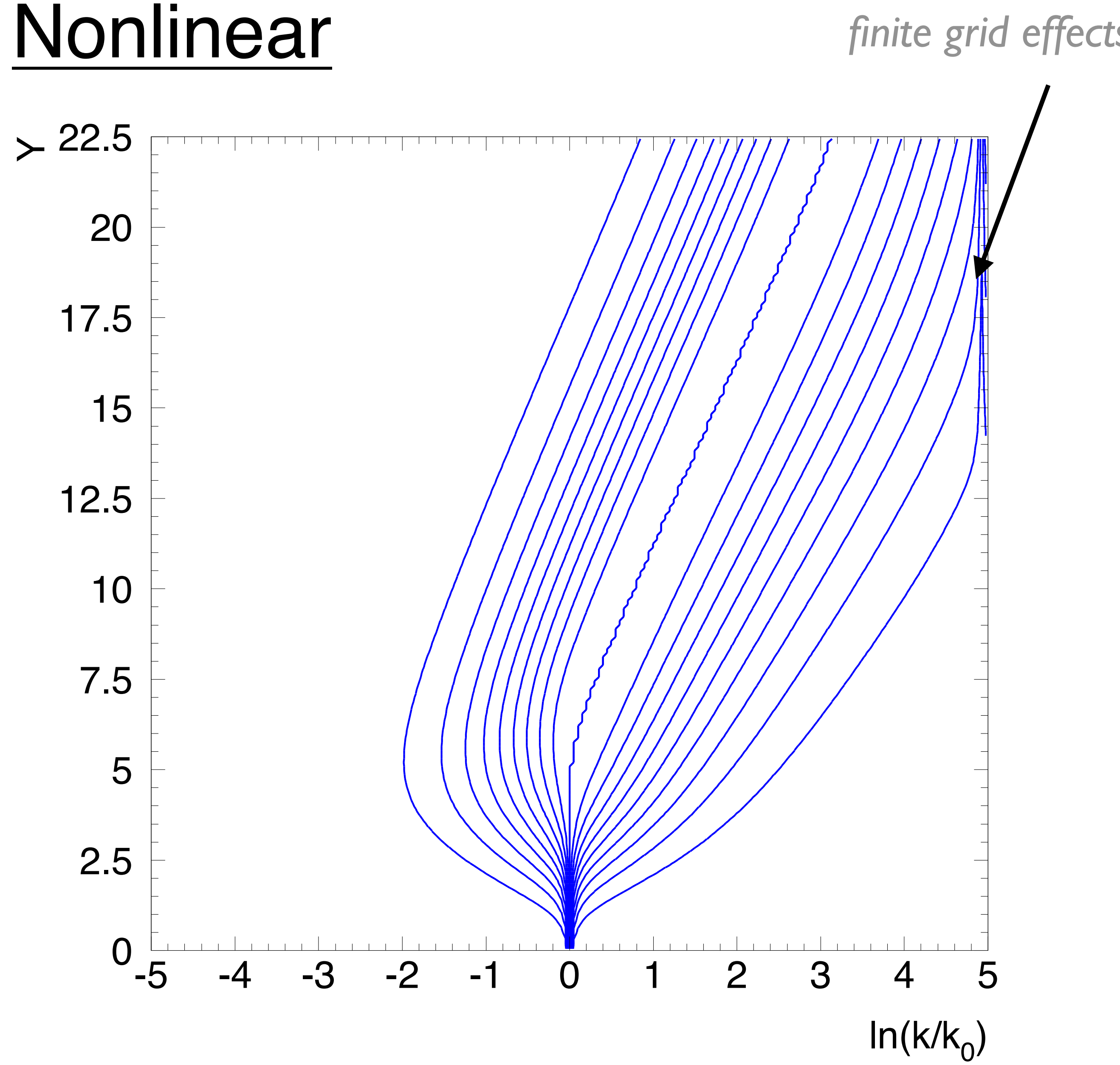

Diffusion suppression in BK equation

Nonlinear

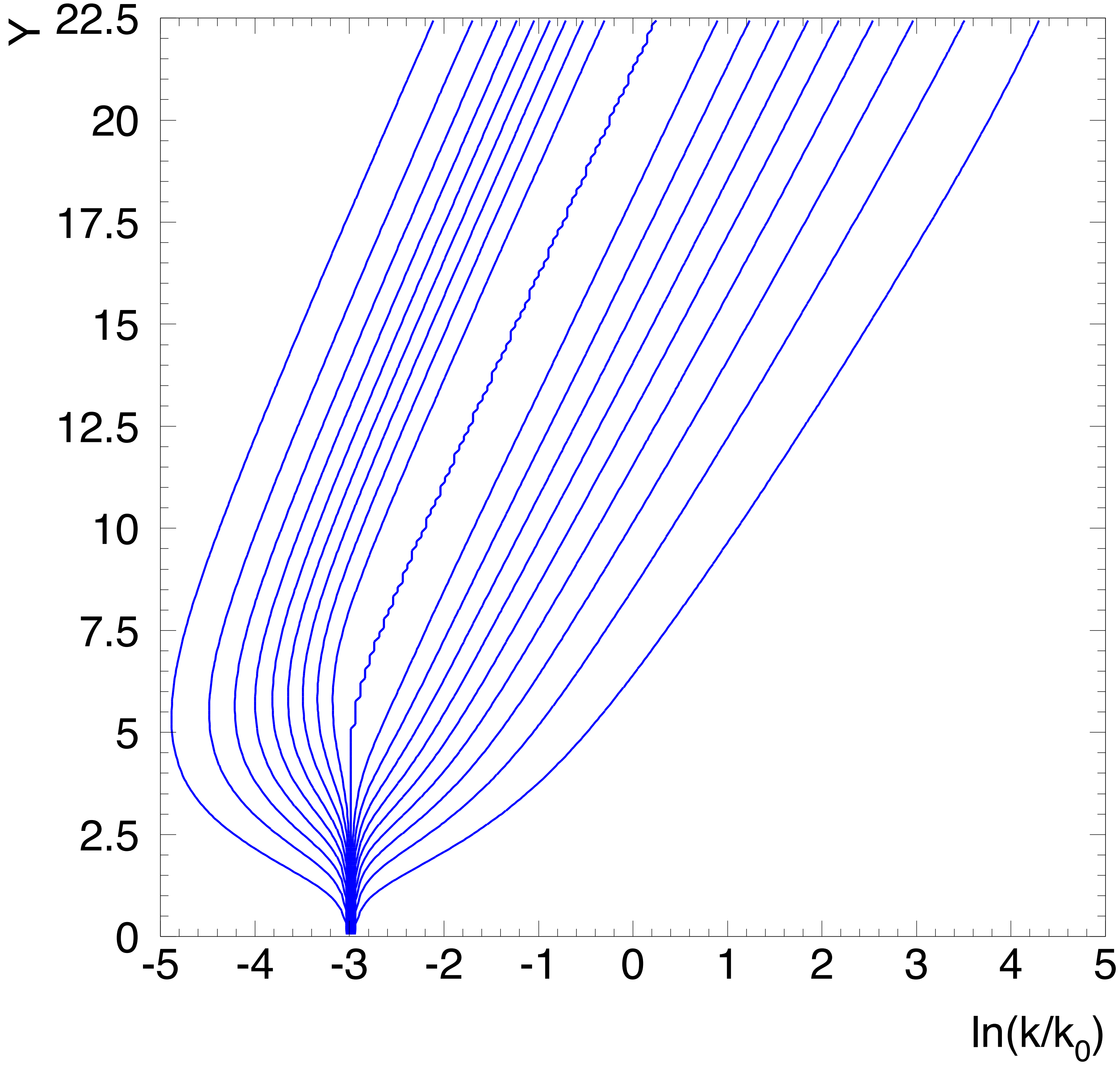

Straight lines:
$\xi = \ln k/k_0 - \lambda Y$

Scaling since solution only on ξ (when $\xi < \xi_s$)

Saturation scale $Q_s(Y)$ defined by the critical line ξ_s

Diffusion to the right of the critical line

However, things become more complicated when impact parameter is taken into account

Phenomenology with BK equation

Examples of HERA inclusive fits to proton reduced cross section using dipole picture and BK evolution

Albacete, Armesto, Milhano, Quiroga, Salgado

Fit including heavy quarks

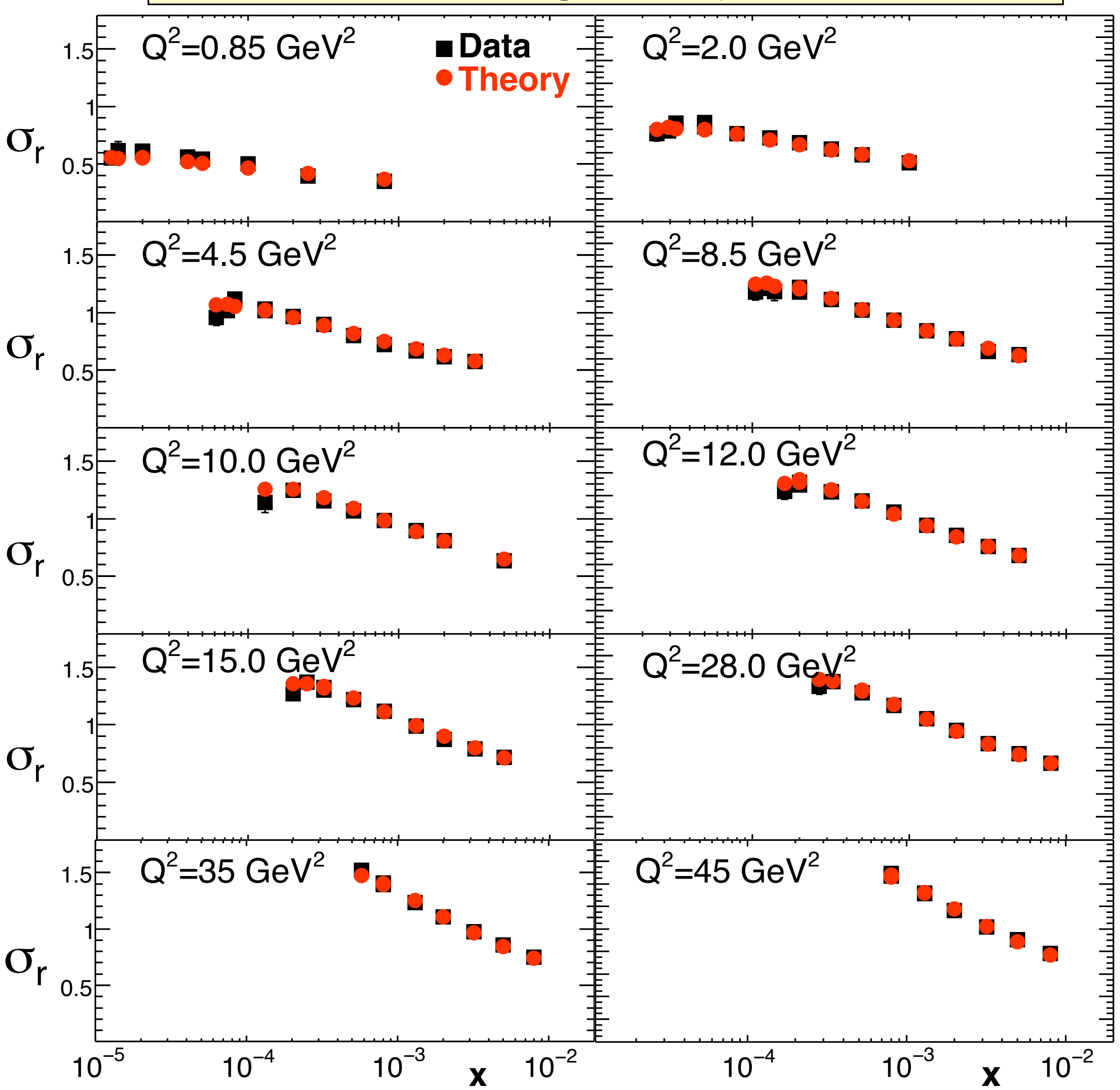

Running coupling BK with leading order impact factor

Beuf, Hanninen, Lappi, Manytsaari

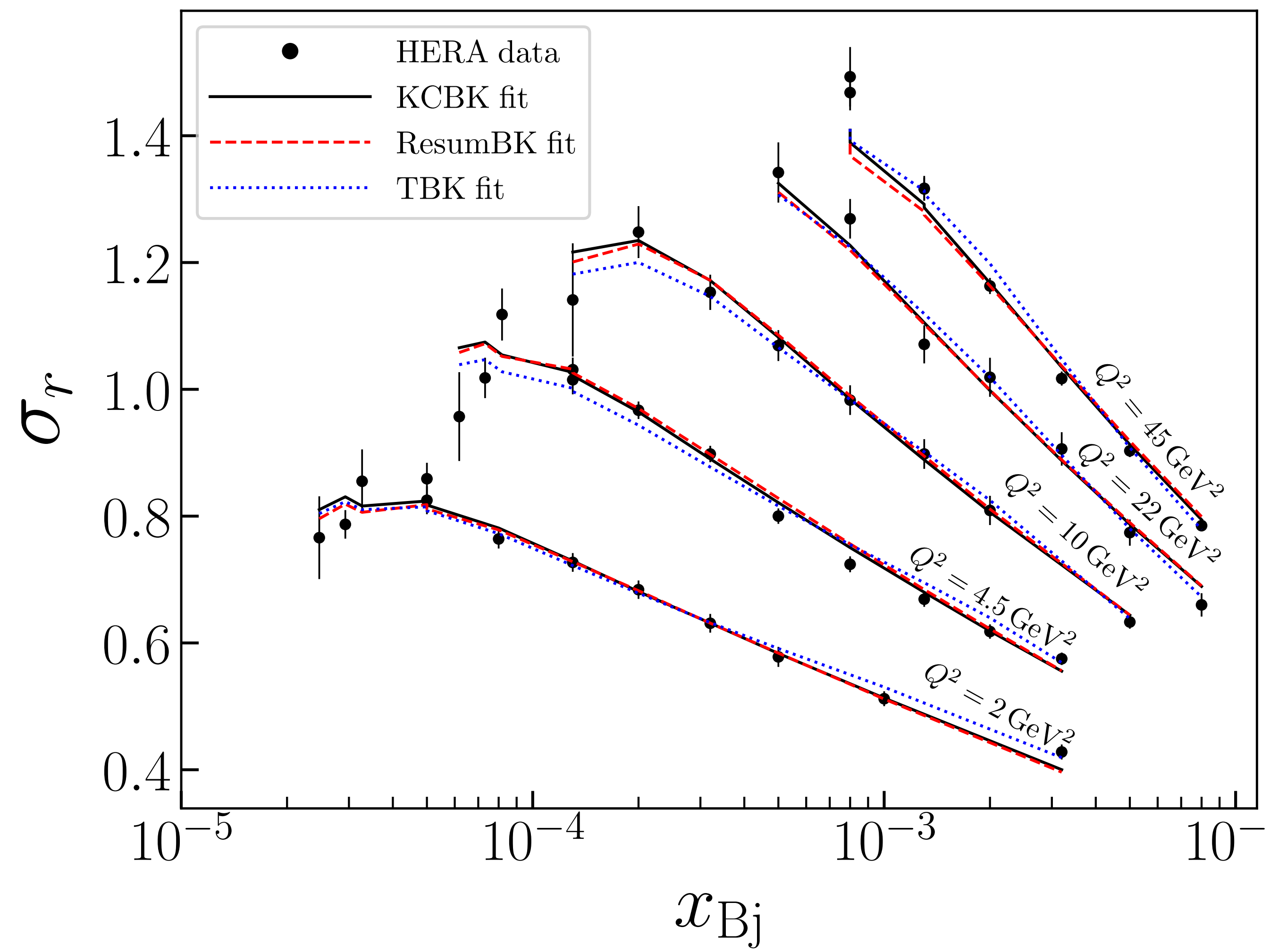

Resummed BK with NLO impact factor

What about spatial distribution of partons ?

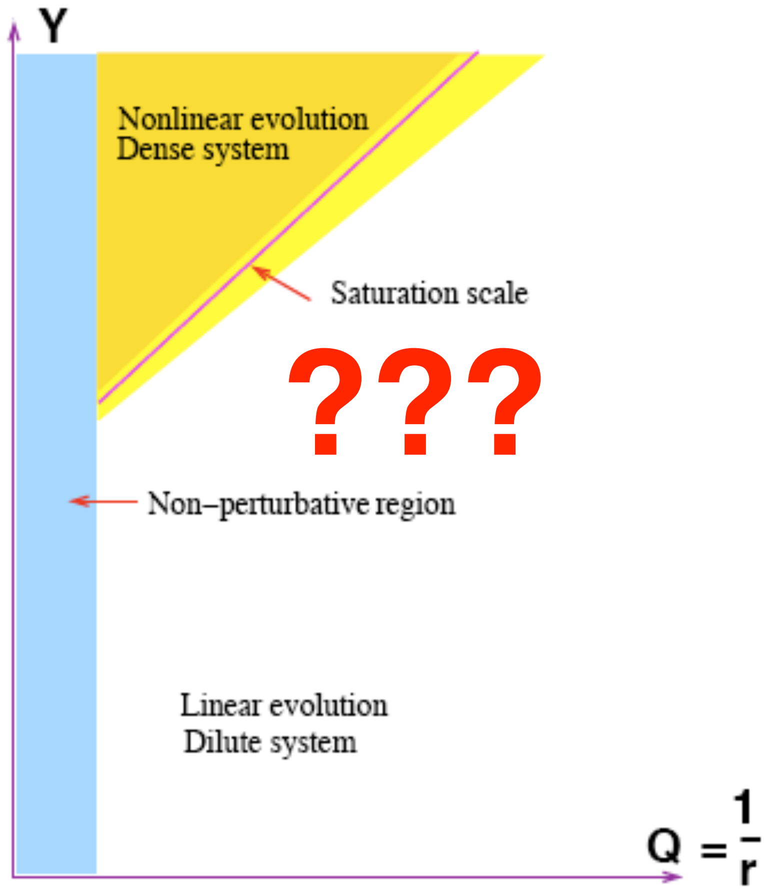

Usual approximation:

$$N(Y;\mathbf{x}_0,\mathbf{x}_1) = N(Y;|\mathbf{x}_0-\mathbf{x}_1|)$$

- The target has infinite size, no impact parameter.
- Local approximation suggests that the system becomes more perturbative as the energy grows.
- But this cannot be true everywhere (IR in QCD)

$$Y = \ln 1/x$$

What about spatial distribution of partons ?

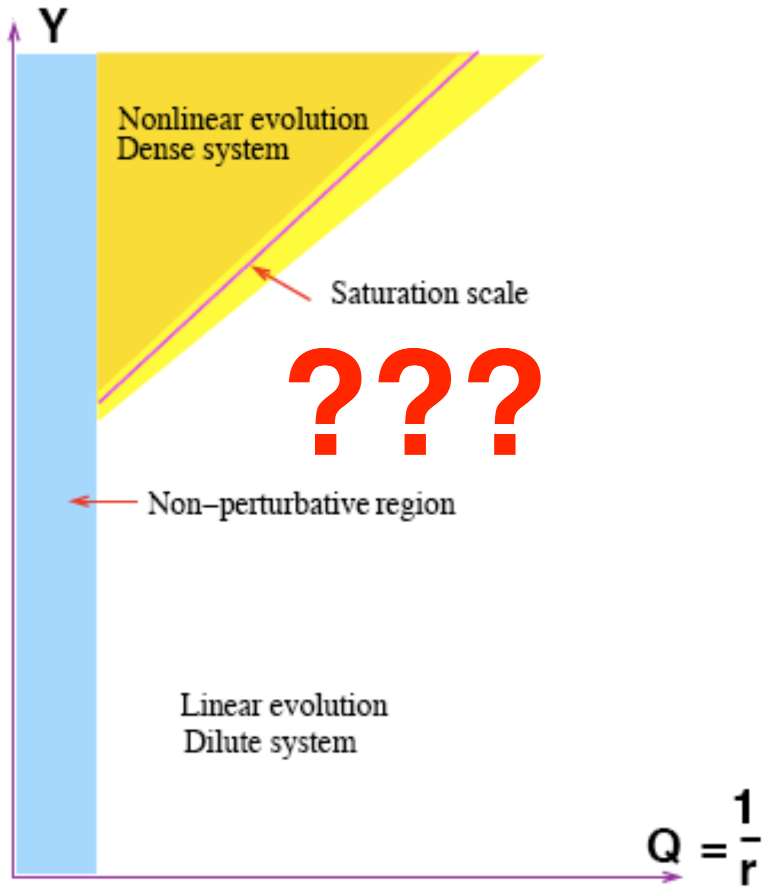

Usual approximation:

$$N(Y; \mathbf{x}_0, \mathbf{x}_1) = N(Y; |\mathbf{x}_0 - \mathbf{x}_1|)$$

- The target has infinite size, no impact parameter.
- Local approximation suggests that the system becomes more perturbative as the energy grows.
- But this cannot be true everywhere (IR in QCD)

$$Y = \ln 1/x$$

Impact parameter profile

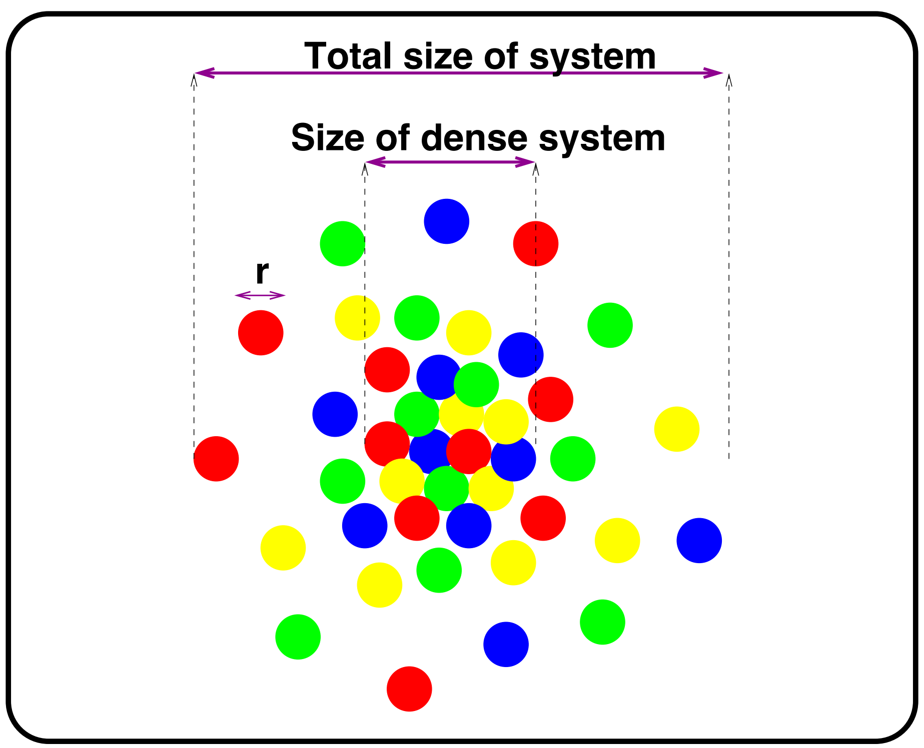

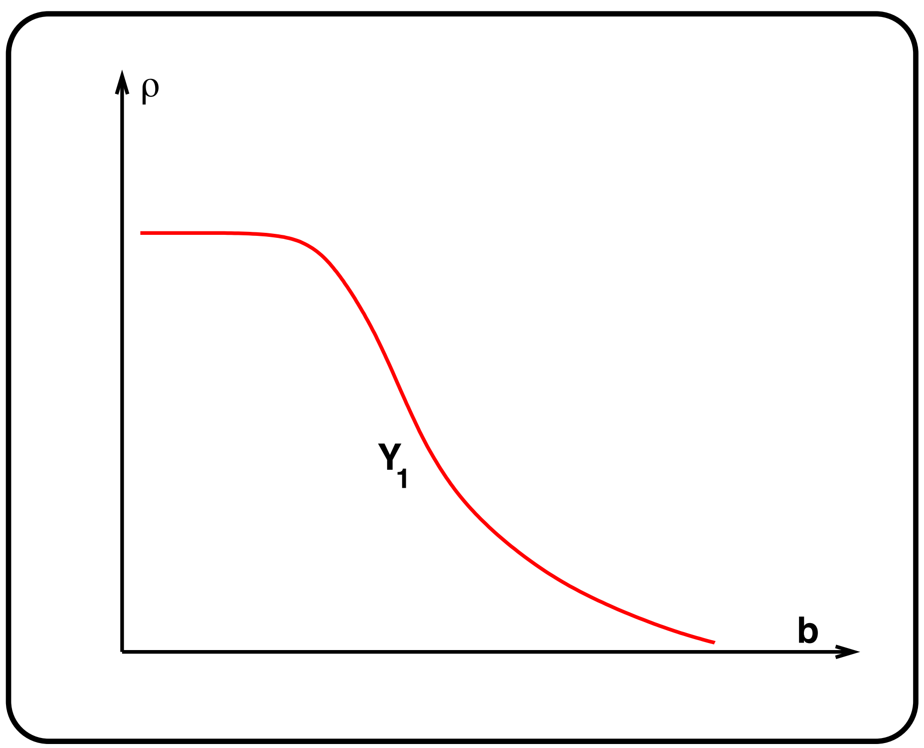

What about spatial distribution of partons ?

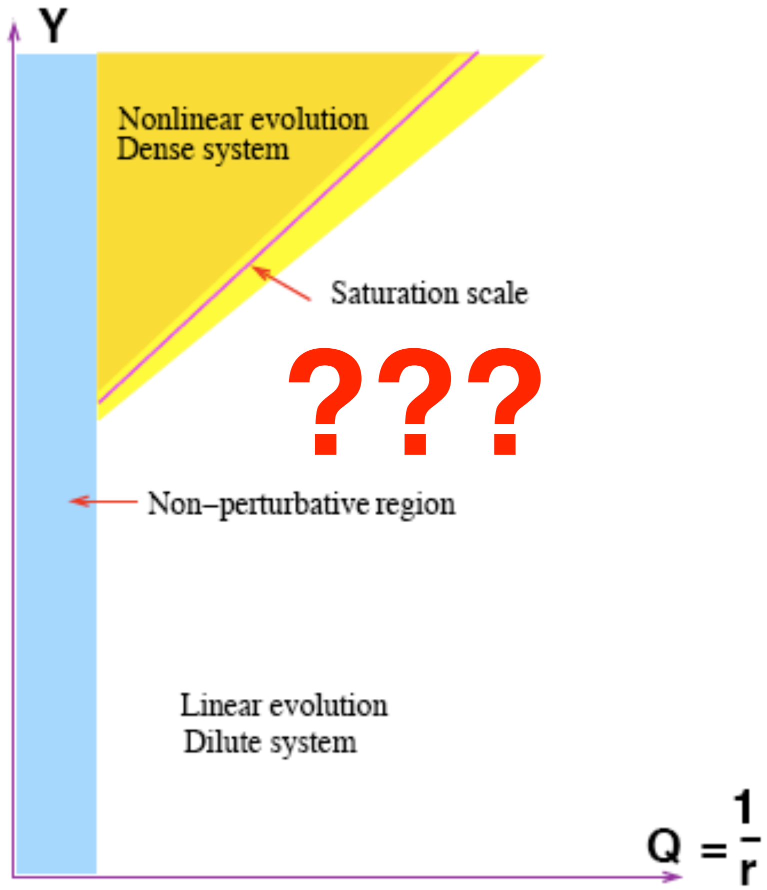

Usual approximation:

$$N(Y; \mathbf{x}_0, \mathbf{x}_1) = N(Y; |\mathbf{x}_0 - \mathbf{x}_1|)$$

- The target has infinite size, no impact parameter.
- Local approximation suggests that the system becomes more perturbative as the energy grows.
- But this cannot be true everywhere (IR in QCD)

$$Y = \ln 1/x$$

Impact parameter profile

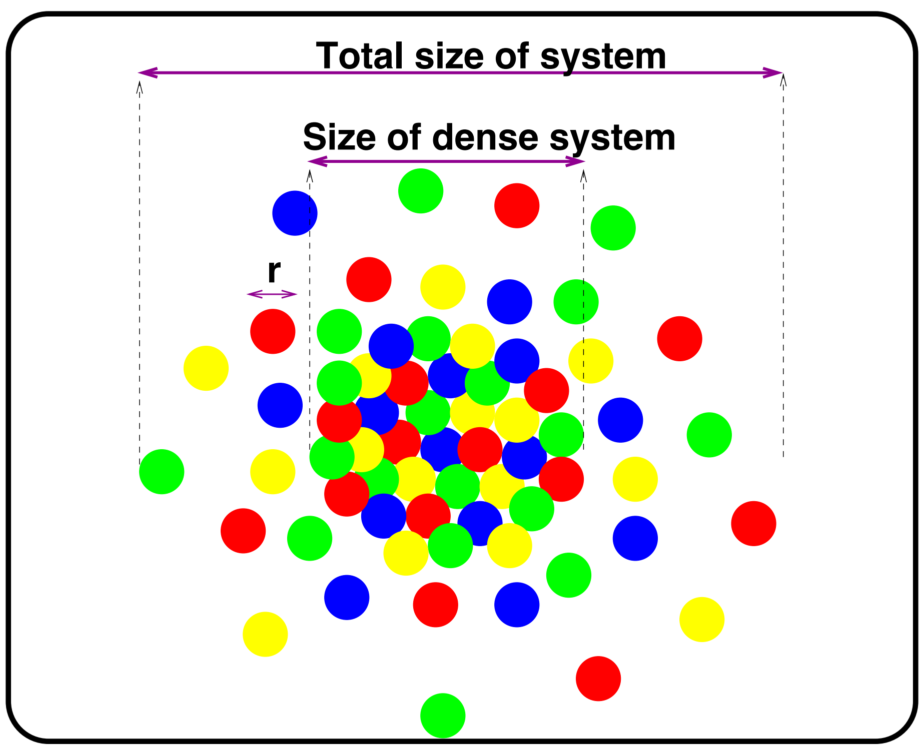

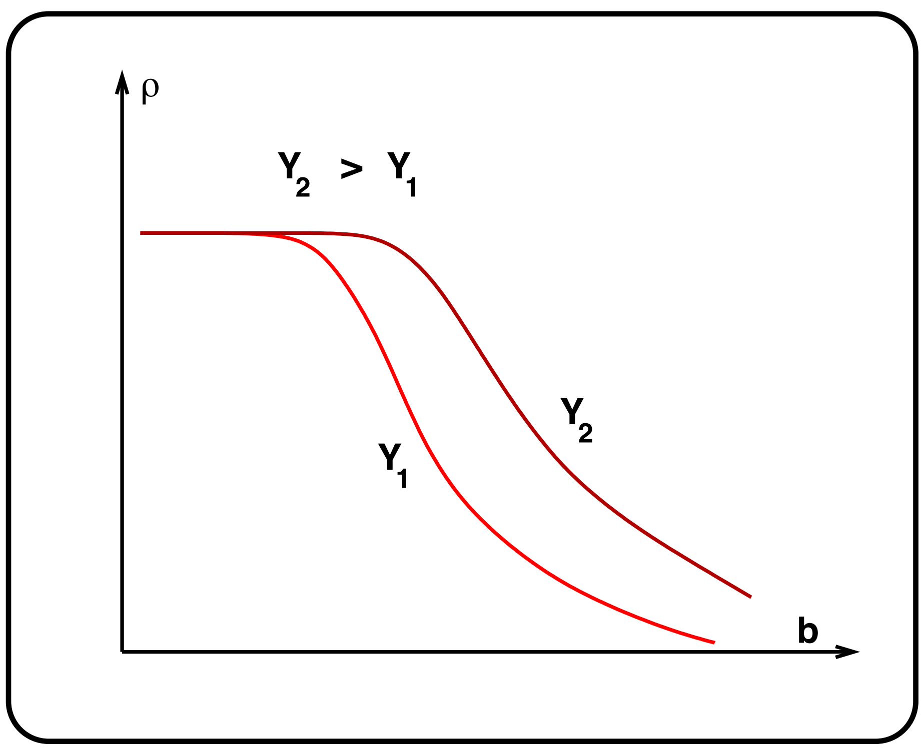

Diffraction in optics

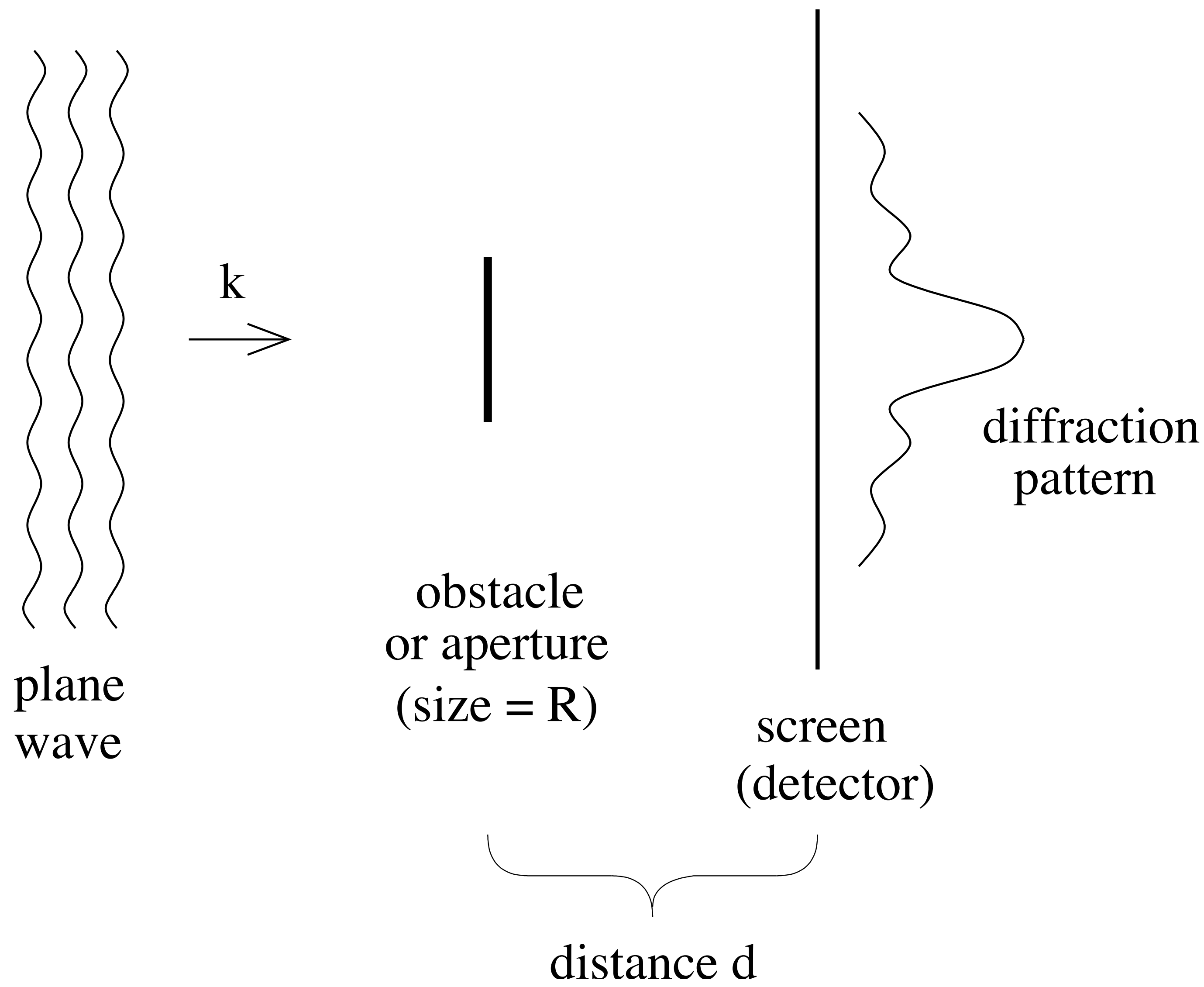

By studying diffraction pattern one can learn about the size of the obstacle and its density

Diffraction in optics and in hadron physics

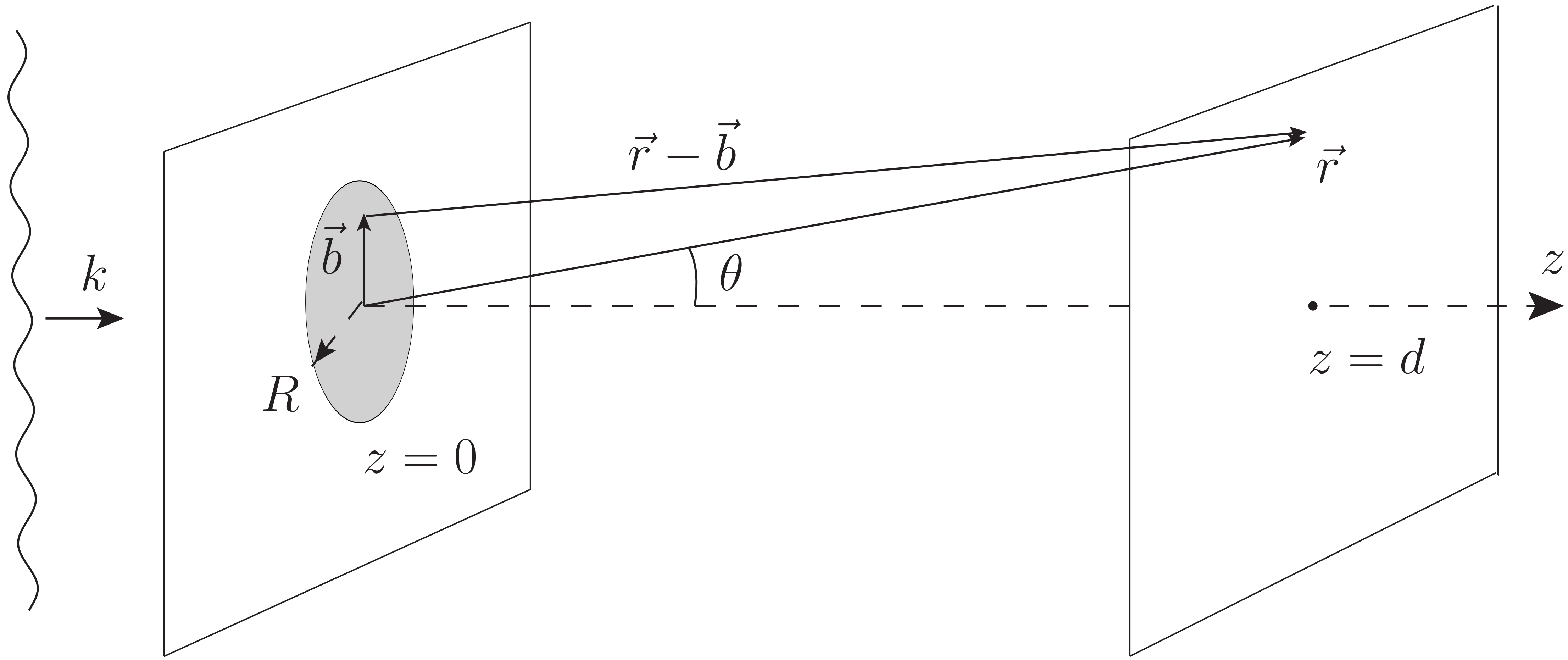

In optics: diffraction is analyzed in terms of angle θ

In particle physics: diffraction is analyzed in terms of Mandelstam invariant **t** : momentum transfer

Elastic production of vector meson

$q\bar{q}$ valence component

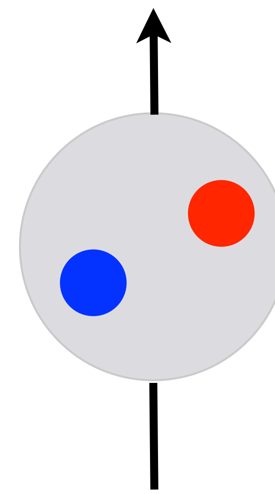

spin=1

J/Ψ	$3\ \mathrm{GeV}$
ρ	$0.77\ \mathrm{GeV}$
ω	$0.782\ \mathrm{GeV}$

Elastic production of meson V in the interaction of photon-proton

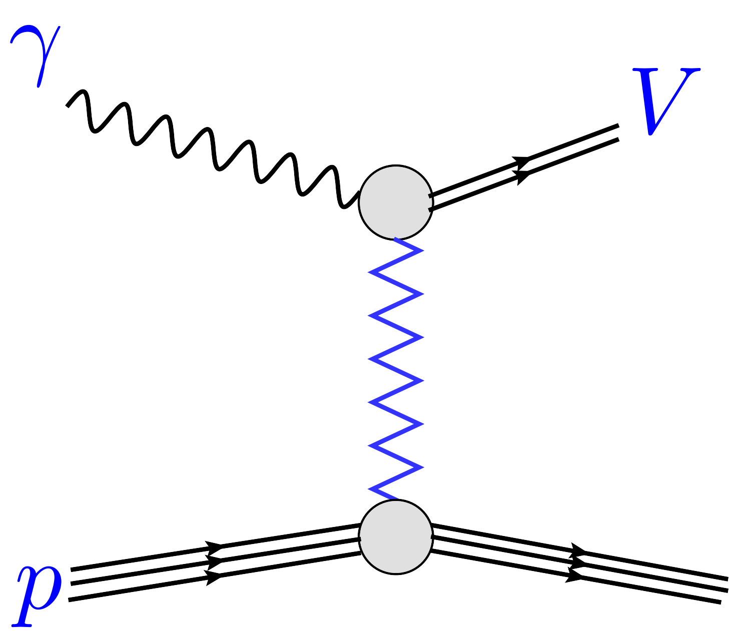

$\gamma p \to J/\psi\, p$ cross section from HERA

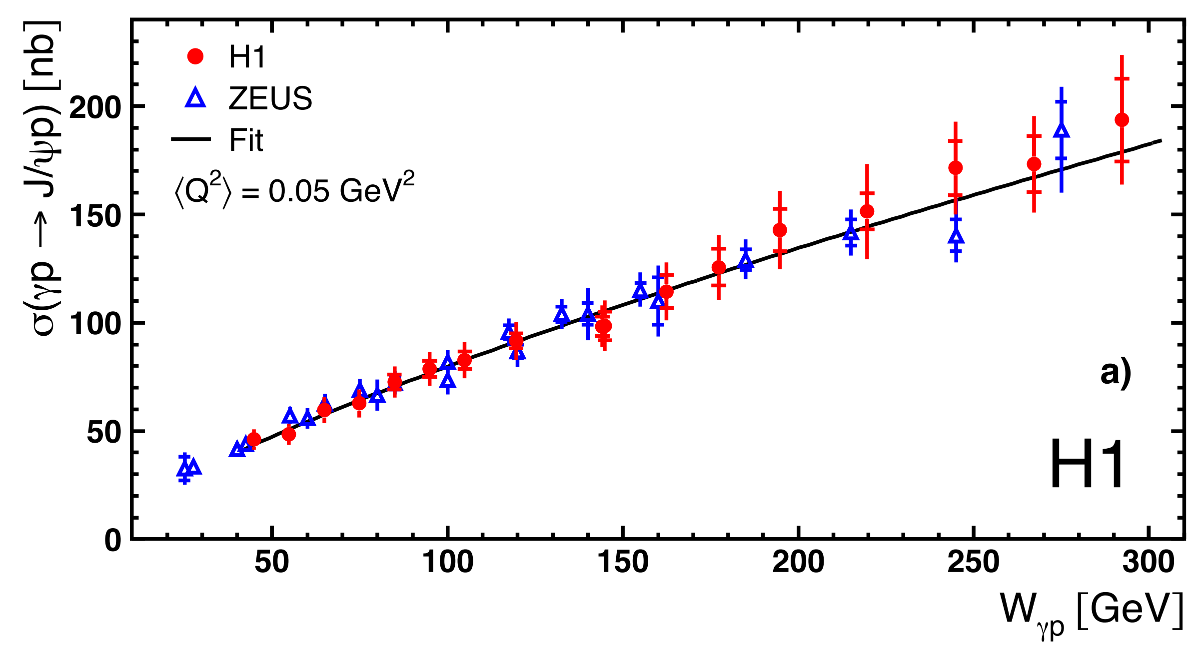

Same process can be measured in UPC ! See talks in this conference

Exclusive diffraction

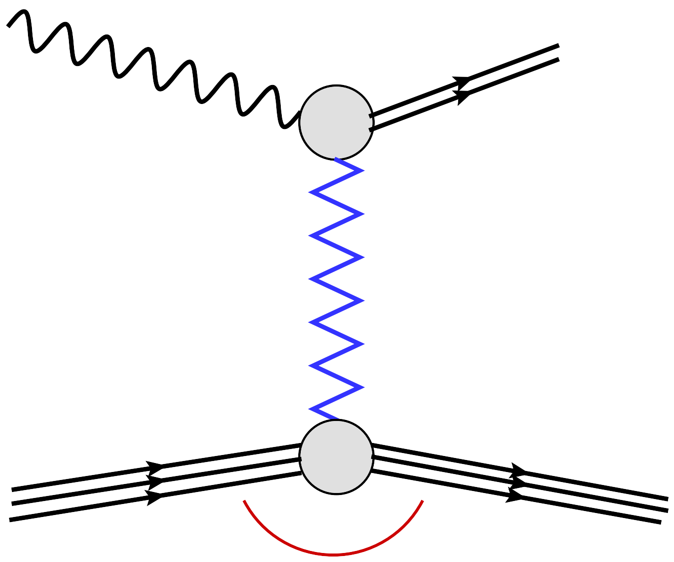

Momentum transfer $t = -\Delta^2$

- Exclusive diffractive production of VM is an excellent process for extracting the dipole amplitude
- Suitable process for estimating the 'blackness' of the interaction.
- t-dependence provides an information about the impact parameter profile of the amplitude.

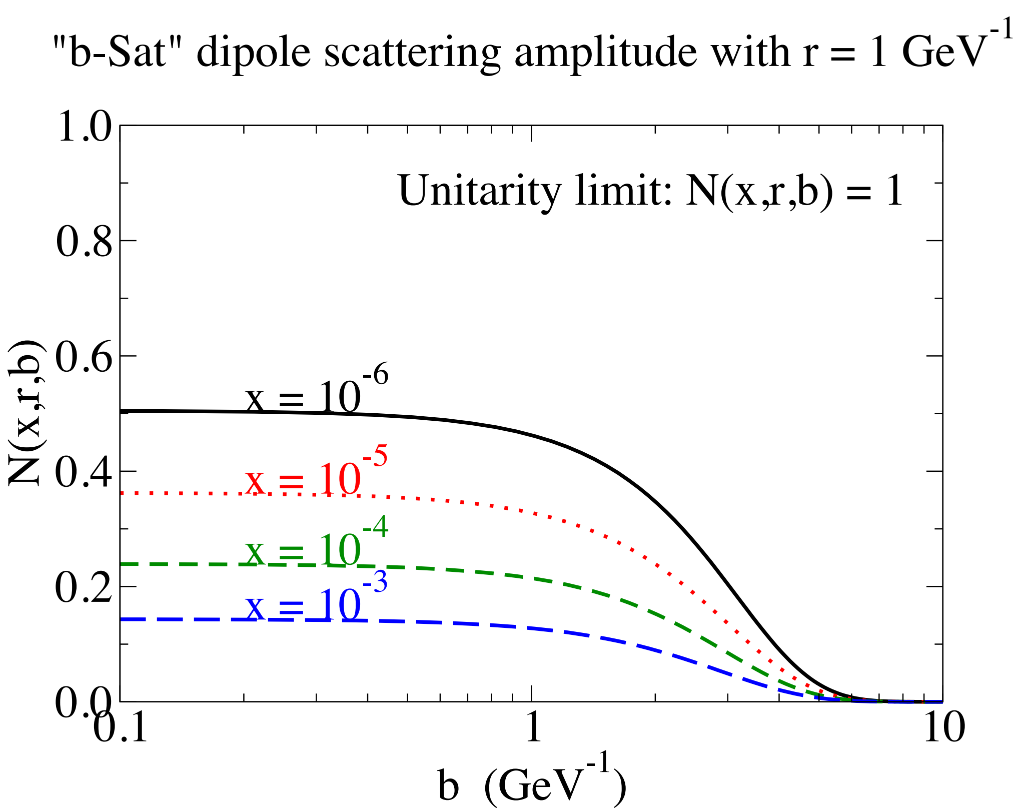

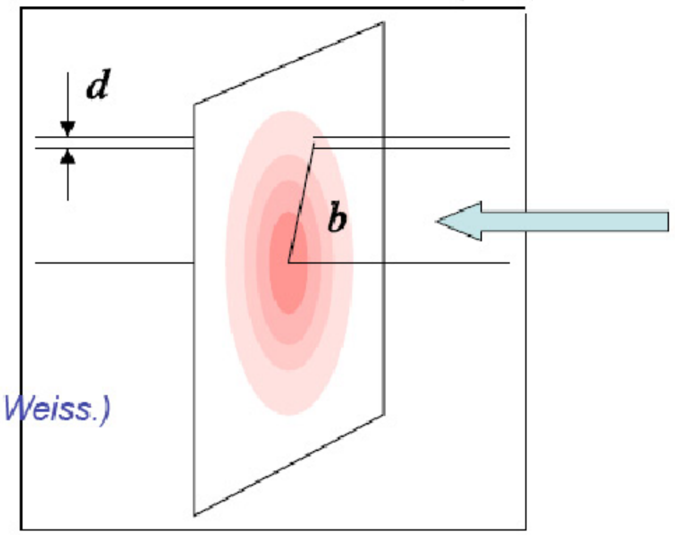

(figure from C. Weiss.)

Central black region growing with decrease of x.

Large momentum transfer t probes small impact parameter where the density of interaction region is most dense.

Extraction of density profile in impact parameter

At high energies:

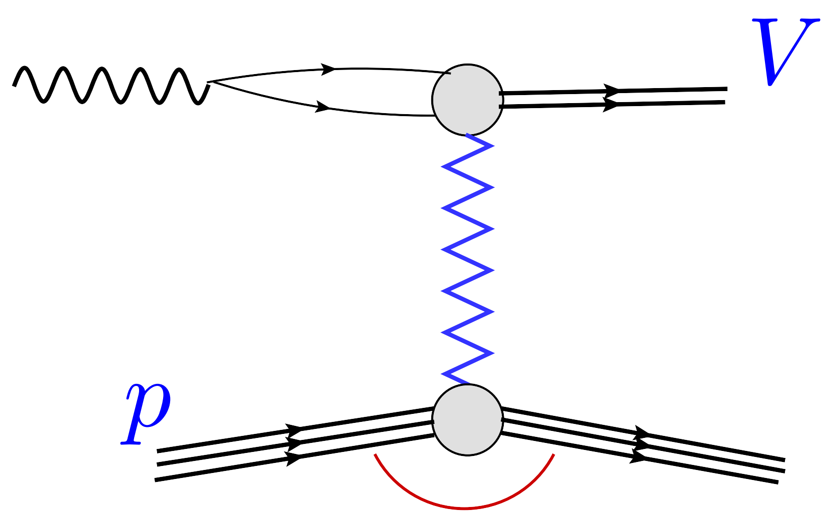

$$\frac{d\sigma}{dt} = \frac{1}{16\pi}|\mathcal{M}(\Delta)|^2$$

$\mathcal{M}$ amplitude for vector meson process

N elementary (quark dipole) amplitude

Momentum transfer $t = -\Delta^2$

$$\mathcal{M}(x, Q, \Delta) = \int d^2\mathbf{r} \int dz \int d^2\mathbf{b}\ \Psi_V^*\ N(x, \mathbf{r}, \mathbf{b}) e^{-i(\mathbf{b}-(1-z)\mathbf{r})\cdot\Delta}\ \Psi_{\gamma^*}$$

Ψ_{γ^*} photon wave function

Ψ_V vector meson wave function

Momentum transfer dependence of the cross section: impact parameter profile